DEVELOPMENT OF EFFECTIVE MODIFIED PALM SHELL WASTE- BASED ACTIVATED CARBON ADSORBENTS FOR POLLUTANTS REMOVAL

FARAHIN BINTI MOHD JAIS

FACULTY OF ENGINEERING
UNIVERSITY OF MALAYA
KUALA LUMPUR

2017

University of Malaya

DEVELOPMENT OF EFFECTIVE MODIFIED PALM SHELL WASTE- BASED ACTIVATED CARBON ADSORBENTS FOR POLLUTANTS REMOVAL

FARAHIN BINTI MOHD JAIS

DISSERTATION SUBMITTED IN FULFILMENT OF THE REQUIREMENTS FOR THE DEGREE OF MASTER OF ENGINEERING (SCIENCE)

FACULTY OF ENGINEERING
UNIVERSITY OF MALAYA
KUALA LUMPUR

2017

University of Malaya

UNIVERSITY OF MALAYA

ORIGINAL LITERARY WORK DECLARATION

Name of Candidate: Farahin Binti Mohd Jais

Matric No: KGA 140043

Name of Degree: Master in Engineering of Science (Environmental)

Title of Project Paper/Research Report/Dissertation/Thesis ("this Work"):

Development of Effective Modified Palm Shell Waste-Based Activated Carbon Adsorbents for Pollutants Removal.

Field of Study: Water and Wastewater Treatment

I do solemnly and sincerely declare that:

(1) I am the sole author/writer of this Work;
(2) This Work is original;
(3) Any use of any work in which copyright exists was done by way of fair dealing and for permitted purposes and any excerpt or extract from, or reference to or reproduction of any copyright work has been disclosed expressly and sufficiently and the title of the Work and its authorship have been acknowledged in this Work;
(4) I do not have any actual knowledge nor do I ought reasonably to know that the making of this work constitutes an infringement of any copyright work;
(5) I hereby assign all and every rights in the copyright to this Work to the University of Malaya ("UM"), who henceforth shall be owner of the copyright in this Work and that any reproduction or use in any form or by any means whatsoever is prohibited without the written consent of UM having been first had and obtained;
(6) I am fully aware that if in the course of making this Work I have infringed any copyright whether intentionally or otherwise, I may be subject to legal action or any other action as may be determined by UM.

Candidate's Signature Date:

Subscribed and solemnly declared before,

Witness's Signature Date:

Name:

Designation:

University of Malaya

UNIVERSITI MALAYA

PERAKUAN KEASLIAN PENULISAN

Nama: Farahin Binti Mohd Jais

No. Matrik: KGA 140043

Nama Ijazah: Sarjana Kejuruteraan Sains (Alam Sekitar)

Tajuk Kertas Projek/Laporan Penyelidikan/Disertasi/Tesis ("Hasil Kerja ini"):

Pembangunan Penjerap Efektif Berasaskan Karbon Diaktifkan Dari Sisa Buangan Tempurung Kelapa Sawit yang Telah Diubah Suai Untuk Pembuangan Pencemaran. Bidang Penyelidikan: Rawatan Air/Rawatan Air Sisa

Saya dengan sesungguhnya dan sebenarnya mengaku bahawa:

(1) Saya adalah satu-satunya pengarang/penulis Hasil Kerja ini;
(2) Hasil Kerja ini adalah asli;
(3) Apa-apa penggunaan mana-mana hasil kerja yang mengandungi hakcipta telah dilakukan secara urusan yang wajar dan bagi maksud yang dibenarkan dan apa-apa petikan, ekstrak, rujukan atau pengeluaran semula daripada atau kepada mana-mana hasil kerja yang mengandungi hakcipta telah dinyatakan dengan sejelasnya dan secukupnya dan satu pengiktirafan tajuk hasil kerja tersebut dan pengarang/penulisnya telah dilakukan di dalam Hasil Kerja ini;
(4) Saya tidak mempunyai apa-apa pengetahuan sebenar atau patut semunasabahnya tahu bahawa penghasilan Hasil Kerja ini melanggar suatu hakcipta hasil kerja yang lain;
(5) Saya dengan ini menyerahkan kesemua dan tiap-tiap hak yang terkandung di dalam hakcipta Hasil Kerja ini kepada Universiti Malaya ("UM") yang seterusnya mula dari sekarang adalah tuan punya kepada hakcipta di dalam Hasil Kerja ini dan apa-apa pengeluaran semula atau penggunaan dalam apa jua bentuk atau dengan apa juga cara sekalipun adalah dilarang tanpa terlebih dahulu mendapat kebenaran bertulis dari UM;
(6) Saya sedar sepenuhnya sekiranya dalam masa penghasilan Hasil Kerja ini saya telah melanggar suatu hakcipta hasil kerja yang lain sama ada dengan niat atau sebaliknya, saya boleh dikenakan tindakan undang-undang atau apa-apa tindakan lain sebagaimana yang diputuskan oleh UM.

Tandatangan Calon Tarikh:

Diperbuat dan sesungguhnya diakui di hadapan,

Tandatangan Saksi Tarikh:

Nama:

Jawatan:

University of Malaya

ABSTRACT

A simple and cost-effective water/wastewater treatment was approached by adsorption technique. While, palm shell-waste based activated carbon widely used in variety field and available in abundance in Malaysia. It was chosen as the basic raw adsorbent before modification can be made. In order to achieve high adsorption performance, special modification of adsorbent need to be made based on types of pollutant to be removed which are in this study, Arsenic removal from groundwater and Methyl Orange & Methylene Blue dye from textile wastewater.

The first modification of Palm Shell waste–based Activated Carbon (PSAC) is for removal of Arsenate ion was synthesized through dual modification. At first, Magnetic Palm Shell waste-based Activated Carbon (MPSAC) was developed via hydrothermal impregnation of nano–magnetite, and secondly it was coated by various amounts of lanthanum (La) followed by calcination. Numerous batch tests were carried out to observe arsenate removal performance. Isotherm data showed that MPSAC–La(0.36) (weight ratio of La to Fe = 0.36) gave the highest adsorption capacity (227.6 mg g^{-1}), which was 16.5 and 1.6 times higher than PSAC and MPSAC, respectively. Based on the pH effect and speciation modeling, arsenate was predominantly removed by precipitation at pH < 8, while it complexed on the surface of $La(OH)_3$ at pH > 8. Lesser La dissolution resulted, owing to a strong binding effect of nano–magnetite with La. XRD, FTIR, FESEM+EDX, and N_2 gas isotherms showed that the coating of nano–magnetite introduced substantial clogging in the micropores of PSAC, but increased meso– and macropores. However, lanthanum oxide/hydroxide (LO/LH) glued the spaces of nano–magnetite to eliminate most pore structures, and effectively removed arsenate as $LaAsO_4$ at pH 6.

University of Malaya

The second modification of PSAC is for Methyl Orange and Methylene Blue dye was developed through triple modification. First, magnetized PSAC (MPSAC) was developed through film coating method followed by second method, co-precipitation to coat MPSAC with SiO_2, which acted as template for $MgCO_3$ crystalline structure. The MPSAC-SiO_2 was then undergo third modification, hydrothermal impregnation method with different molar ratio, $MgNO_3$: urea proceed with calcination to form MPSAC-SiO_2@$MgNO_3$. Several batch studies were completed to compare the adsorption performance. The isotherm tests show MPSAC-SiO_2@$MgNO_3$(0.46) with highest $MgNO_3$ molar ratio gave the highest Methyl Orange adsorption capacity, Q_{max}=1091.6 mg g^{-1} which about 2.7 times higher than PSAC, 378.37 mg g^{-1}. While, it only gave 471.82 mg g^{-1} Methylene Blue removal capacity which was 1.15 times higher than PSAC, 409.54 mg g^{-1}. Meanwhile, pH studies reported MPSAC-SiO_2@$MgNO_3$(0.46) capable to remove both dye at high capacity at most pH range. Through triple modification, XRD, FTIR, FESEM+EDX, and N_2 gas isotherms analysis reported micropore structure was reduced, blocked and eventually disappeared after dye was loaded on adsorbent surface caused morphological changed indicated high accumulation of adsorbed dye on the surface. To conclude, both modified MPSAC–La(0.36) and MPSAC-SiO_2@$MgNO_3$(0.46) are considered as new competitive granular materials due to its high sorption capabilities, easy magnetic separation and high regeneration rate for both types of pollutant.

University of Malaya

ABSTRAK

Rawatan air/air sisa secara mudah dan kos efektif telah didatangi oleh teknik penjerapan. Sementara, karbon diaktifkan dari sisa buangan tempurung kelapa sawit telah digunakan secara meluas dalam pelbagai bidang dan boleh didapati dengan mudah di Malaysia. Ia dipilih sebagai asas penjerap sebelum pengubahsuaian dilakukan. Dalam usaha untuk mencapai prestasi penjerapan yang tinggi, pengubahsuaian khas penjerap perlu dibuat berdasarkan jenis bahan pencemar yang akan dikeluarkan iaitu dalam kajian ini, penyingkiran Arsenik daripada air bawah tanah dan pewarna Metil Jingga & Metilena biru daripada air sisa tekstil.

Pengubahsuaian pertama karbon diaktifkan berasaskan sisa buangan tempurung kelapa sawit (PSAC) adalah untuk penyingkiran Arsenate telah dihasilkan melalui dwi pengubahsuaian. Pada mulanya, karbon diaktifkan dari sisa buangan tempurung kelapa bermagnet (MPSAC) telah dibangunkan melalui hidroterma nano magnetit, kemudian disalut dengan pelbagai jumlah lantanum (La) diikuti oleh pengkalsinan. Beberapa ujian berkumpulan telah dijalankan untuk melihat prestasi penyingkiran Arsenate. Data isoterma menunjukkan bahawa MPSAC-La (0.36) (nisbah berat La untuk Fe = 0.36) memberikan kapasiti penjerapan yang paling tinggi (227.6 mg g-1), iaitu 16.5 dan 1.6 kali lebih tinggi daripada PSAC dan MPSAC. Berdasarkan kesan pH dan pemodelan penspesiesan, sebahagian besar Arsenate dikeluarkan secara mendakan pada pH <8, dan kompleks pada permukaan La $(OH)_3$ pada pH> 8. Hanya sedikit La luntur, oleh kerana kesan yang kuat mengikat nano -magnetite dengan La. XRD, FTIR, FESEM + EDX, dan isoterma gas N_2 menunjukkan bahawa penyalutan nano magnetit menyebabkan liang mikro PSAC berkurang, dan liang meso dan makro meningkat. Walau bagaimanapun, lantanum oksida / hidroksida (LO / LH) mengisi ruang antara nano magnetit dan

University of Malaya

menghapuskan kebanyakan struktur liang, dan berkesan menngeluarkan Arsenate sebagai $LaAsO_4$ pada pH 6.

Pengubahsuaian kedua PSAC adalah untuk Metil Jingga dan Metilena Biru telah dibangunkan melalui tiga kali pengubahsuaian. Pertama, PSAC bermagnet (MPSAC) telah dibangunkan melalui kaedah salutan filem diikuti oleh kaedah kedua, mendakan SiO_2 pada MPSAC, yang bertindak sebagai templat untuk struktur kristal $MgCO_3$. MPSAC-SiO_2 kemudiannya menjalani pengubahsuaian ketiga, kaedah pengisitepuan hidroterma dengan nisbah molar berbeza, MgNO3: urea diikuti pengkalsinan untuk membentuk MPSAC-SiO_2 @ $MgNO_3$. Beberapa kajian kumpulan telah dijalankan. Ujian isoterma menunjukkan MPSAC-SiO_2 @ $MgNO_3$ (0.46) dengan nisbah molar $MgNO_3$: urea tertinggi memberikan kapasiti penjerapan Metil Jingga tertinggi, Q_{max} = 1091.6 mg g^{-1} kira-kira 2.7 kali lebih tinggi daripada PSAC, 378.37 mg g^{-1}. Manakala, ia hanya memberikan 471.82 mg g^{-1}, kapasiti penyingkiran Metilena Biru iaitu 1.15 kali lebih tinggi daripada PSAC, 409.54 mg g^{-1}. Sementara itu, kajian kesan pH melaporkan MPSAC-SiO_2 @ $MgNO_3$ (0.46) mampu untuk menjerap kedua-dua pewarna pada kapasiti tinggi pada kebanyakan nilai pH. Melalui tiga kali pengubahsuaian, XRD, FTIR, FESEM + EDX, dan gas N_2 isoterma analisis melaporkan struktur liang mikro telah berkurang, tersumbat dan akhirnya hilang selepas pewarna terjerap pada permukaan menyebabkan morfologi berubah menandakan penjerapan pewarna pada permukaan terkumpul tinggi. Kesimpulannya, kedua-dua MPSAC-La (0.36) dan MPSAC-SiO_2 @ $MgNO_3$ (0.46) penjerap yang telah diubah suai boleh dianggap sebagai bahan berbutir kompetitif baru kerana keupayaan penjerapan yang sangat tinggi, pengasingan magnetic secara mudah dan kadar penggunaan semula yang tinggi untuk kedua-dua jenis bahan pencemar**.**

University of Malaya

ACKNOWLEDGEMENTS

Immeasurable appreciation and deepest gratitude for the help and support are extended to the following persons who in one way or another have contributed in making this study possible.

Prof. Shaliza Ibrahim, my main supervisor for her research adviser, support, advices, guidance, valuable comments, suggestions, and for her time and effort in checking this dissertation.

Prof. Min Jang, my co-supervisor for his positive encouragement, guidance, patience in correcting and editing manuscript to be published together with me and for all the experimental results analysis guidance.

Public Service Department (JPA), my sponsored scholarship for 3 semesters.

Mrs. Rozita Yusop, Environmental Engineering Laboratory Assistant, for her guidance in the laboratory.

My family, family-in law and my beloved husband, for all their spiritual support, love and care.

Ms. Nuzaima Che Mood & Syafiqah Janurin, my supportive friends, for her courage words along this study journey.

University of Malaya

TABLE OF CONTENTS

University of Malaya

University of Malaya

University of Malaya

University of Malaya

LIST OF FIGURES

University of Malaya

University of Malaya

University of Malaya

LIST OF TABLES

University of Malaya

LIST OF SYMBOLS AND ABBREVIATIONS

As	:	Arsenic
As(V)		Arsenate
BET	:	Brunauer-Emmett-Teller
IPD	:	Intra Particle Diffusion
IUPAC	:	International Union of Pure and Applied Chemistry
JCPDS	:	Joint Committee on Powder Diffraction Standards
K_L	:	Langmuir isotherm constant
K_{diff}	:	Diffusion control rate constant
mg	:	milligram
mg g^{-1}	:	milligram per gram
mg L^{-1}	:	milligram per liter
ml	:	milliliter
pH_{pzc}	:	Point of Zero Charge
Q_{max}	:	Maximum adsorption capacity
q_{eq}	:	Amount of solute adsorbed per unit weight of the adsorbent
µg L^{-1}	:	microgram per liter
R^2	:	Coefficient of determination
ΔH°	:	Change of entropy
ΔS°	:	Change of enthalpy
ΔG°	:	Change of Gibbs free energy

University of Malaya

LIST OF SCHEMES

University of Malaya

CHAPTER 1: INTRODUCTION

Chapter Summary

The aim of this chapter is to give a brief introduction on the overall study, which consists of the study on arsenic and dye removal (methylene blue and methyl orange dye). The introduction chapter contained freshwater and wastewater profile summary, problem statement, scope of research, objectives of research, and research outline.

1.1 General Introduction

Water has become scarce over the years and has been to a critical level. Rapid urbanization, fast population growth, uncontrolled agricultural activities, lack of environmental awareness and natural disasters are some examples contributed to global water issues. Either freshwater or wastewater issues, both need full attention from the eyes all around the world.

a) Freshwater

Freshwater can be classified into two categories: 1) surface water 2) groundwater. The surface water is defined as water found on top of the ground, for example water in the lake, river and sea. While, groundwater is defined as water found under the ground, such as in the spaces and cracks in soils, rocks and sands. The groundwater is stored underground and steadily move through aquifers (geological formations of soil, rocks and sands).

University of Malaya

Surface water has always been the top source used by many countries that has an abundance surface water, but for countries with a lack of surface water, groundwater will be the important alternative source of water to be consumed. However, more work and costs are needed to use the groundwater as a daily supply as compared to the surface water.

Almost half of the world's groundwater source is being used by countries such as China and those in the South Asia region (India, Nepal, Bangladesh and Pakistan). Researchers have found that continuous extraction of groundwater will worsen the water crisis in the South Asia region. World Water Development Report (WWDR) concluded in year 2015 that 748 million people worldwide still use untreated groundwater for daily used, where South Asia contributed to the most number of people.

Groundwater acts as a solvent, which is dissolved minerals from rocks, soil and sand that came in contact with it. Calcium (Ca^{2+}), chloride (Cl^{-}), bicarbonate (CO_3^{2-}), magnesium (Mg^{2+}), potassium (K^{+}), sodium (Na^{+}) and sulfate (SO_4^{2-}) are the common minerals dissolved in groundwater. These minerals would not cause harm to the consumer unless the concentration of the dissolved minerals are higher than the allowable concentration.

University of Malaya

b) Wastewater

Wastewater is a general term used for water that has been in contact with any by-product, products, raw material or waste from residential, commercial, or industrial activities or processes. Originally, wastewater is considered as treated freshwater that has been channeled to a different use with a different water quality standard. When the freshwater has been used, it becomes wastewater. Different use of freshwater will produce different types of wastewater.

Wastewater sources can be classified into several categories: 1) Domestic activities, which is water used for residential activities, such as drinking, bathing, cleaning, food preparation and watering the lawn. 2) Commercial activities, such as beauty salons, furniture refurnishing, and auto body repair shops. In commercial activities, the wastewater produced is more polluted than residential activities because the use of chemical products, such as paint, dye and lubricant contained a high concentration of inorganic contaminant. 3) Institutional activities is similar with the domestic activities, but in a larger quantity, which are originated from shopping mall, hospital and school. 4) Industrial activities use water for a variety of purposes, such as for heating, cooling, by-product waste carrier, solvent, for dilution and food manufacturing.

Industrial and commercial activities may contribute to a high discharge of inorganic contaminant and pollutant, which could affect wastewater treatment quality using the conventional method. Specialized treatment is needed to treat a certain industrial and commercial wastewater discharge, for example the textile manufacturing wastewater. Generally, industrial wastewater contained a high concentration of suspended solids, heavy metals (in example nickel, cadmium, calcium, iron and sodium), Biological Oxygen Demand (BOD), Chemical Oxygen Demand (COD), and ammonia. Different industry discharge will have different types of pollutant based on its activities.

University of Malaya

For example, textile manufacturing industry involved several main steps; spinning, weaving, dyeing, printing, finishing, and garments manufacturing. Dyeing, printing and finishing processes involve the use of various chemicals, such as solubilizes, dispersants, levelling agents, soaping agents, and dyeing agents. Furthermore, in printing process, the chemicals used are vat levelling agents, thickeners, binders, stain removers, and anti-back staining agents. Moreover, the cationic, non-ionic, anionic, reactive and cold water soluble softeners flake or paste were commonly used for the finishing process. The use of these textile chemicals contribute to the high amount of pollutant in the wastewater.

Other than textile chemicals, the application of dyes on the manufactured textile also contributed to the high amount of pollutant in the wastewater. Different types of textile use different types of dye. Cellulose fibers (cotton, linen and rayon), protein fibers (wool, cashmere and silk) and synthetic fibers (polyester, nylon and spandex) are the three main fibers used in the textile industry. Cellulose fibers textile commonly uses the reactive dyes (remazol, cibaron F), direct dyes (congo red and methyl orange), naphtol dyes (fast yellow GC and fast blue B), and indigo dyes (indigo white and tyrian purple). Furthermore, the acid dyes (azo dye) and lanaset dyes (blue 5G) were used for the protein fibers textile and finally, the basic dyes (methylene blue), dispersed dyes (dispersed yellow 218), and direct dyes were used for synthetic fibers.

University of Malaya

1.2 Problem Statement

a) Freshwater

Due to the uncontrolled agricultural activities and the lack of environmental conscious by farmers, the groundwater source has been contaminated. Chemical pesticides, herbicides and fertilizers contained nitrate (NO_3^-) and arsenic (As) were seen facilitate agricultural activities. The unseen results from these act were not focus at early stage. Nitrate and arsenic contained pesticides, herbicides and fertilizers that were sprayed at the plant or poured on the soil will be dissolved into the groundwater through the soil and sand. High concentration of nitrate and arsenic in the groundwater will cause serious health problem towards a long-time consumer either an animal or a human being.

Untreated industrial effluents and municipal wastewater are another source of groundwater contamination problem. Central Pollution Control Board of India found untreated effluent as the dominant source of groundwater pollution, which has a trace of heavy metal, such as Mercury (Hg), Lead (Pb), Zinc (Zn) and Cadmium (Cd) that were present in the contaminated groundwater. As we know in India, it is considered as an urban slum country with a high population growth. Some region still depends on a shallow aquifer as their source of drinking water. Without treatment, the shallow aquifer has a high risk of having a high concentration of contamination.

A long term consumption of the contaminated groundwater will bring harm towards the consumers. As stated before, heavy metal contamination in groundwater will contain a silver color pollutant called mercury, a toxic pollutant that will cause abortion, neurological disorder, brain impairment, and retardation in children's growth. However, certain heavy metal is colorless and difficult to be detected by the naked eye, but it will still harm the consumers. Normally, people always interpret clear water as clean and uncontaminated, but it is not always the case. For example, arsenic can only be detected by using a heavy metal equipment test. Arsenic contamination causes a disease called

University of Malaya

arsenicosis and there is no effective treatment for it. It is the major disease caused by a contaminant poisonous drinking water.

Naturally, arsenic is found in groundwater due to the climate and geological changes. Arsenic can be in the organic and inorganic form, but the inorganic form of arsenic is highly toxic than the organic form. The organic form of arsenic (Arsenobetaine and arsenocholine) can be found in fish and shellfish, while the inorganic form of arsenic (As^{+3}, As^{+5}) can be found in groundwater, soil and sediments. Arsenic can be found in response to the natural (geochemical mobilization) or anthropogenic sources (mining activities). Inorganic arsenic release from iron oxide is the most common source of high concentration of arsenic (>10µg/L) in groundwater. The World Health Organization has underlined the allowable arsenic concentration in drinking water, which is lower than 10µg/L.

Exposure to a high level of inorganic arsenic through drinking, breathing or skin contact can cause vomiting, diarrhea and nausea. Furthermore, a long-term exposure to the high level of inorganic arsenic can cause several types of cancer, skin lesion and gastrointestinal injuries. Fortunately, the organic arsenic that can be found in seafood are non-toxic to human.

University of Malaya

b) Wastewater

The textile manufacturing industry does not need special skills for employment. Thus, it provides millions of job opportunity to people, especially in the developing countries, such as India, Vietnam, Myanmar, Bangladesh, and Sri Lanka. Unfortunately, lack of knowledge in this field causes global wastewater treatment problem to rise. This problem was not addressed earlier and people were not aware of the importance to treat the textile wastewater.

Textile manufacturing industry uses freshwater in abundance during the dyeing and finishing processes. Thus, an abundance of wastewater has been produced from this industry. Among all industries, textile manufacturing wastewater was labelled as the most polluted based on the type of pollutants found in the effluent and the volume of effluent discharge.

Removal of the dye materials during wastewater treatment is very crucial because the quality of water is highly influenced by its color. Moreover, most type of dyes are toxic and carcinogenic, where it is difficult to degrade the dye molecule due to its stability to light and the oxidation reaction and its complex structure that is consists of the aromatic compound become barriers to treat the wastewater-contained dye through the conventional method.

Meanwhile, methyl orange and methylene blue are common dyes used in the textile industry. Methyl orange is an anionic dye and methylene blue is a cationic dye. Both dyes carry different characteristics, but still caused the same impact, which is toxic. In addition, the presence of the dyes in water will lead to the lack of light penetration into the water and reduce the aqua photosynthesis activities. Meanwhile, the hazardous impact towards human health are toxic blood, liver problem, upper respiratory tract problem, and central nervous system problem.

University of Malaya

1.3 Scope of Research

The fundamental scope of this research is to treat polluted water. Adsorption technology was applied in this research because it is simple and cost-effective as compared to the other current technologies such as electrocoagulation. However, arsenic and dye are different in terms of physical, chemical and toxicity characteristic. Thus, a different modified adsorbent was developed for different water treatments from the same raw palm shell waste-based activated carbon. Meanwhile, a simulated arsenic water and dye water were made in the laboratory and all experimental studies were conducted using the laboratory scale.

1.4 Objectives of Research

The main objectives of this study were to develop new materials with high adsorption rate to remove arsenic in the groundwater and dyes wastewater (Methylene Blue and Methyl Orange). The specific objectives were as follows:

a) Arsenic in groundwater

- To prepare MPSAC–La adsorbents with different Fe:La mass ratio entitled as MPSAC-La (0.084), MPSAC-La (0.16), MPSAC-La (0.32), and MPSAC-La (0.36) adsorbent.
- To characterize the raw PSAC, MPSAC, and MPSAC–Las adsorbents by several characterization techniques (XRD, FT-IR, FESEM+EDX, N2 gas isotherm, and pH_{pzc}).
- To compare the arsenate adsorption capacities, kinetics, pH, temperature, and co–existing anions behavior on adsorbents.
- To analyze arsenate removal mechanism on MPSAC-La adsorbent.

University of Malaya

- To investigate the MPSAC-La and MPSAC adsorbents regeneration, and the recyclability in arsenate removal.

b) Dyes wastewater

- To prepare the MPSAC-SiO_2@Mg adsorbents with a different Si:Mg mass ratio entitled as (0.06), MPSAC-SiO_2@$MgNO_3$ (0.12), MPSAC-SiO_2@$MgNO_3$ (0.23), and MPSAC-SiO_2@$MgNO_3$ (0.46).
- To characterize the raw PSAC, MPSAC and MPSAC-SiO_2@$MgNO_3$ adsorbents by several characterization techniques (XRD, FT-IR, FESEM+EDX, N2 gas isotherm & pH_{pzc})
- To compare the methylene blue and methyl orange adsorption capacities, kinetics, pH and ionic strength behavior on adsorbents.
- To analyze the methylene blue and methyl orange removal mechanism on the MPSAC-SiO_2@$MgNO_3$ adsorbent.
- To investigate the MPSAC-SiO_2@$MgNO_3$ and MPSAC adsorbents regeneration and recyclability in dye removal.

1.5 Research Outline

Incorporation of the double layer, Magnetite and Lanthanum at a higher ratio into the palm shell waste-based activated carbon improved the adsorbent performance in arsenic removal. Meanwhile, the tri layer, Magnetite, Sodium Silicate, and Magnesium Nitrate that were incorporated into the palm shell waste-based activated carbon at a higher ratio were observed to be a better adsorbent for the methyl orange dye as compared to the methylene blue dye.

University of Malaya

To explain further, this thesis was organized into five chapters. The chapters in this thesis are composed of: 1) introduction on the groundwater and wastewater; 2) literature review on water pollution, arsenic in groundwater, textile dye wastewater, current treatment technologies, types of adsorbent existed, palm shell waste-based activated carbon characteristic and modification advantageous, isotherm and kinetic models; 3) methodology on equipment used and procedure carried out during the whole research; 4) results and discussion for the whole research; 5) conclusion.

University of Malaya

CHAPTER 2: LITERATURE REVIEW

Chapter Summary

This chapter was divided into nine sections to explain further about pollution, types of water and wastewater treatment, types of adsorbent available, detailed characteristic of palm shell waste-based activated carbon, its modification trend and characteristics, followed by isotherm and kinetic model that were applied to analyze the experiment data.

2.1 Pollution History

Pollution is an issue that will have no ending without any environmental awareness and practice from everyone. It is an ancient issue that has been happening since the Paleolithic Age where archaeologist found stone tools scraps. They also believe that the use of the first wood-burning is the beginning of air pollution, which will give adverse effects towards the environment. The beginning of pollution that affected the environment and human health happened after World War II, when they first used nuclear weapon to destroy Hiroshima and Nagasaki in Japan. Exposure to nuclear radiation may cause birth defect, mutation, cancer, and even death. This incident was one of the example of air, water and land pollution that occurred for a long period of time.

When World War II ended, industrialization, urbanization and agricultural activities began to increase uncontrollably. People tried their hardest to improve the economy with variety of ways without being aware of the adverse effects. Industries began to increase their quantity and quality of manufacturing products and started using synthetic materials, such as synthetic dyes and plastics in the manufacturing process. At the time, wastewater produced were discharged without proper treatment, followed by the use of inorganic insecticide and pesticide for agricultural activities as they thought it is more efficient to kill pests and produce good quality agricultural product.

University of Malaya

As time passed by, these scenarios showed its impact towards the environment and health. Some of the synthetic material used for manufacturing process were not biodegradable and high in toxicity. When the waste was accumulated in the water course, it caused water pollution and increased the health risk of people who consumed it. This is one of many example of human activities that caused pollution.

2.2 Water Pollution

Water pollution is defined as water bodies (lake, river, sea, groundwater, and aquifers) containing harmful elements. It occurred when pollutants entered the water bodies directly or indirectly and no adequate treatment has been used to remove the pollutants. (Wikipedia, 2016). On the other hand, Lloyd (1992) described water pollution as the addition of harmful thing into the water by human, which caused the chemical composition, temperature, and biological composition of the water to alter to a certain extent that will eventually affect the environment and humankind (R. Lloyd, 1992).

2.1.1 Sources of Water Pollution and Its Impact

a) Organic Matters

Dissolved Natural Organic Matters in the water causes foul smell and is normally caused by untreated discharged domestic or industrial waste into the water course (Heath, 1995; R. Lloyd, 1992). However, a major fraction that contributes to the Dissolved Natural Organic Matters in water is humic substances (Kaiya, Itoh, Fujita, & Takizawa, 1996). When the humic substances interact with the potential pollutants such as chlorine that is used in water disinfection process, it may interact and produce carcinogenic compounds. Furthermore, the interaction of humic substances in the ozonation process may

University of Malaya

lead to biodegradable-by-products production and eventually promote microbial growth (Suffet, Maccarthy, MacCarthy, & Suffet, 1988).

b) Excessive nutrients

The excessive nutrients occur when agricultural run-off and biodegradables were discharged in the water. By concerning on nitrate and phosphate, the increment of these two nutrients may result in algae bloom (Blaas & Kroeze, 2016). Excessive nutrient causes algae to grow in abundance and stimulate the growth of phytoplankton where a high phytoplankton density will cause dissolved oxygen depletion. This phenomenon is called eutrophication (Heath, 1995).

c) Suspended Solids

Suspended solids are defined as mass (mg) or concentration (mg L-1) of the organic and inorganic substances in the water bodies by flowing movement. Typically, suspended solids composed of fine particles with a diameter less than 62 µm (Waters, 1995). Naturally, all streams carry suspended solids without causing any harm. However, at a certain condition where the anthropogenic interrupts the natural condition (Ryan, 1991), the amount of suspended solids is increased and will lead to adverse impact towards the physical, chemical and biological characteristic of the water bodies, such as reduced light penetration and infilling stream (D. S. Lloyd, Koenings, & Laperriere, 1987).

University of Malaya

d) Toxic chemicals

i) Metals

Metals in water generally are called as trace metals or heavy metals. Cobalt, zinc, manganese, fluoride, and calcium are some of the general metals that are present in water bodies. (Heath, 1995). It enters the water bodies through natural or anthropogenic activities. Consuming a few of the heavy metals in water at an allowable concentration is essential for health, but higher concentration will cause a negative effect (USEPA, 2016). Industries such as chemical, textile, and electroplating industries are a few examples of heavy metals source (arsenic, mercury, lead and silica) in the water bodies (He et al., 2008) . In many developing countries, domestic, industrial, and agricultural wastewater are usually discharged into any water bodies without having a proper treatment (A. D. Gupta, 2008).

ii) Dyes

Dyes are used as coloring agents in textile, food, cosmetics, paper, and plastic manufacturing industries (B. Chen et al.). When wastewater containing dyes were discharged into any water bodies, it will cause the water bodies to change its physical properties (color). Most of the dyes are toxic, mutagenic and carcinogenic (Soni, Sharma, Srivastava, & Yadav, 2012). Dyes also prevent light penetration in the water bodies and eventually reduce the photosynthetic activities in the water.

University of Malaya

2.3 Arsenic in Groundwater

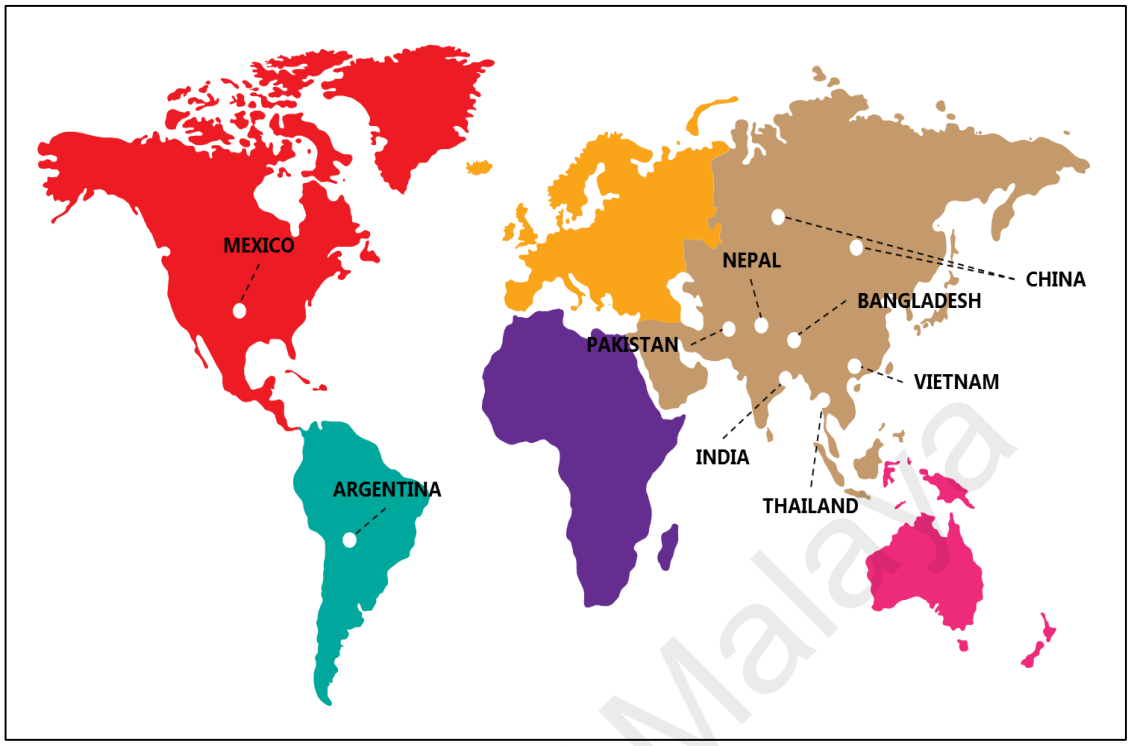

Figure 2.1 Countries with arsenic contaminated groundwater risk

Arsenic (As) contamination and mobilization in the groundwater has already become a global issue affecting millions of people worldwide (Hafeznezami et al., 2016). However, the world population were only aware of the toxicity effect of arsenic in the groundwater in the year 1992, where the first contamination was reported in Bangladesh (D Chakraborti & Roy, 1997).

Currently, the World Health Organization (WHO) underlined that the groundwater is considered to be contaminated with arsenic if its concentration in the groundwater is more than 10 µg/L. Arsenic contamination in the groundwater has been reported in not less than 100 countries with estimated affected population of more than 200 million people (Murcott, 2012; Naujokas et al., 2013). Until the year 2009, a total of 140 million people are consuming arsenic-groundwater as their daily water source (Ravenscroft, Brammer, & Richards, 2009). Asian countries, especially India and Bangladesh are the countries with the worst arsenic-groundwater contamination (Dipankar Chakraborti et al., 2013).

University of Malaya

Based on previous studies, the government of Bangladesh and India installed tube wells to prevent the risks of water-borne diseases and provided safe drinking groundwater supplies to their citizens. There are 8.6 million tube wells were recorded in Bangladesh alone. Unfortunately, the tube well installation is only able to prevent water-borne diseases, yet, they are still being exposed to arsenic groundwater consumption. A report on tube wells in India itself mentioned that there are 48.1% of tube wells that had arsenic concentration in the groundwater (>10 µg/L), while 23.8% of the tube wells had more than 50 µg/L of arsenic in the groundwater (Dipankar Chakraborti et al., 2009).

2.3.1 Source of arsenic

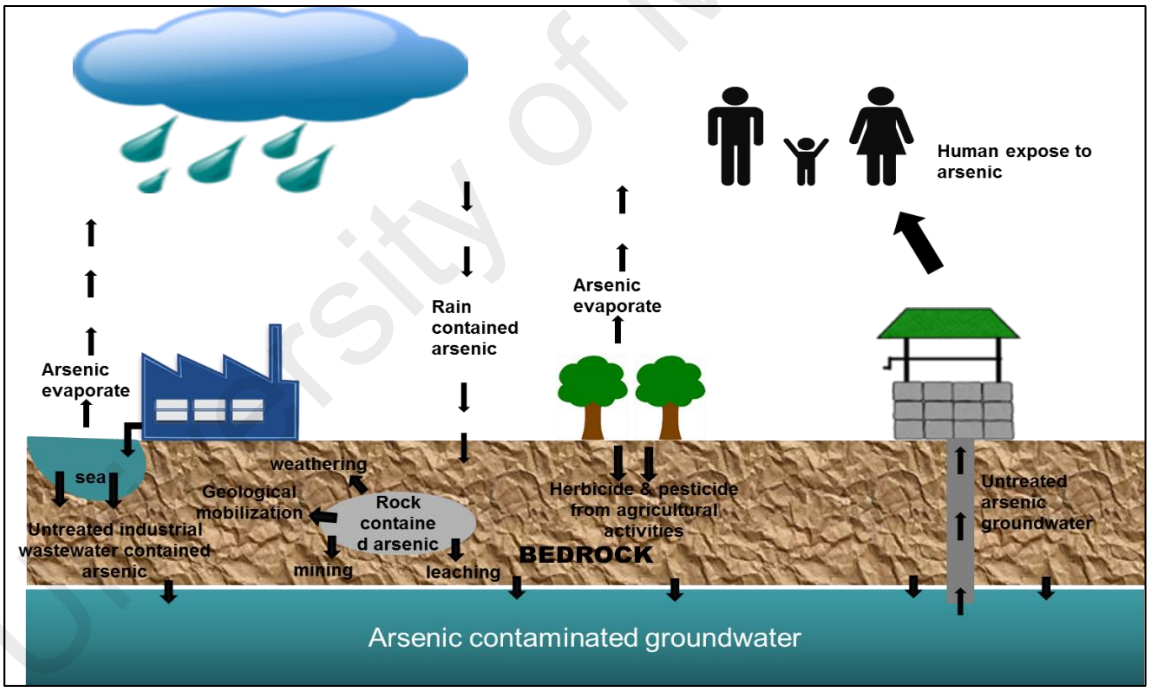

Figure 2.2 The cycle of arsenic source in groundwater and the human exposure pathway through ingestion

A long time ago, arsenic presents naturally, even in earth's crust, sediment, soil, water, air, and in living organisms (Mandal & Suzuki, 2002). Arsenic is a metalloid element that is available in abundance in the earth's crust. Among the 245 minerals that are naturally available, arsenic was nominated to be the first twenty mineral to be most available

University of Malaya

(Mandal & Suzuki, 2002). Arsenic might co-precipitate at high concentration with iron hydroxides or sulfides in sedimentary rocks (Mandal & Suzuki, 2002). In addition, arsenic is available in more than 200 different mineral forms, whereby, about 60% of arsenic are available in arsenate form, 20% in sulfides and sulfosalts, while other 20% present as arsenide, arsenite, oxide, elemental arsenic and silicate (Wedepohl, 1969).

Arsenic was found to be more concentrated in soil than rocks (Peterson, Benson, & Zieve, 1981). Usually, unpolluted soils may contain in between 1-40 mg Kg^{-1} of arsenic, whereby, sandy soils and derived granites have the lowest arsenic concentration as compared to the organic and alluvial soils (Kabata-Pendias & Pendias, 1992). Thus, different type of soils will have different level of arsenic concentration.

Levels of arsenic in soils will eventually affect the level of arsenic in the groundwater. Factors such as redox potential, climate, organic and inorganic element in soils are closely related to the level of arsenic in soils (Mandal & Suzuki, 2002). The physical and geochemical characteristic of arsenic causes accumulation and mobilization in groundwater at a naturally high concentration (Smedley & Kinniburgh, 2002). Arsenic may be mobilized through several natural occurrences such as rock weathering reactions, volcanic emissions, and biological activity (Smedley & Kinniburgh, 2002).

Importantly, the natural source of arsenic was not a threat to human and the environment, but the combination between the natural source and the anthropogenic source is the main thing to tackle. Some examples of human activities that are causing arsenic contamination are the use of arsenical pesticides fertilizers, the use of arsenic as additive in livestock feed, mining activities, and industrial waste disposal (Mandal & Suzuki, 2002; Smedley & Kinniburgh, 2002). Although the arsenical product usage is decreasing, the use of arsenic in wood preservation still remain the same.

University of Malaya

In the year 1955, arsenic was used widely for manufacturing insecticide and pesticide, a total of 37,000 tons of white arsenic were produced globally in the form of pesticide (Heishman, Olson, & Shelton, 1960). Lead Arsenate, Copper Acetoarsenite, monosodium Methanearsonate (MSMA), and Disodium Methanearsonate are some of the pesticides example that were used back then. Additionally, weed killer herbicide containing the inorganic arsenic (Sodium Arsenite) was widely used back in the 1890s.

Meanwhile, during the mining activities, arsenic was exposed to the environment from the mine and extraction plants. After the mine has closed down, the waste rock dumps and tailing dams containing arsenic experienced weathering, while the acid mine drainage was produced due to the sulfur and arsenic bearing mineral being oxidized by the water run-offs and infiltrated through rain water (Sánchez-Rodas, Luis Gómez-Ariza, Giráldez, Velasco, & Morales, 2005).

2.3.2 Arsenic Characteristic

Arsenic has the chemical and physical characteristics of being between a metal and a non-metal. Thus, arsenic was called as metalloid or semi-metal element. Arsenic may be present in an organic or inorganic form.

Based on the mobilization sensitivity of arsenic at a typical pH of groundwater, pH6.5 to 8.5, it was classified to have high sensitivity among other metalloid and oxyanion element. It may exist in several oxidation numbers (-3, 0, +3, and +5). Commonly, when arsenic was found in natural water, it present in an inorganic form, either Arsenite (+3) or Arsenate (+5) (Jedryczko, Pohl, & Welna, 2016). Moreover, Arsenate is commonly in water (AsO_4^{3-}, $HAsO_4^{2-}$, $H2AsO_4^{-}$), while Arsenite (AsO_3^{3-}, $As(OH)_3$, $As(OH)_4^{-}$, $AsO_2OH_2^{-}$) are the common species available in natural water (Zongliang, Senlin, & Ping,

University of Malaya

2012). At a common pH for groundwater and natural water (pH6.5 to 8.5), water tends to have aerobic conditions where this natural occurrence will lead arsenic to present dominantly in Arsenite form, while the predominant form is Arsenate (Katsoyiannis, Hug, Ammann, Zikoudi, & Hatziliontos, 2007).

On the other hand, the organic arsenic are said to be less toxic than the inorganic arsenic while based on the inorganic arsenic itself, Arsenite was reported to be more toxic than Arsenate (Zongliang et al., 2012). The ability of Arsenite to react with sulfur containing compound and generated the Reactive Oxygen Species makes it being more toxic (Hughes, Beck, Chen, Lewis, & Thomas, 2011).

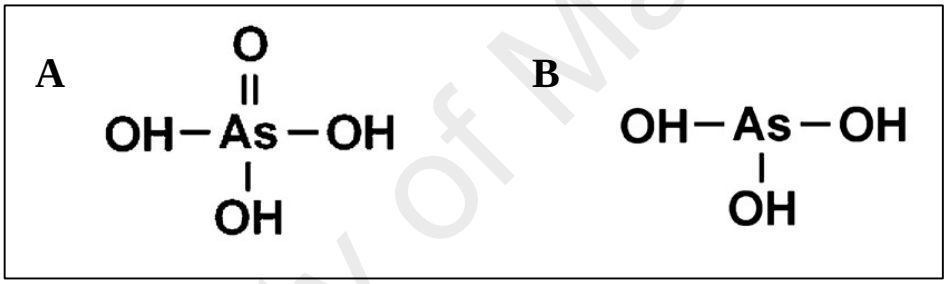

Figure 2.3 the molecular structure of A) arsenate and B) arsenite

2.3.3 Impact towards Human Health

Arsenic was classified as a Class I human carcinogen (Humans, Organization, & Cancer, 2004). A long term ingestion of drinking water source containing inorganic arsenic may result to a serious health complication. The World Health Organization (WHO) underlined several serious diseases that may affect people who consume arsenic contaminated groundwater, for example having the effect on the respiratory tract, skin, liver, kidney, and gastrointestinal tract. WHO also reported the first case related to arsenic contaminated water exposure on the 19th century when the victim experienced hyperkeratosis, pigmentation changes, and skin cancer (Compounds, 2001).

University of Malaya

A summary on several health effects caused by arsenic exposure are listed below:

i) Respiratory Effect

Long term exposure to inorganic arsenic may cause laryngitis, trachea bronchitis, rhinitis, nasal congestion and shortness of breath (Naqvi, Vaishnavi, & Singh, 1994).

ii) Carcinogenic Effect

Hundred years ago, arsenic was used as medicine to treat chronic diseases. However, a number of medicated patients experienced a symptom where the number of their basal cells and squamous cell carcinomas of their skin were increased ("Reports of Societies," 1887). Previous research studies reported that most arsenic contaminated groundwater area such as Bangladesh, India, and Argentina will have an increased cancer risk, which is due to the consumption of arsenic contaminated drinking water (Hopenhayn-Rich et al., 1996; Report, Toxicology, Toxicology, Studies, & Council, 2001). Significantly, lung, skin, bladder, kidney, and liver are the common vital organ being attacked by the cancer cells that are caused by arsenic contaminated groundwater.

iii) Gastrointestinal Effect

At a high arsenic dosage consumption, acute arsenic poisoning may occur, which will show symptoms such as dry mouth and throat, heartburn, moderate diarrhea or abdominal pains, and cramps. Meanwhile, at a low dosage consumption, gastritis and lower abdominal discomfort may occur (Naqvi et al., 1994).

iv) Dermal Effects

High concentration of arsenic consumption will cause several skin diseases, for example melanosis, keratosis, hyperkeratosis, Bowen’s disease, and cancer.

University of Malaya

Hyperpigmentation also may occur where the skin area tend to be a little darker (Shannon & Strayer, 1989).

2.4 Textile Dyeing Wastewater

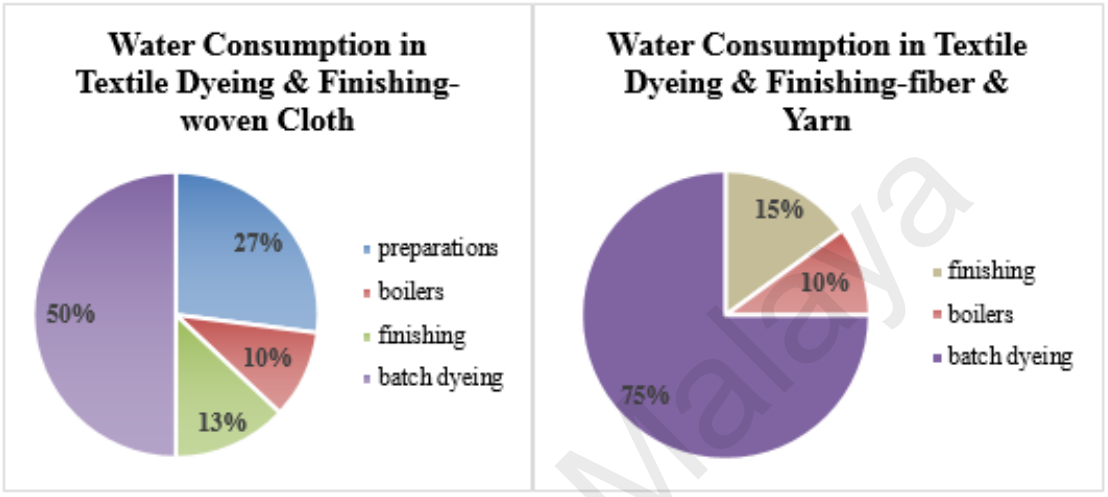

Figure 2.4 Water consumption in the textile dyeing & finishing-woven cloth, and water consumption in the textile dyeing and finishing-fiber & yarn
Source: (Envirowise, 1997)

Figure 2.4 illustrated the water consumption in the textile dyeing & finishing-woven cloth and the water consumption in the textile dyeing and finishing-fiber & yarn data in pie charts. Both pie charts show the batch dyeing process consumed the largest amount of freshwater followed by finishing and boilers.

China and India recorded to be the two largest textile dyeing industry contributor in the world (Lin & Moubarak, 2013). The textile dyeing and finishing industrial sector was reported to create a major water pollution and has been classified as one of the most chemically intensive industries in the world, where it is considered to be the first water pollution contributor after agricultural sector. Statistically, there are more than 3,600 individual textile dyes being manufactured and more than 8,000 chemicals were used in various textile manufacturing process, especially in dyeing and printing processes (Baiocchi et al., 2002).

University of Malaya

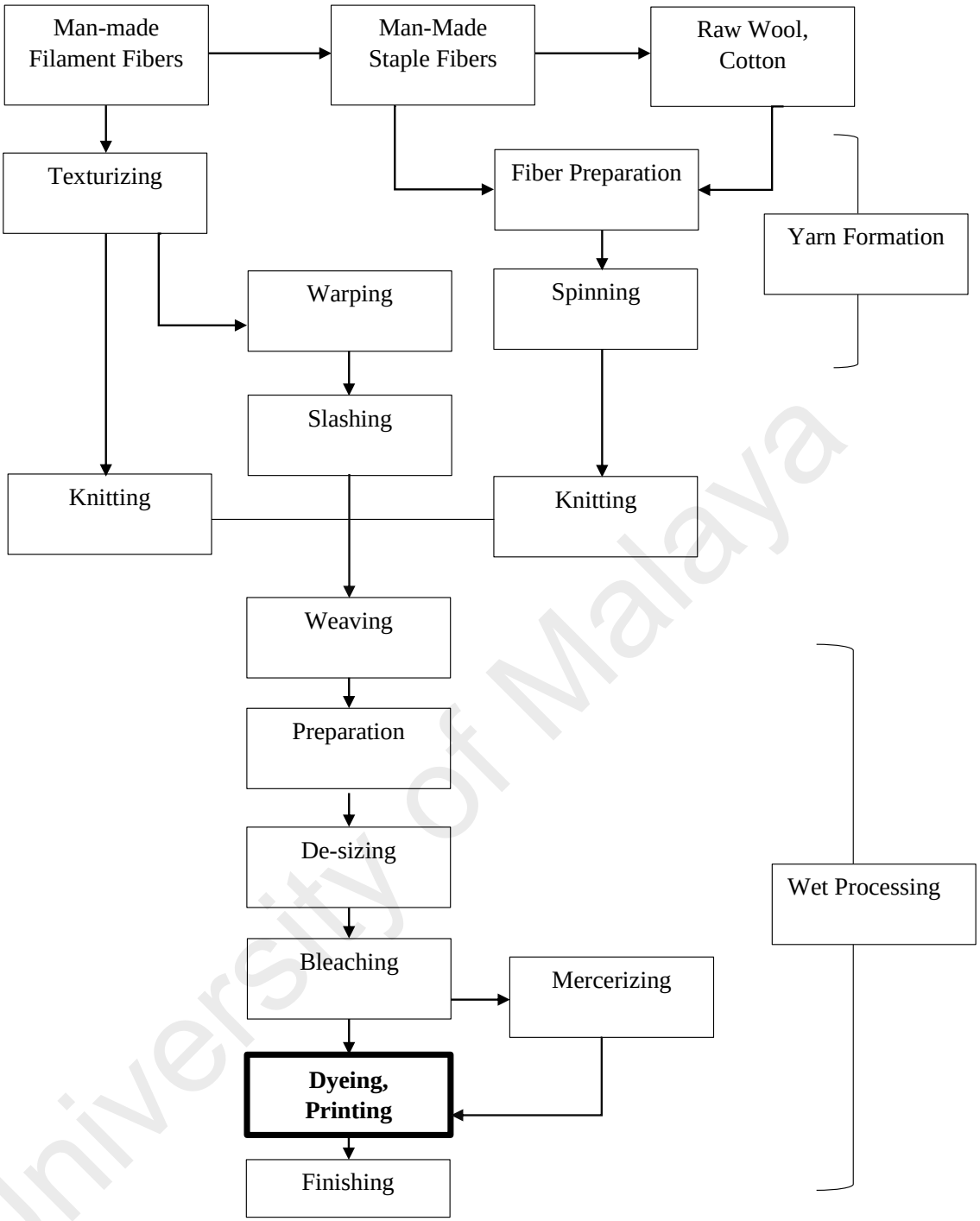

Figure 2.5 Flow diagram of various steps involved in processing textile in a cotton mill
(Babu, Parande, Raghu, & Kumar, 2007)

University of Malaya

Mercerization

Mercerization is a process to improve the dye uptake into the cotton fiber and fabric by treating it in a concentrated NaOH solution (8-24%). The cotton material will be washed-off after 1-3 minutes of soaking time. The used NaOH solution was then recovered by the membrane techniques. The alternative recovery method, which is $ZnCl_2$ helps to increase the weight of fabric and in the dye uptake, where it will also allow NaOH to be recovered easily. Additionally, the process is environmental friendly and does not required neutralization by acetic or formic acid (Karim, Das, & Lee, 2006).

Bleaching

Bleaching is a process to decolorize the creamy appearance of fabric due to the natural color of yarn. In order to produce a pale and bright shades of color on fabric, hypochlorite will be used as bleaching agents. Hypochlorite chemical produced toxic chlorinated organic-by-product during the bleaching process. The other alternative to replace hypochlorite is peracetic acid, which is an environmental friendly bleaching agent. It is decomposed into a biodegradable product, oxygen and acetic acid. The advantage of using the peracetic acid is that the fabric will experience less damage as compared to when using hypochlorite (Rott & Minke, 1999).

Dyeing

The dyeing process involved an abundant uses of freshwater (hot water) to transfer the dyes color onto the cotton fiber and fabric. The color of the dye is obtained from auxochrome and chromophore functional group of the dye molecular compound, which will contribute to water pollution (Szymczyk, El-Shafei, & Freeman, 2007). The world's

University of Malaya

most popular fabric being used in the textile manufacturing industry, which is cotton needs a total of 0.6-0.8 kg NaCl, 30-60 g of dye and 70-150 L of freshwater to dye a 1kg of cotton fabric (Chakraborty, De, Basu, & DasGupta, 2005).

At the end of the dyeing process, abundance of wastewater is produced from various treatment processes containing a high concentration of salt (NaCl) and a highly colored dyed water. The wastewater produced needs to be treated before it can be reused or discharged into any water bodies. The common treatment methods used to treat dyed wastewater are coagulation and membrane process. However, these processes are only effective for diluted dyed wastewater (Babu et al., 2007).

Finishing

Finishing process is done to improve the specific properties in the finished fabric and various finishing agent, such as softening agent, cross-linking and waterproofing were used, and eventually contribute to water pollution. For the past years, the most environmental friendly product being used in the finishing process is formaldehyde based cross-linking agents. However, formaldehyde will undergo evolution in which it will liberate chemical products and cause toxicity to the water used during the cross-linking reaction.

University of Malaya

Table 2.1 List of wastewater generated in each cotton dyeing manufacturing process

Process	Wastewater
Fiber preparation	Little or no wastewater generated
Yarn spinning	Little or no wastewater generated
Slashing/sizing	BOD, COD, metals, cleaning waste, size
Weaving	Little or no wastewater generated
Knitting	Little or no wastewater generated
Tufting	Little or no wastewater generated
Desizing	BOD from water-soluble sizes, synthetic size, lubricants, biocides, anti-static compounds
Scouring	Disinfectants and insecticide Residue, NaOH, detergents, fats; oils, pectin, wax, knitting lubricants, spin finishes, spent solvents
Bleaching	Hydrogen peroxide, sodium silicate or organic stabilizer, high pH
Singeing	Little or no wastewater generated
Mercerizing	High pH, NaOH.
Heat setting	Little or no wastewater generated
Dyeing	Metals, salt, surfactants, toxics, organic processing Assistance, cationic materials, color, BOD, sulfide, acidity/Alkalinity, spent solvents.
Printing	Suspended solids, urea, solvents, color, metals, heat, BOD, foam.
Finishing	BOD, COD, suspended solids, toxics, spent solvents.

2.4.1 Type of Dyes

Dyes can be classified into various types based on their chemical composition and characteristic. Thus, the type of dye being used in the textile-dyeing manufacturing industry varies depending on the type of fabric they produce.

Commonly, textile dyes carry these general characteristics, which are (Christie, 2007):

- Strongly absorb at visible spectrum wavelength.
- Consists of polyaromatic compounds.
- Water soluble except for dispersed dye, pigments, and vat dyes.
- Resistant against biological degradation.

Based on Christie et al. (2007) in the Environmental Aspects of Textile Dyeing, textile dyes were classified based on its application methods (basic, acid, direct), the type of

University of Malaya

interaction between the dye and the fabric (reactive), the structural characteristic (azo) or the historical characteristic (vat).

a) Azo dyes

Azo dyes, such as Methyl Orange (anionic dye) consists of one or more double-bonded nitrogen units linking the aromatic units. The problem with azo dyes is the capability to break down and form certain aromatic amines.

b) Basic dyes

Methylene Blue (cationic dye) is classified under the basic dye and the characteristic of the basic dye is it carries the amino group (positive charged) that is attached to the larger aromatic structures. Thus, it gives both water solubility and affinity to the fabric, such as nylon that contains a dominant negative charge.

c) Acid dyes

Usually, acid dyes carry sulfonic acid group that gives them negative charge characteristic. Under acidic conditions, amino groups in protein or polyamides fibers become positive and eventually attract the negative dye anions.

d) Reactive dyes

Reactive dyes contain the functional group that are bind to the chromophore allowing covalent bonds to be formed with the cellulosic and protein fibers. Reactive dyes are not being absorbed onto the biomass to any degree.

e) Disperse dyes

Originally, dispersed dyes were developed for acetate fibers. The characteristic of disperse dye is low solubility, which helps to color fibers that have a very high hydrophobicity.

Methylene Blue and Methyl Orange dyes were used in this research as they are the two typical dyes being used in the textile dyeing process. Furthermore, both dyes carry

University of Malaya

different characteristics. Brief explanations on the Methylene Blue and Methyl Orange dyes' characteristics are stated as below:

i. Methylene Blue dye characteristic

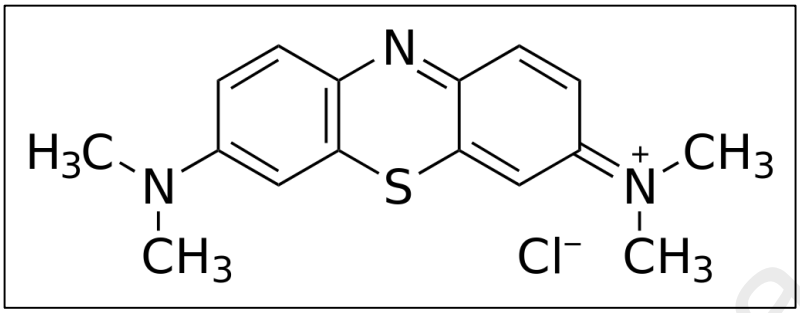

Figure 2.6 Methylene Blue dye molecular structure

Figure 2.6 shows the molecular structure of Methylene Blue with the molecular formula $C_6H_{18}N_3SCl$. At standard room temperature, Methylene Blue will appear as odorless, solid, and dark green powder, which will produce blue color when it is dissolved in water (N. W. E. contributors). It is classified as cationic dye, with the maximum absorption of light around 670 nm that is being used in many industries, including the textile manufacturing industry (Umoren, Etim, & Israel, 2013) (W. contributors). To emphasize, the Methylene Blue dye is known as an organic dye that is commonly used in dyeing variety types of fabric materials including cotton, wool, acrylic fibers, and silk (Tabbara & El Jamal, 2012).

University of Malaya

ii. Methyl Orange dye Characteristics

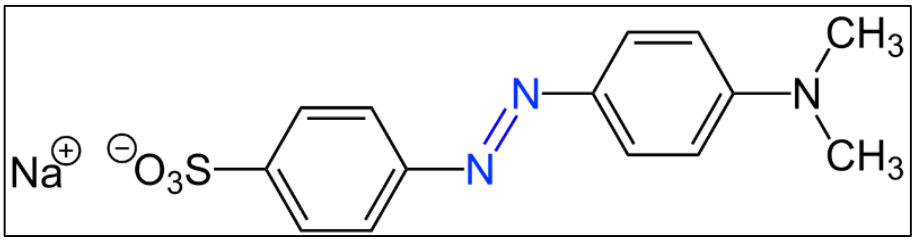

Figure 2.7 Methyl Orange dye molecular structure

Figure 2.7 shows the molecular structure of Methyl Orange dye (acidic anion mono azo dye) with the molecular formula $C_{14}H_{14}N_3NaO_3S$ (Jain & Sikarwar, 2008). It was listed in one of the most important class of commercial dyes and is categorized as a stable dye in either visible or near UV light (Nam, Kim, & Han, 2002). Methyl Orange dye usually shows a different color at different solution medium, such as red color in acidic solution, and yellow color in basic solution (W. contributors). Thus, it is commonly used as a color indicator in chemical laboratories. Other than that, Methyl Orange dye also usually being used in printing, photography and textile industries (C. Guo, Xu, He, Zhang, & Wang, 2011). However, Methyl Orange dye is classified as an azo dye, which is known to be carcinogenic because of the degradation of the Methyl Orange into aromatic amines (Guivarch, 2004). Thus, the detoxification and discoloration of azo dye will have an increasingly important environmental significance in the recent years (Guivarch, 2004).

University of Malaya

2.4.2 Impact of Dye Wastewater towards Environment

Textile wastewater contains various types of pollutant, for example trace metals, BOD, COD, suspended solids and many more. Meanwhile, the dye itself contributes to a high concentration of color in wastewater. Water containing dyes gives a bad color and may cause diseases such as ulceration of skin, nausea, severe skin irritation, and dermatitis when being consumed or exposed to it (Tüfekci, Sivri, & Toroz, 2007). It formed barrier in water and blocks the sunlight penetration, which is the essential for photosynthesis of aquatic plants (Laxman, 2009) where it will in turn causes the BOD level to increase and the total photoautotrophic plants to decrease (Tüfekci et al., 2007). Among various types of dye, reactive dyes were classified under the inorganic substances in textile wastewater that caused toxicity towards aquatic environment (Blomqvist, 1996). However, the organic dyes will also bring harm towards the aquatic environment through chemical and biological changes, which will lead to reduction of DO (Tholoana, 2007).

The level of dye pollution in water is strongly depending on the quantity of freshwater and the types of chemical used during the manufacturing process (Laxman, 2009). The problem with textile dye is that it is difficult to be degraded as it contained a large amount of organic substances, which also prevents it from aerobic degradation. The worst problem is the ability of the dye to undergo reduction process and forms carcinogenic agents under the anaerobic conditions (Jain, Bhargava, & Sharma, 2003), whereas some of carcinogenic compound is formed through the azo dye degradation. More importantly, human that are in contact with the Methyl Orange and Methylene Blue dyes may experience vomiting, cyanosis, jaundice, shock, and tissue necrosis (Azami, Bahram, Nouri, & Naseri, 2012).

University of Malaya

2.5 Conventional Water & Wastewater Treatment

In water or wastewater treatment technologies, there are three treatment stages called as primary, secondary, and tertiary treatment processes. The primary treatment is commonly installed to remove the suspended solids, large waste, and coarse particles from the water or wastewater, whereby screening, sedimentation, flotation, and filtration processes were used. After the primary treatment, the water or wastewater will be treated using the secondary treatment, whereby the biological pollutants will be removed. At this treatment stage, the aerobic or anaerobic treatment process will be installed. Lastly, in order to obtain safe water for a specific use, the remaining pollutants, which are commonly chemicals, inorganic waste or any particles that were not removed significantly during the primary and secondary treatment will then be removed during the tertiary treatment (Vinod Kumar Gupta, Ali, Saleh, Nayak, & Agarwal, 2012). Likewise, Tchobanoglous and Burton (1991) defined the tertiary treatment or also known as the advanced treatment as the additional combination of the treatment process or the operation used to reduce or remove other residual suspended solids and other constituents that are not remarkably removed by the conventional secondary treatment (Tchobanoglous & Burton, 1991).

The high cost of installation, operation and maintenance of certain treatment processes, and the difficulty in implementation are some of the factors that made some countries such as India unable to provide a low-cost drinking water supply equipment, for example by installing shallow tube wells in the aquifer. However, the drinking water supplied from tube wells were reported to contain arsenic concentration more than the allowable limit for a safe drinking water. Meanwhile, other drinking water supply alternative such as harvesting rainwater is an inconvenient way to be practiced because of the expensive installation cost (Ahmed, 2001). On another note, the dye wastewater produced by the textile manufacturing industry usually contained a high organic load, a strong and

University of Malaya

resistant color that needed to be treated. In order to incur a low cost and simple treatment, the biological treatment process is commonly used. Unfortunately, biological treatment does not efficiently remove the organics and colors from the dye wastewater since most of the dye molecules consist of a very complex structure and a non-biodegradable characteristic due to their chemical nature and molecular size. These factors resulted in a high sludge formation at the end of the treatment process (Yuan, Wen, Li, & Luo, 2006).

In between a variety of the tertiary treatment technologies, the most commonly used to treat arsenic contaminated groundwater are ion exchange, aerobic and anaerobic microbial degradation, coagulation and flocculation, membrane separation, advanced oxidation process, solvent extraction, precipitation, electrocoagulation, electrolysis and adsorption for a safe drinking water use and also to treat the dye wastewater in order for it to be reused or discharged into any watercourse.

a) Ion Exchange

In domestic water treatment, ion exchange treatment is used to remove nitrate and other natural organic matter. It is also widely used in household laundry detergent and water filters to generate soft water by exchanging Ca^{2+} and Mg^{2+} with Na^{+} and H^{+} on resin surface (W. contributors). The ion exchange process involved the exchange of toxic ion in water or wastewater with non-toxic ion from solid material (Naden, 1984). There are two types of ion exchange, which are anion and cation exchange, whereby in anion exchange, the toxic anion is exchanged with anion on the resin surface, while in cation exchange, the toxic cation is exchange with cation on the resin surface. The most common resin (ion exchanger) used are zeolite, sodium silicate, polystyrene sulfonic acid, and acrylic. Ion exchange treatment is usually used to remove low concentration of contaminants (250 mgL^{-1}). Thus, resin modification is needed in order to optimize the

University of Malaya

contaminant removal capacity. However, ion exchange resin is easily polluted by the toxic ion exchanged caused by the removal capacity that is reduced from time to time. Thus, resin regeneration is needed to increase its removal capacity back again, but this process incurred a high cost (VITO, 2010).

Ahmed et al. (2001) reported in his study that the oxidation treatment process is usually used as the pre-treatment to convert As (III) to As (IV) before further treatment can be made. Oxygen, ozone, free chlorine, permanganate, hypchlorite, hydrogen peroxide, and Fulton's reagent are some of the oxidizing agent used to oxidize As (III). However, in developing countries, they usually use atmospheric oxygen, hypochloride and permangate as the oxidizing agent (Ahmed, 2001).

The organic dye (Methylene Blue and Methyl Orange) can be treated using the chemical oxidation method with an almost complete mineralization of the organic pollutants. The oxidation with Fenton's reagent is proven to be the effective technology for the destruction of various numbers of toxic and organic pollutant. Unfortunately, Fenton's oxidation are not very suitable for pollutants with alkaline solution and the sludge produced at the end of the oxidation process is high, which will resulted in a high cost to dispose of the sludge (Dutta, Mukhopadhyay, Bhattacharjee, & Chaudhuri, 2001).

b) Microbial Degradation

Biological treatment or microbial degradation is classified as an eco-friendly method, which are gaining more interest nowadays. Fungi, bacteria, algae, enzymes and yeasts are some of the microorganisms used to remove a wide range of dyes through anaerobic, aerobic, and anaerobic-aerobic treatment processes (Vinod K Gupta, Rastogi, & Nayak, 2010). The microbial degradation is usually used for the removal of synthetic dyes. This treatment process is usually cheap, has a low operation cost, and produced

University of Malaya

non-toxic decolorized and mineralized product. However, various types of the dyes are chemically stable and resistant to microbiological attack (Forgacs, Cserháti, & Oros, 2004).

Zouboulis et al. (2005) reported in his study that the biological remediation treatment process was used to convert As (III) to As (V) and succeeded to reduce the arsenic concentration from 60 to 80 µg/L to a final concentration lower than 10 µg/L. However, over ten months treatment period, buy using the XPS analysis, he found that only a partial of the As (III) was converted into As (V) (Zouboulis & Katsoyiannis, 2005). This showed that the biological remediation is not a very efficient pre-treatment process.

c) Coagulation & Flocculation

Coagulation and flocculation are processed involving the use of coagulant and flocculant. Coagulation is the rapid mixing process, where the coagulants will be added during the rapid mixing process. Coagulants are chemicals used to aid the removal of total suspended solid and color present in the untreated water. The coagulant will destabilize the stable colloidal particle to become a settable particle in the form of flocs, which will then be separated and removed through the downstream clarification or filtration treatment process (Gebbie, 2006). Meanwhile, Flocculation is a process after the rapid mixing process. The aim of flocculation is to form larger sizes of particles that will suit the next process. It is a unit process treatment that will allow the collision between small size particles. When the small particles collide with themselves, the particles will stick to each other and flocculate, which will increase their sizes and become floc (Hendricks, 2006).

University of Malaya

The coagulation-flocculation treatment process is more efficient for As (V) than As (III) removal where $FeCl_3$ acts as a better coagulant than $Al_2(SO_4)_3$. The disadvantage of using the coagulation-flocculation treatment is the high volume of arsenic-concentrated-sludges produced at the end of process (R. Singh, Singh, Parihar, Singh, & Prasad, 2015). Moreover, the sludge treatment incurred a high cost and these limitations make this treatment to be less suitable (Mondal, Bhowmick, Chatterjee, Figoli, & Van der Bruggen, 2013).

Coagulation of the dye wastewater has been used for many years as the main treatment or pre-treatment due to its low capital cost (Anjaneyulu, Chary, & Raj, 2005). However, the major barrier of coagulation process is thehigh sludge generation and ineffective decolorization of some soluble dyes (Hai, Yamamoto, & Fukushi, 2007). The sludge production can only be minimized in small volume of highly colored effluent, which will directly be treated after the dyeing bath (Golob, Vinder, & Simonič, 2005). On the other hand, due to the development of synthesis technology, a large number of innovative dyes with complex structures have been developed, which contributed to the difficulties in using the coagulation process (Y. Yu, Zhuang, Li, & Qiu, 2002).

d) Membrane Separation

Membrane separation or membrane filtration is a treatment process used to separate heterogeneous particle from liquids or gaseous state through a selective barrier (membrane). Reverse osmosis, ultrafiltration, microfiltration and pervaporation are the major membrane separation processes used widely. Membrane filtration is used to remove color, heavy metals, COD, and total dissolved solids from wastewater (SHUKLA, KUMAR, & BANSAL, 2008). The advantage of membrane separation is the compact system with easy control operation and maintenance. However, the ultrafiltration process is only capable to treat low molecular weight organic material, while the reverse osmosis

University of Malaya

consumed high energy. Another disadvantage of membrane separation is the flux decline caused by membrane fouling. This problem reduced the rate of pollutant removal and its efficiency (Ledakowicz, Solecka, & Zylla, 2001).

The application of membrane technology to treat the dye wastewater is very effective (Ledakowicz et al., 2001). However, the main drawbacks of the membrane treatment process are having a high cost, frequent membrane fouling, requiring different pre-treatments, depending upon the type of influent wastewater and production of concentration dyebath that needed the proper treatment before it can be disposed to the environment (Robinson, McMullan, Marchant, & Nigam, 2001).

e) Advanced Oxidation Process

Advanced Oxidation Process (AOP) is the term used for multi-oxidation process involving a highly reactive hydroxyl radical generation where one oxidation process is not sufficient for water or wastewater treatment (Yoon, Lee, & Kim, 2000). AOP techniques, such as Ultra Violet (UV) photolysis and Fenton's reagent oxidation are capable to degrade organic pollutants at normal pressure and temperature. These techniques have already been applied at full scale, while techniques such as photo catalysis and ultrasound are only applied at a pilot scale on laboratory benches (Parsons, 2004).

The advantage of AOP is the organic contaminants will be oxidized to CO_2. Photo catalysis is one of AOP being used for organic pollutant degradation. It involves the use of UV or solar energy to excite electron from the valence bond of the photo catalyst to the conduction band with a series of reaction to form hydroxyl radicals. Hydroxyl radicals have a high oxidizing potential and can attack many organic pollutants. TiO_2, ZnO, ZrO_2,

University of Malaya

Cds, and ZnS are the common photocatalysts used in photo catalysis process that are suitable for a wide range of organic pollutants (Kabra, Chaudhary, & Sawhney, 2004).

f) Precipitation

Precipitation mechanism involved the conversion of dissolved contaminants into solid precipitated by reducing the contaminant's solubility to make it easily skimmed off from the water surface. Precipitation process is usually used to remove ionic metal and organic pollutants, but the presence of oil and grease in water may cause precipitation problems. The rule in precipitation process is low contaminant's solubility. Thus, some chemicals will be added or water temperature will be reduced in order to reduce solubility. Some of the chemical additives used are Alum, Ferric Chloride, lime, Sodium Bicarbonate and Ferrous Sulphate. Unfortunately, chemical addition technique used at commercial level consumes high cost.

The precipitation treatment process is simple and able to remove 60% of the pollutant. Normally, wastewater from metal plating industries and water recycling will install this treatment process to treat their wastewater before discharging it to the environment. However, the end process by-product (sludge) is produced at a high volume and the sludge produced is highly toxic as it contained all the precipitated contaminant removed during the precipitation treatment, which will then be dumped at a general landfill (Cavaco, Fernandes, Quina, & Ferreira, 2007).

g) Electrocoagulation

Electrolysis is a process whereby oxidation and reduction takes place when the electric current is applied into the electrolytic solution (Kuokkanen & Kuokkanen, 2013). Electrocoagulation consists of electrolysis element, whereby the anode is called as 'sacrificial anode', which produced metal ion that will act as the coagulant agents in the

University of Malaya

water to be treated (Emamjomeh & Sivakumar, 2009; Holt, Barton, & Mitchell, 2005). The electrode used in the electrocoagulation treatment process is usually made of iron, aluminum or stainless steel because they are readily available, non-toxic, and cost-effective (X. Chen, Chen, & Yue, 2000; Kumar, Chaudhari, Khilar, & Mahajan, 2004).

A previous study examined the ability of As (III) and As (V) removal using the electrocoagulation process by installing three different electrodes, namely aluminum, iron and titanium. Study results showed that arsenic removal is better when using the iron electrode than the other two electrodes (Kumar et al., 2004). However, electrocoagulation has several limitations, one of which the sacrificial anode will be eroded by time as a result of oxidation. The eroded anode will be dissolved into the treated water and needs to be replaced regularly. Meanwhile, impermeable oxide surface will be formed on the cathode surface making the pollutant removal efficiency to be reduced. Lastly, the electricity used for this treatment might be expensive depending on how long the treatment process is taken (Sahu, Mazumdar, & Chaudhari, 2014).

h) Adsorption

Adsorption is a phase transfer process. It happened when the chemical species from the fluid phase attached to the surface of the liquid or solid phase. In water or wastewater treatment, adsorption has been proved to be the efficient treatment process to remove a variety of contaminant in water to be treated. Adsorbent (usually solid phase), adsorbate (chemical species in fluid phase) are two principles needed to succeed in the adsorption mechanism. Whereas, adsorbent must have an active and energy-rich site to enable it to interact with the adsorbate. The reverse process of adsorption is called as desorption. It occurred when the adsorbate is attached on the surface and the adsorbent is detached (Worch, 2012). Usually, desorption will be done after the adsorption process in

University of Malaya

order to regenerate the surface of adsorbent. Thus, it can be reused again for another treatment cycle.

As adsorption is a surface process, surface area of the adsorbent is the important key to determine the efficiency of the adsorbent. An engineered adsorbent usually has a high porosity with a surface area in the range of 102 -103 m^2g^{-1}, which is caused by its internal surface constituted by the pore walls. Contrastingly, the external surface is typically below 1 m^2 g^{-1} (Worch, 2012).

The adsorption process typically undergoes three different steps, which are:

1) **Mass transfer**: the adsorbate particle molecules attached to the outer surface of adsorbent.
2) **Intra particle diffusion**: the adsorbate particles went into the adsorbent pores.
3) **Physical or chemical sorption**

There are two different types of adsorption mechanism, named as physical sorption and chemical sorption. Physical sorption involves weak intermolecular forces between adsorbent surface and adsorbate. Meanwhile, the chemical sorption involves the chemical bond between adsorbate and adsorbent surface. The other differences between the physical sorption and chemical sorption are that physical sorption does not share their electron. The adsorption does not occur at a specific site and the heat from the physical sorption is low compared to the chemical sorption (Faust & Aly, 2013).

University of Malaya

2.6 Type of Adsorbents

The commercial adsorbents are adsorbent produced commercially, whereby the cost for commercial adsorbents are more expensive as compared with a low-cost adsorbent. Low-cost adsorbents are typically cheaper than the commercial adsorbents because they derived from waste products either from agricultural or industrial by-product.

Because there are various types of adsorbents, several adsorbent characteristics need to be considered, which are selectivity, surface area, and regeneration ability. There are adsorbents with multiple adsorbate particle selectivity and single adsorbate particle selectivity. The surface area for each adsorbent is different, for example the activated carbon has a very high surface area. High surface area helps the adsorbent to react with the adsorbate more efficiently. Regeneration ability gives the capability for the adsorbent to be reused again. There are some adsorbent capable to be recycled more than three times. Thus, a high regeneration ability significantly helps to reduce the water or wastewater treatment cost.

2.6.1 Commercial Adsorbent

a) Silica gel

Silica gel or silicon dioxide, SiO_2 is a clear, transparent or translucent adsorbent. Some of the silica gel manufactured contained alumina blended in them. Commonly, silica gel is produced in the form of micro spherical particle known as beads, but there is also granule, pellets and powder form of silica gel. Silica gel is commercially used as desiccant to control humidity, food preservation, and various medical apparatus. Additionally, it is also being used in adsorption treatment process to remove hydrocarbon (Knaebel, 2008).

University of Malaya

b) Activated alumina

Activated alumina adsorbent is made up of Aluminum Oxide, Al_2O_3. It is a white, tan or opaque adsorbent. Commonly, activated alumina is produced in the form of balls, pellets, powder or granules sizes. Commercially, activated alumina is used as a catalyst or desiccant. The other usage of activated alumina is for the removal of fluoride (Ghorai & Pant, 2005) and arsenic (T. S. Singh & Pant, 2004) through the adsorption treatment.

c) Zeolite

Most zeolites are aluminosilicate, which are made up of alumina and silica. Thus, it generally appears in white, opaque and chalk-like. The zeolite characteristic is influenced by the amount of alumina in it. A high amount of alumina gives the hydrophilic characteristic to it, while the low amount of alumina gives the hydrophobic characteristic to it. All commercial zeolites consist of a very fine crystal structure bound together by its binder with a uniform microporous structure (Knaebel, 2008). Usually, zeolites are used for gas or liquid drying, oxygen separation from air, purification of hydrogen and many more.

d) Polymer

Polymer adsorbent is spherical beads with opaque appearance. It colors depends on its manufacturing product, which is commonly in black, orange, brown, white or tan. Typically, polymer is made up of polystyrene or divinyl-benzene copolymer with a spherical shape and a high pore volume. Currently, polymer is used in decolorization, industrial wastewater treatment, purification of antibiotics and vitamins, and VOC recovery from off-gases. The disadvantage of polymer is that it is ten times more expensive

University of Malaya

than other commercial adsorbent. In addition, polymer tends to shrink and swell upon cyclic use (Knaebel, 2008).

e) Activated carbon

Activated carbon is a burned organic material (wood, tree trunk, fruit shells) until it formed charcoal, which is a black color adsorbent with high porosity. The activation of the burned organic material (carbon material) created the internal structure that consists of varied pore structures where the dominant pore structure is micropore followed by macropore and mesopore structures (Kasaoka, Sakata, Tanaka, & Naitoh, 1987). The types of organic material used in the burning process will influence the amount of ash produced at the end. The alkali ash formed at the pore surface can be removed by acid washing or by impregnation with other elements.

Commonly, the activated carbon is produced at different granule sizes (fine, medium, and coarse grain). Different activated carbon size gives different pollutant removal adsorption capacity. Activated carbon with a fine particle size has the highest surface area as compared to a coarse size. Effective surface area is generally ranges from 300 to 1500 m^2g^{-1} depending on the base of the organic material and the activation method (Knaebel, 2008).

University of Malaya

2.6.2 Low Cost Adsorbent

i. Industrial by-product

a) Fly ash

Combustion of the coal will produce a by-product known as fly ash. Researchers believed that fly ash is potentially able to substitute the use of a commercial adsorbent (zeolite or activated carbon) for wastewater or water treatment. Additionally, fly ash contained a high percentage of silica, alumina and magnetite. However, the performance of fly ash to be a great adsorbent is strongly affected by the origin of the fly ash and the chemical treatment (M. Ahmaruzzaman, 2011). On the other hand, fly ash was used widely to remove the heavy metals from water and wastewater. It is able to remove Pb, Cd, Cr, Ni, As, and Hg and it has been reported that fly ash from coal-char can also remove As (V) at the adsorption capacity of 34.5 mg g^{-1} (Pattanayak, Mondal, Mathew, & Lalvani, 2000).

a) Used tire

Thoroughly, used tires have been a major disposal issue in many countries. Researchers have found a solution to reduce the used tire dumping issue by recycling the waste and utilizing it for rubber tiles and blocks or for cement manufacturing ingredients. However, the cost of making waste tire into rubber powder is expensive and it is virtually non-biodegradable and covers a lot of space at the landfill (Mousavi, Hosseynifar, Jahed, & Dehghani, 2010). Contrastingly, used tire has a high carbon content and in this recent years, Ali et al. (2012) have reported that there are many research studies using used tires as a raw material to synthesize adsorbent for phenol and various dye removals (Ali, Asim, & Khan, 2012). Meanwhile, Mousavi et al. (2010) found another use of used tire, which

University of Malaya

is as an adsorbent where he reported in his study that it has a gray color consisting of a heterogeneous pore size and shape with a high surface area. It is capable to remove Pb at the adsorption capacity of 22.35 mg g^{-1} (Mousavi et al., 2010).

b) Blast furnace slag

A large volume of granular blast furnace slag was produced from steel plants. It was utilized as fillers or as slag cement, and was also converted into a cost-effective adsorbent for toxic organic contaminant in water and wastewater. In order for a raw blast furnace slag to be converted into a good adsorbent, it has to be activated by the activation method (Ali et al., 2012). Gupta et al. (1988) revealed the used of the blast furnace slag as adsorbent by activating it through oven-dried method at a certain temperature and found that the activated blast furnace slag has a high surface area of 107 m^2g^{-1}. Then, he used the finished product to remove the malachite green dye and as a result, 99.9% of the dye concentration was removed at a low concentration (G. Gupta, Prasad, Panday, & Singh, 1988). The main disadvantage of using a blast furnace slag as adsorbent is that the blast furnace slag was classified as a non-product. Thus, the production cost is expensive (Nilforoushan & Otroj, 2008). In various pH environment, slag properties may change and toxic element in slag may be released through leaching (Yan, Moreno, & Neretnieks, 2000).

c) Peat

Peat is a porous structure with a complex material containing lignin and cellulose. It has been used in many studies to remove heavy metals, dyes and oil from water and wastewater. The ability of raw peat to directly be used as an adsorbent for wastewater or water treatment is insignificant because raw peat has low stability and mechanical strength, and it is difficult to regenerate (Smith, MacCarthy, Yu, & Mark Jr, 1977). Sun

University of Malaya

et al. (2003) revealed that raw peat structure has to be chemically modified using the plyvinylalcohol and formaldehyde in order to break the limitations. The modified peat-resin particles contained polar functional groups (acids and alcohols) and act as a good adsorbent for dye removal (Sun & Yang, 2003).

ii. Agricultural waste

a) Sugar cane bagasse

Bagasse pith is sugar industry waste by-product that is available in abundance with no cost (Amin, 2008). Sugar cane bagasse consists of cellulose (45%), hemicellulose (28%), and lignin (18%) (Pehlivan et al., 2013). It also contained hydroxyl and carboxyl group, which shows the capacity to adsorb dye molecules by complexation or ion exchange mechanisms (Dávila-Jiménez, Elizalde-Gonzalez, & Peláez-Cid, 2005).

b) Rice husk ash

Rice husk is obtained during the separation of rice from paddy through the rice mills processing industry. It is widely used as fuel in boiler furnace to produce steam. Rice husk ash is available in abundance and consumes almost no cost (Lakshmi, Srivastava, Mall, & Lataye, 2009). It has a good adsorption capacity and has been used to study various dye and heavy metal removal capacities.

c) Palm shell

Palm shell waste contains a high carbon content obtained from the palm oil milling process, which is produced as an agricultural waste in some tropical countries. The raw palm shell itself is available in abundance and cheap. To make palm shell waste a better material for adsorption, it needs to be burned into ash and activated using a

University of Malaya

specific activation method. The activation process will help the palm shell waste ash to have high porosity, surface area and density. In this research study, palm shell waste based activated carbon has been used as the basic raw material to remove arsenic in both groundwater and dye (methylene blue and methyl orange) in textile industrial wastewater. The justification will be described further in the next section.

University of Malaya

2.7 Palm Shell-Waste Based Activated Carbon

To recall, adsorption is simple, easy to operate treatment process and widely used to treat variety of pollutant at a high removal capacity as compared to others. However, high adsorption performance is influenced by the type of adsorbent used. Thus, it is important to select a great basic adsorbent before any modification can be made to treat the pollutant in water or wastewater at optimum performance. As mentioned in the previous section, there are many types of adsorbent synthesized by researchers and the palm shell-waste based activated carbon was classified as the agricultural waste product that is being utilized as an adsorbent.

Malaysia was reported to be the largest palm oil producer worldwide. Generally, there are about 2.4 million tons of palm oil shell waste generated every year. Meanwhile, Malaysia's neighboring country, Thailand recorded over 100 thousand tons of palm oil shell waste produced by 16 different palm oil mills factories every year where they were disposed to the landfills (Lua & Guo, 2001; Prasertsan & Prasertsan, 1996). The palm shell-waste production and disposal attracted many researchers to find ways to utilize it and eventually reduced the volume of palm shell waste disposed to landfills. Many ways to utilize the palm shell waste were studied by researchers, such as for light weight concrete material, combustion steam fuel and as adsorbent.

In general, palm shell waste is a porous waste product containing a very rich carbon structure. To produce a great adsorbent, a high pore surface area is one of the important characteristics to determine the adsorption performance. Thus, palm shell waste needs to undergo several preparation methods to improve its adsorption characteristics. Hence, palm shell waste-based adsorbent production has to undergo two preparation steps, which is carbonization and activation. Carbonization is a process whereby air moisture in the palm shell waste will be taken out through the heating process at extreme temperature for

University of Malaya

several hours. This process will reduce palm shell waste weight and increase pore surface area. Then, palm shell waste need to undergo activation process or known as oxidization process, either by gas or chemical treatment before it can be classified as the palm shell waste-based activated carbon. At the end of the preparation process, a light-weight and very high porosity activated carbon is produced.

The production of the activated carbon, either the commercial or low cost adsorbent is almost the same. However, the difference is in the source of material. This research study chose to use palm shell-waste based activated carbon as it was available in abundance in Malaysia and cheap as compared to other materials. It will also contribute to waste dumping reduction in Malaysia and other palm shell producer country.

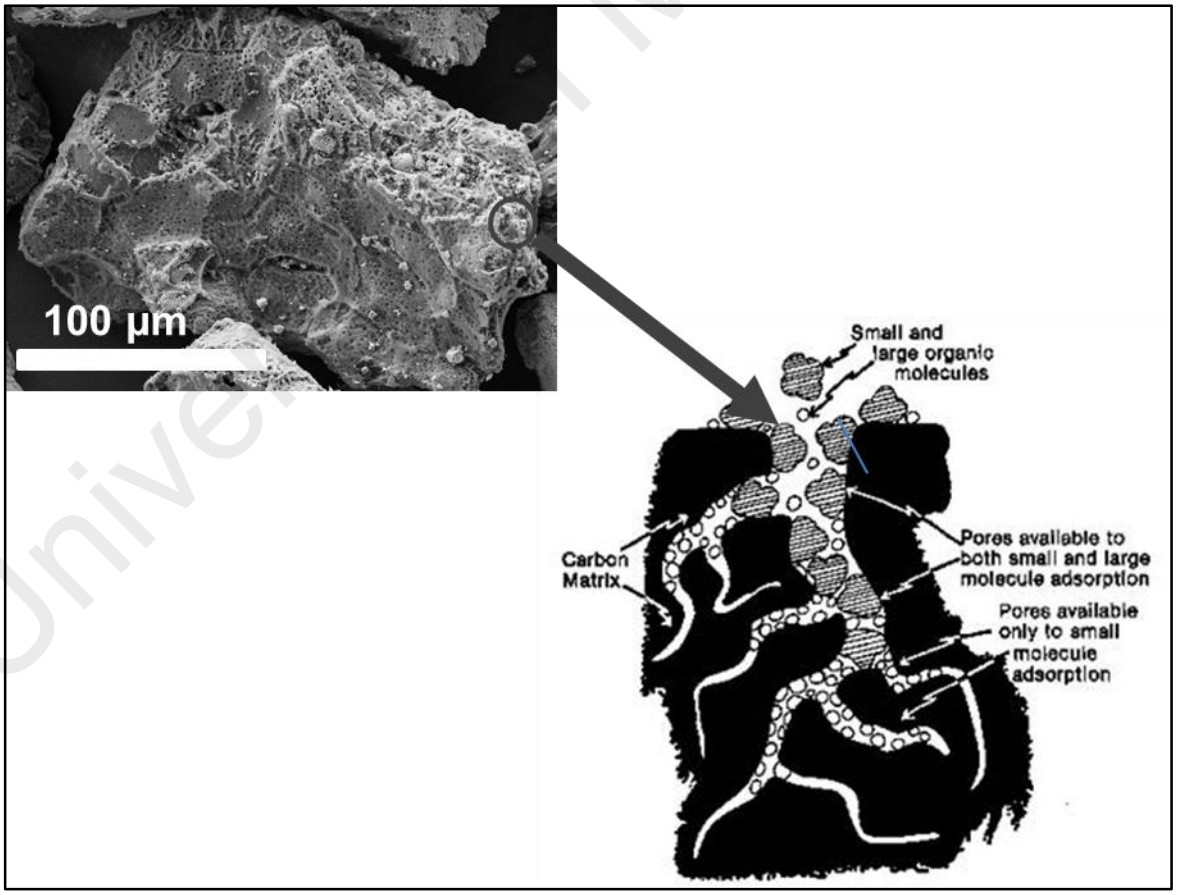

Figure 2.8 The general activated carbon pore structure
Source: http://www.wateensolutions.com.au/page/carbon-filter

University of Malaya

Furthermore, palm shell has the ability to be modified and eventually, increases its carbon porosity, which is one of the important aspect to determine the adsorption capability. This is because, the higher the adsorbent's porosity, the better the adsorption capacity by the adsorbent. Other than that, palm shell has a high lignin content, but low cellulose content where these characteristics allow the palm shell to be activated at a short time due to a less fibrous structure as compared to the other types of activated carbon (Daud & Ali, 2004).

2.7.1 Importance of Surface Modification

The general activated carbon's microporous structure allows to adsorb a large amount of pollutant in a small enclosed space. The adsorptive structure of activated carbon consists of the ordered carbon with aromatic planes similar to graphite. However, the graphite consists of a well-ordered aromatic planes, while activated carbon consists of the angular orientation of aromatic planes.

Commonly, activated carbon comprises of heteroatoms, for example oxygen, sulfur, hydrogen and nitrogen, whereby in carbon matrix, the heteroatoms are present in the form of functional groups (carboxyl, carbonyl, phenols) and oxygen atom acts as the predominant atom in the functional group. The adsorption capacity of the activated carbon is strongly controlled by the types of functional group present in the carbon matrix of activated carbon. Interestingly, the types of activation treatment, either wet or dry treatment influences the types of oxygen surface complexes (functional group) (Gaur, 2012). Laszlo et al. (2001) proposed that the characteristics of activated carbon surface, either basic or acidic depend on the delocalized electron of the carbon structure (Laszlo & Szűcs, 2001).

University of Malaya

Nevertheless, a wide surface area and a high microporous structure owned by the activated carbon gives an advantage for arsenic ion to accommodate in the activated carbon's microporous structure (Asadullah et al., 2014). The Arsenic uptake was not very efficient. Additionally, the microporous structure arises a problem in adsorbing a large-sized dye molecule, whereby the large-sized dye molecule was not fitted into the porous structure of the activated carbon. Other than that, the activated carbon surface is lack of polarity (Asadullah et al., 2014). Hence, reducing the surface affinity towards the adsorbate (Yin, Aroua, & Daud, 2007).

The type of pollutant to be removed is heavily dependent on the activated carbon surface chemical features. Thus, the surface chemical modification of the activated carbon is important to produce an adsorbent for a specific pollutant removal. Thus, pollutant can be removed at optimum capacity. This is because the surface chemical modification method by oxidation usually will produce a high hydrophilic structure activated carbon with a rich functional group containing oxygen (Rios et al., 2003).

University of Malaya

2.7.2 Activated Carbon Surface Modification Techniques

a) Physical modification

Heat treatment is a common method under the physical modification techniques. This method helps to enhance the physical characteristics (BET area and total pore volume) of activated carbon. Other than that, heat treatment also helps the acidic characteristic of activated carbon to be reduced to basic character by reducing the oxygen containing functional group. High temperatures at more than 700˚C might be used for this method because the majority of oxygen containing the functional group can be decomposed at 800˚C to 1000˚C (Figueiredo, Pereira, Freitas, & Orfao, 1999).

b) Chemical modification

Chemical modification technique was aimed to reduce the internal surface area and pore volume of the activated carbon. Other than that, the aim of the chemical modification is to increase the acidic surface on the activated carbon since the heavy metal in water, such as arsenic is more favorable to adsorb on a negatively charge acidic character than basic character. The chemical modification uses oxidation method by introducing oxidizing agent to create an acidic functional group on the activated carbon surface. Unfortunately, the oxidation method will cause the activated carbon pore structure to deconstruct. Thus, researchers have found that by introducing alkaline solution treatment, the OH- ion from the alkaline solution, it will react with the activated surface of the functional group and eventually reduce the pore destruction risk.

The most important method in the surface modification is surface impregnation method. It is a method whereby the fine chemicals or metal particles are distributed evenly on the activated carbon pore surface. The impregnation method increases the advantages of using activated carbon as the adsorbent, such as to promote a built-in catalytic

University of Malaya

oxidation capability and synergism between the impregnator and activated carbon. Meanwhile, the most advantageous is that it optimizes the activated carbon adsorption capacity.

Gaur et al. (2012) explained that the modification of the activated carbon by metal impregnation method has increased interest among researcher because it enhance the activated carbon sorption capacity in example fluoride and Arsenic in water (Gaur, 2012).

2.7.3 Advantageous of Magnetic Modification

Activated carbon, either in granular or fine particle sizes are widely used in water or wastewater treatment as adsorbent. However, the activated carbon usage has its own limitation because it is difficult to separate and regenerate when all the activated carbon surface pore is fully used or exhausted. Traditionally, exhausted activated carbon was separated using the filtration method and this leads to exhausted activated carbon especially the fine sized activated carbon to block the pore filter where eventually will reduce the filtered activated carbon collected for regeneration (Reza & Ahmaruzzaman, 2015).

By introducing the Iron Oxide nanoparticles (Fe_2O_3) through chemical modification method, the activated carbon limitation can be overcome. The Fe_2O_3-activated carbon or also known as the magnetically activated carbon is effective and has a low-cost adsorbent that is able to remove both the organic and inorganic pollutant from water (Mezohegyi, van der Zee, Font, Fortuny, & Fabregat, 2012). Furthermore, magnetically activated carbon is easy to separate when exhausted by introducing the external magnetic field without the need for filtration, which will eventually reduce the operation cost.

University of Malaya

2.7.4 Advantages of Multi Metal Oxide/Hydroxide Modification

Nowadays, researchers have put their concern on the synthesized adsorbent with low cost preparation but showing optimum adsorption capacity. Bimetallic oxide or hydroxide modification is the answer. It was prepared by a double coat activated carbon using a different metal oxide or hydroxide. There are many researchers already succeeded in producing a good bimetallic adsorbent, such as Zhang et al (2005) that abled to synthesize the Fe-Ce bi metal oxide adsorbent for arsenate removal (Y. Zhang, Yang, Dou, He, & Wang, 2005) and Lu et al. (2016) that synthesized the Ni-Fe layered double hydroxide for methyl orange dye removal (Lu et al., 2016). However, the bimetallic oxide or hydroxide synthesized by them are nanoparticles and are not magnetically separable. Practically, it is not very suitable to be used in real situations.

Nevertheless, the modified activated carbon by the bimetallic oxide or hydroxide will overcome these limitations. The activated carbon porous structure provides a wide medium for the nano-metal oxide or hydroxide particle to coat on the outer surface and forms a layer. As previously discussed, activated carbon itself is a good adsorbent. Hence, by introducing a bilayer nano-metal oxide or hydroxide layers on the activated carbon's outer surface, the modified bimetallic oxide or hydroxide activated carbon will integrate their own unique characteristics and eventually, enhance the adsorption capacity (Kong, Wang, Hu, & Olusegun, 2014).

As this research is focusing towards the magnetically modified palm shell-waste based activated carbon, the Iron Oxide, Fe_2O_3 nanoparticle will be the first layer modifying the activated carbon outer surface, while, the second layer for modification is determined based on the pollutant to be removed.

University of Malaya

i. MPSAC-La

For the removal study, the activated carbon was modified by coating the outer surface with a nano-magnetite, Fe_2O_3 to form a magnetically palm shell-waste based activated carbon and will eventually increase the affinity towards the arsenate ion. Then, the magnetically palm shell-waste based activated carbon was impregnated with Lanthanum oxide or hydroxide. Lanthanum was chosen to be the second layer coating the activated carbon because it is a non-toxic metal (Jang, Park, & Shin, 2004). It is important to identify the toxicity of the metal because the metal impregnated to the activated carbon might leach out during the adsorption treatment process. Lanthanum oxide or hydroxide is capable to remove arsenate at high removal capacities over a wide pH range (Xie et al., 2014; W. Zhang, Fu, Zhang, & Zhang, 2014). Therefore, no specific pH has to be adjusted in order to remove the arsenate at a high capacity. Modifications of the palm shell-waste based activated carbon by the nano-magnetite, Fe_2O_3 and Lanthanum oxide or hydroxide, LO/LH improve the adsorbent characteristic. Whereby, the modified adsorbent will have the capability to be separated easily by using external magnetic field and enhanced capability in arsenate removal.

i. MPSAC-SiO_2@$MgNO_3$

Contrastingly, Methyl Orange and Methylene Blue dyes removal study still remained the magnetically palm shell-waste based activated carbon characteristics, but modified the second layer with silica and finally, coated the silica layer with metal oxide or hydroxide of Magnesium (nitrate salt). Silica is an inorganic material and non-metal but is classified as good stabilizers. It is biocompatible and chemically inert, and does not affect the redox reaction at the core surface (J. Yu, Jiang, Hao, & Liu, 2015). Furthermore, silica provides abundance of silanol group (-OH group) on the silica layer that allows various functional group to be activated on the coated surface (Fisli, Yusuf, Krisnandi, &

University of Malaya

Gunlazuardi, 2014; J. Yu et al., 2015). However, pure silica consists of neutral frame-structure that causes limitations in the cation-exchange capacities and reactivity (Parida, Dash, Patel, & Mishra, 2006; Xu, Chu, & Luo, 2006), which leads several researchers to study the silica modification by introducing metal oxide into the silica. Silica-nano-magnetite has already been synthesized and investigated by Shariati et al. (2014) to remove the methyl orange, while the silica coated magnetic nanocomposite was synthesized and investigated by Yu et al. (2015) to remove methylene blue. However, the adsorption capability results were not significant.

Magnesium oxide or hydroxide has been widely investigated and were used as an adsorbent for various pollutants. It acts as a catalyst and catalyst support for a variety of organic reactions and gives good performance in dye removal (Nga, Hong, Dai Lam, & Huy, 2013). Additionally, Magnesium oxide or hydroxide is a unique oxide with a high ionic character, simple stoichiometry, and can produce crystal structure with a variety of particle sizes and shapes (Fakhri & Adami, 2014). Furthermore, it is also a non-toxic metal, environmentally friendly with a high reactive surface and adsorption capacity (Nga et al., 2013). Previous study showed that pHpzc of MgO is 12.4, which makes it more suitable for anionic dye removal (Crittenden, Howe, Hand, Tchobanoglous, & Trussell, 2012). By integrating three types of adsorbent materials on the surface of activated carbon, the adsorption capacity for methyl orange or methylene blue dyes potentially will have an optimum increment.

University of Malaya

2.8 Equilibrium Isotherm Model

Fundamental physiochemical data provided by the sorption equilibrium was used to evaluate the applicability of sorption processes as a unit of operation. Commonly, sorption equilibrium is described by an isotherm equation, whereby the parameter equation indicates the surface properties and adsorbent affinity at a constant pH and temperature. The accuracy of isotherm model to the experimental equilibrium data is determined based on the coefficient of determination, R2, which is the closest R^2 to unity that will provide the best fit for the isotherm model. The most two common isotherm models usually used are Langmuir and Freundlich models. Langmuir isotherm model tends to give the best fit data for a high concentration experimental data, while Freundlich tends to give the best data for a low concentration experimental data (Ho, Porter, & McKay, 2002).

2.7.1 Langmuir isotherm model

Initially, Langmuir adsorption isotherm model was developed to explain the gas-solid phase adsorption mechanism onto the activated carbon; and this model was applied to analyze the performance of other types of adsorbents (Langmuir, 1916). Basically, Langmuir isotherm equation model explained the monolayer (Vijayaraghavan, Padmesh, Palanivelu, & Velan, 2006) and homogeneous adsorption, whereby each molecules have the constant enthalpies and sorption activation energy (Kundu & Gupta, 2006). It is characterized by a plateau, which is an equilibrium saturation point when the molecules already occupied all the active sites, then no adsorption can occur further (Demirbas, Kobya, & Konukman, 2008).

University of Malaya

The linear form of Langmuir model equation can be expressed as shown below.

The Langmuir equation described as:

$$q_{eq} = \frac{Q_{\max} K_L C_{eq}}{1 + K_L C_{eq}} \tag{2.1}$$

Where q_{eq} is the amount of solute adsorbed per unit weight of the adsorbent (mg g^{-1}), C_{eq} is the equilibrium concentration of solute in the bulk solution (mg L^{-1}), Q_{max} is the maximum adsorption capacity (mg g^{-1}), and K_L is the Langmuir constant related to the energy of adsorption

2.8.2 Freundlich Isotherm model

Assuming that the adsorption is held onto the heterogeneous surface of adsorbent, the Freundlich model is a better fit for the isotherm data. In the Freundlich model, chemisorption and physisorption are applicable to the monolayer and multilayer adsorptions, respectively. Originally, Freundlich isotherm model was developed to describe the animal charcoal adsorption mechanism, where the ratio of adsorbate adsorbed onto the adsorbent in the solute at different concentrations were not constant (Md Ahmaruzzaman, 2008). Conceptually, Freundlich isotherm model characterized the amount of adsorbate adsorbed as the total adsorption on all sites, with a stronger binding sites are occupied first until the adsorption energy exponentially decreased upon the completion of adsorption process (Zeldowitsch, 1934).

The linear form of the Freundlich equation is expressed as:

$$\log q_{eq} = \log K_F + \frac{1}{n} \log C_{eq} \tag{2.2}$$

Where K_F and n are the Freundlich isotherm constants related to the adsorption capacity and adsorption intensity, respectively.

University of Malaya

2.9 Adsorption Kinetic Model

Adsorption kinetic model was used to estimate the sorption rate and to determine the possible reaction mechanisms happened (Robati, 2013). Several kinetic models, including the pseudo first order kinetic model, pseudo second order kinetic model, and intra particle diffusion model were used for these studies.

2.8.1 Pseudo first order kinetic model

Lagergren et al. (1898) developed the pseudo first order kinetic model for the sorption study of oxalic acid and malonic acid onto charcoal (Lagergren, 1898). The earliest application of the pseudo first order kinetic model was to investigate the sorption of cellulose triacetate from the chloroform onto calcium silicate (Trivedi, Patel, & Patel, 1973).

Generally, the pseudo first order equation of Lagergren (Lagergren, 1898) is expressed as:

$$\frac{dq_t}{dt} = k_1(q_e - q_t) \tag{2.3}$$

Where q_e and q_t are the equilibrium sorption capacity and at time, t respectively (mg g^{-1}). K1 is the rate constant (l min^{-1}). The integration of equation brings the equation into:

$$\log(q_e - q_t) = \log(q_e) - \frac{k_1}{2.303}t \tag{2.4}$$

The parameter k_1 (qe –qt) does not represent the number of available sites. The parameter log (qe) is an adjustable parameter and always found not equal to the intercept of plot log (qe –qt) vs t, whereby in a true first order log (qe) must be equal to the intercept of a plot of log (qe-qt) vs t (Y. Ho & G. McKay, 1998).

University of Malaya

2.9.2 Pseudo second order kinetic model

The earliest application of the pseudo second order kinetic model in the solid or liquid systems was used to explain the reaction mechanism between soils and minerals (Griffin & Jurinak, 1974; Kuo & Lotse, 1972)

The pseudo second-order kinetic model is based on the equilibrium adsorption is expressed as (Y. S. Ho & G. McKay, 1998):

$$\frac{t}{q_t} = \frac{1}{K_2 q_{eq}^2} + \frac{t}{q_{eq}} \tag{2.5}$$

where q_e (mg g^{-1}) and q_t (mg g^{-1}) are the amount of adsorbate adsorbed at equilibrium and specific time, respectively. And, K_1 (min^{-1}) and K_2 [g (mg $min)^{-1}$] are the rate constant of the pseudo first-order and the pseudo second-order kinetic models, correspondingly.

2.8.3 Intra particle diffusion model

Weber and Morris has developed the intra particle diffusion model in the year 1962 (W. Weber & Morris; W. J. Weber & Morris, 1963).

The IPD kinetic model can be formulated by:

$$q_t = k_i t^{0.5} + C \tag{2.6}$$

where k_i [(mg g^{-1} $min^{-1/2}$)] is the intraparticle rate constant.

Multi linearity in q_t against $t^{0.5}$ plot is considered as there are two or three steps involved in the reaction process (Sun & Yang, 2003). The first step indicates the external surface adsorption or instantaneous adsorption occurred, following by the second step that indicates the gradual adsorption where the intra particle diffusion acts as the

University of Malaya

controlling step and the third step is indicated as the final equilibrium step, where slow movement of solute from mesopore or macropore into micropores occurred (F.-C. Wu, Tseng, & Juang, 2009).

University of Malaya

CHAPTER 3: MATERIALS AND METHODOLOGY

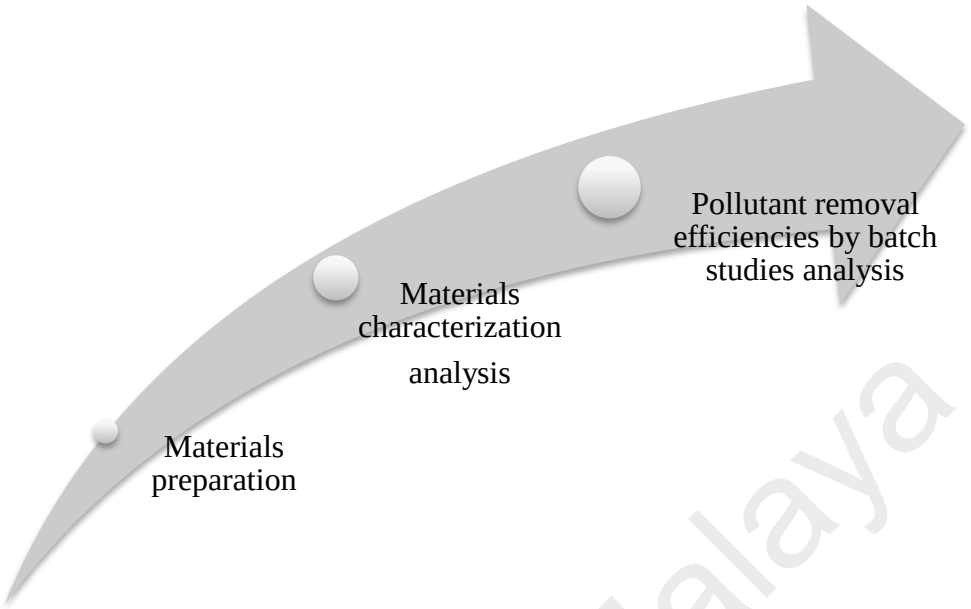

3.1 Materials

The Palm Shell Waste-Based Activated Carbon Adsorbents (PSAC) (75-150 µm) was purchased from Bravo Green Sdn. Bhd., Kuching, Malaysia. The PSAC was used as a host material for:

a) Nano–magnetite and La (hydr) oxide to remove arsenate, whereby Fe (II) Sulfate Heptahydrate ($FeSO_4 \cdot 7H_2O$), La (III) Chloride Heptahydrate ($LaCl_3 \cdot 7H_2O$), and Sodium Hydroxide (NaOH) were used for material preparation, while Sodium arsenate Heptahydrate ($Na_2HAsO_4 \cdot 7H_2O$) was used for arsenate stock solution to simulate the polluted water containing arsenate. Dilute HCl and NaOH were used for pH adjustments. All chemical solutions were purchased from R&M Chemical.

b) Nano-magnetite, Silica and $MgNO_3$ were used to remove the Methyl Orange and Methylene Blue dyes, whereby Fe (II) Sulfate Heptahydrate ($FeSO_4 \cdot 7H_2O$), Sodium Hydroxide (NaOH), Sodium silicate, (Na_2SiO_3), Magnesium Nitrate Hexahydrate ($Mg(NO_3)_2.6H_2O$) were used for material preparations. Methyl

University of Malaya

Orange (MO) and Methylene Blue dye (MB) were used for Methyl Orange and Methylene Blue dyes stock solution. Dilute HCl and NaOH were used for pH adjustments. All chemical solutions were purchased from R&M Chemical.

3.2 Equipment

a) Material preparation and sample analysis

An oven (Memmert Laboratory Oven) was used for drying purposes and for heating samples up to 160^{o}c. However, muffled furnace (Dae Heung Science, Korea) was used when higher temperature is needed. The Ultrasonic Cleaning Bath (E120H, Elmasonic E) was used for the preparation of material for Arsenic removal. An orbital shaker (SK-300, Lab Companion) was used for all batches of test experiments. The pH measurement was taken using Bante920 Benchtop pH/ORP/°C/°F meter and the Inductively Coupled Plasma Optical Emission Spectrometry (ICP–OES, Optima 5300V, Perkin Elmer) was used to determine the Arsenic (As), Iron (Fe), Lanthanum (La) ion concentration. The concentration of Methyl Orange and Methylene Blue dyes were determined by using the UV-visible spectrometer (Spectroquant® Pharo300).

b) For characterization analysis

Morphological changes of adsorbent particles were examined using the field emission scanning electron microscopy (FESEM, FEG Quanta 450, EDX–OXFORD). X–ray powder diffraction (XRD, PANalytical, EMPYREAN) was used to verify the presence and the type of element over a range of 20° to 80°. Texture characterization was performed on the N_2 adsorption–desorption isotherm, which was obtained at 77 K using the TriStar II 3020 (Micrometrics®, USA). The specific surface area and the pore specific volume were measured by the Brunauer–Emmett–Teller (BET) method, whereas the pore

University of Malaya

diameter and pore size distribution were determined by the Barret–Joyner–Halenda (BJH) method. Fourier transform infrared spectroscopy (FTIR, Perkin Elmer, FTIR–spectrum 400) was carried out to analyze the changes in the functional group on the oxide surfaces, as well as the structural stability of the materials. The pH of the point of zero charge (pH_{PZC}) were determined using a pH drift method (Lopez-Ramon, Stoeckli, Moreno-Castilla, & Carrasco-Marin, 1999) with a 0.1 M NaCl solution at pH 2~12 (± 0.1). The pH_{pzc} of the adsorbent was determined by plotting the graph of the initial pH against the change in pH ($pH_{final} - pH_{initial}$).

3.3 Materials Preparation

3.3.1 Preparation of Lanthanum and Nano-Magnetite Composite Incorporated Palm Shell Waste-Based Activated Carbon (MPSAC-Las)

a) Preparation of Magnetized Palm Shell Waste–Based Activated Carbon (MPSAC)

Hydrothermal wetness impregnation method

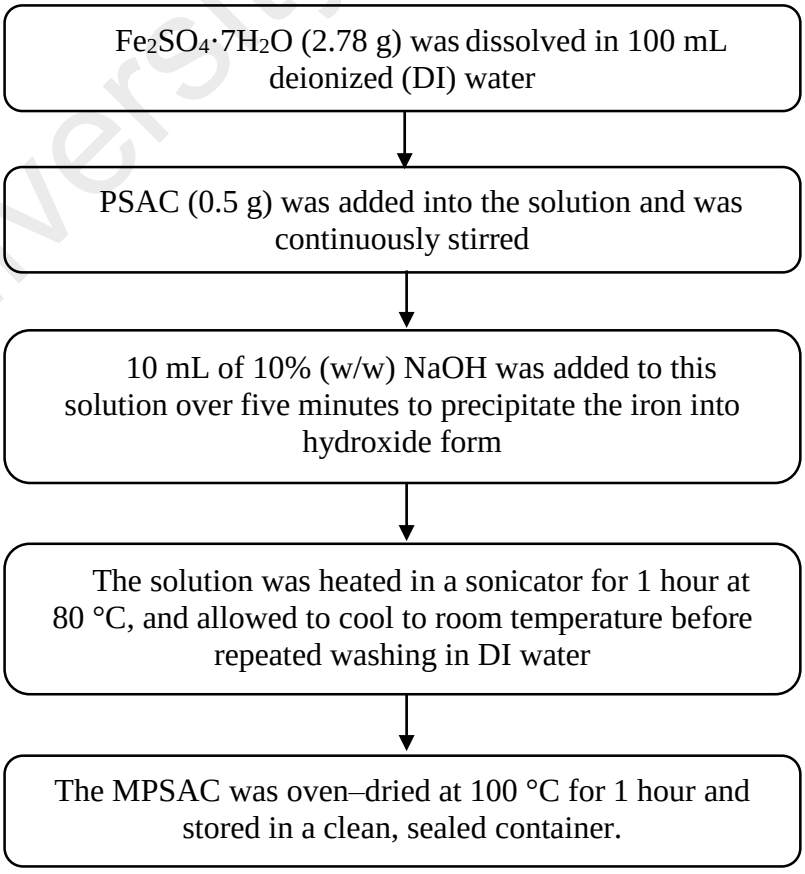

University of Malaya

b) Preparation of lanthanum impregnated MPSAC (MPSAC-Las)

Hydrothermal wetness impregnation method

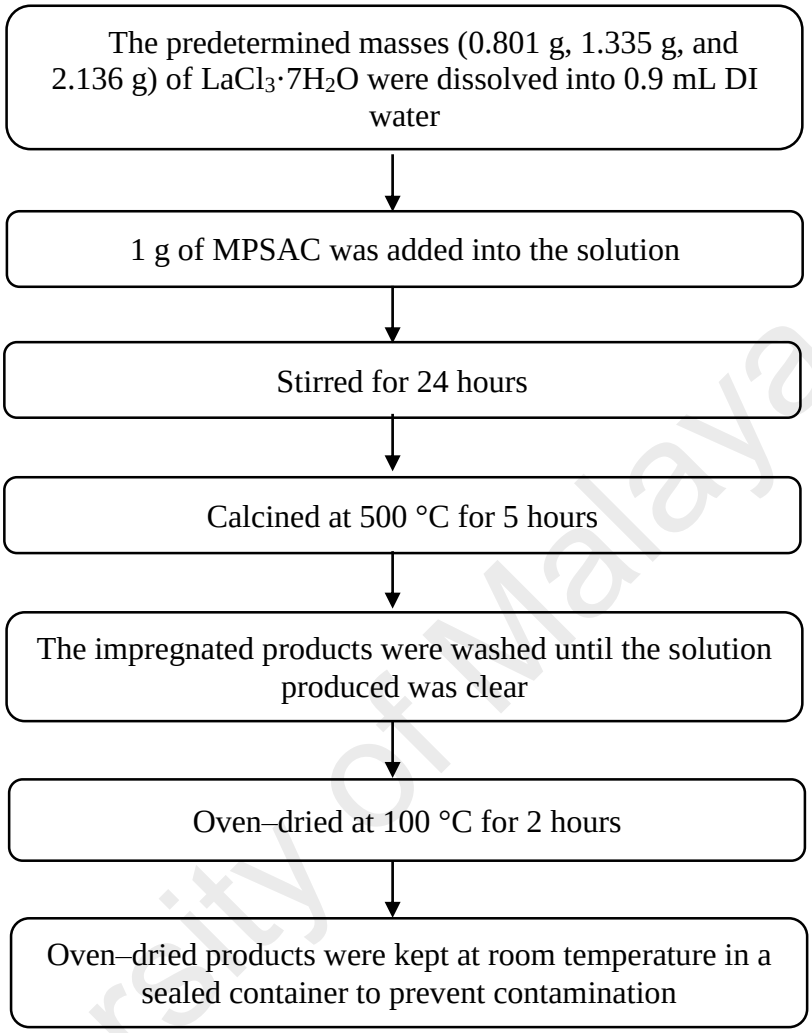

Aqua–regia extraction was added to determine the volume of Fe and La in the MPSAC–La. The weight ratios of La to Fe were 0.084, 0.23, 0.28, and 0.36, which were designated as MPSAC–La (0.084), MPSAC–La (0.23), MPSAC–La (0.28), and MPSAC–La (0.36), respectively.

University of Malaya

3.3.2 Preparation of $MgNO_3$-SiO_2 incorporated into nano-magnetite Palm Shell Waste-Based Activated Carbon

a) Preparation of Magnetic Palm Shell Waste–Based Activated Carbon (MPSAC)

Film coating method

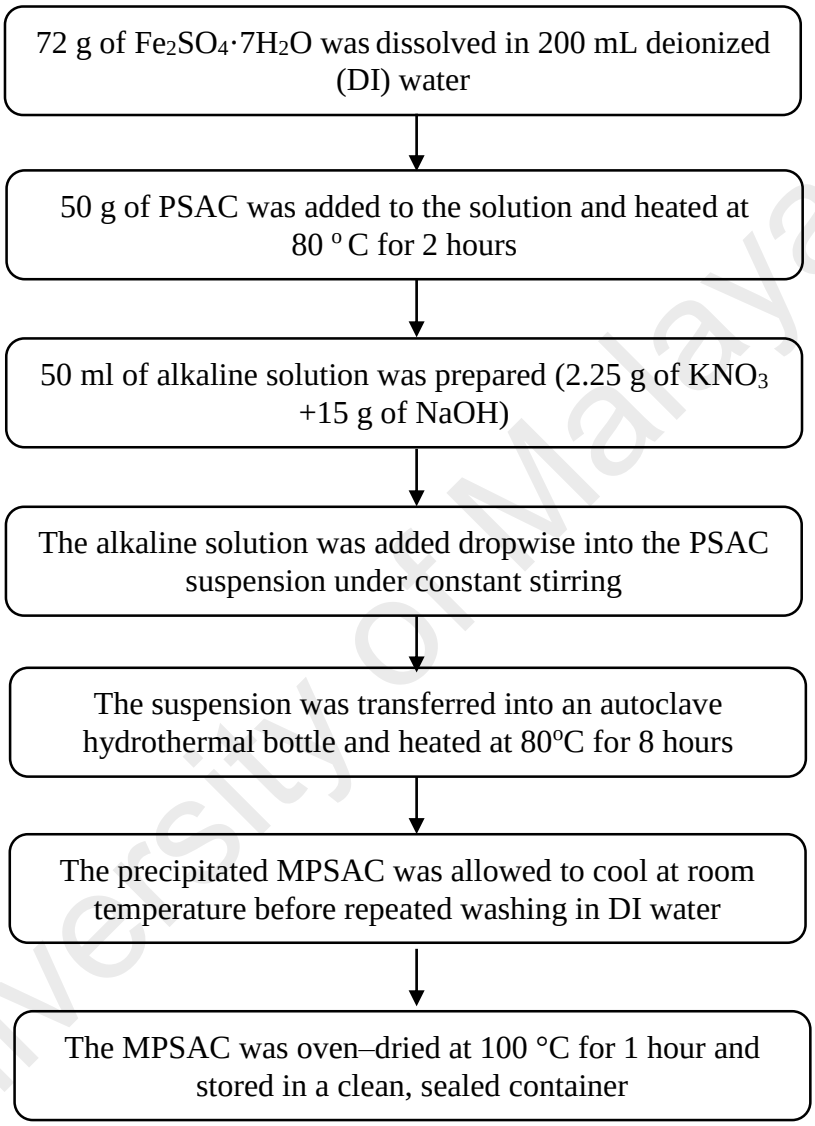

University of Malaya

b) Preparation of Silica coated Magnetic Palm Shell Waste–Based Activated Carbon (MPSAC-SiO_2)

Co-precipitation method

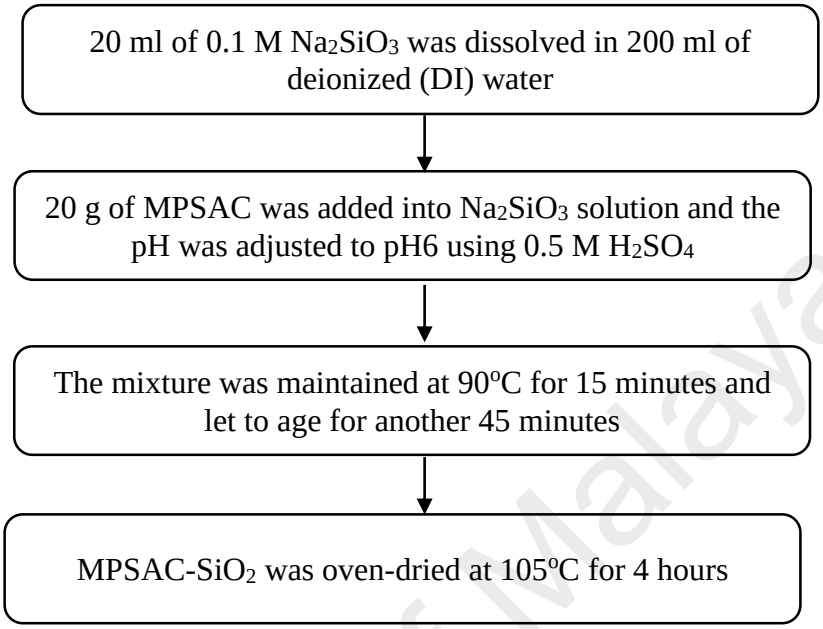

c) Preparation of MPSAC-SiO_2@$MgNO_3$

Hydrothermal method

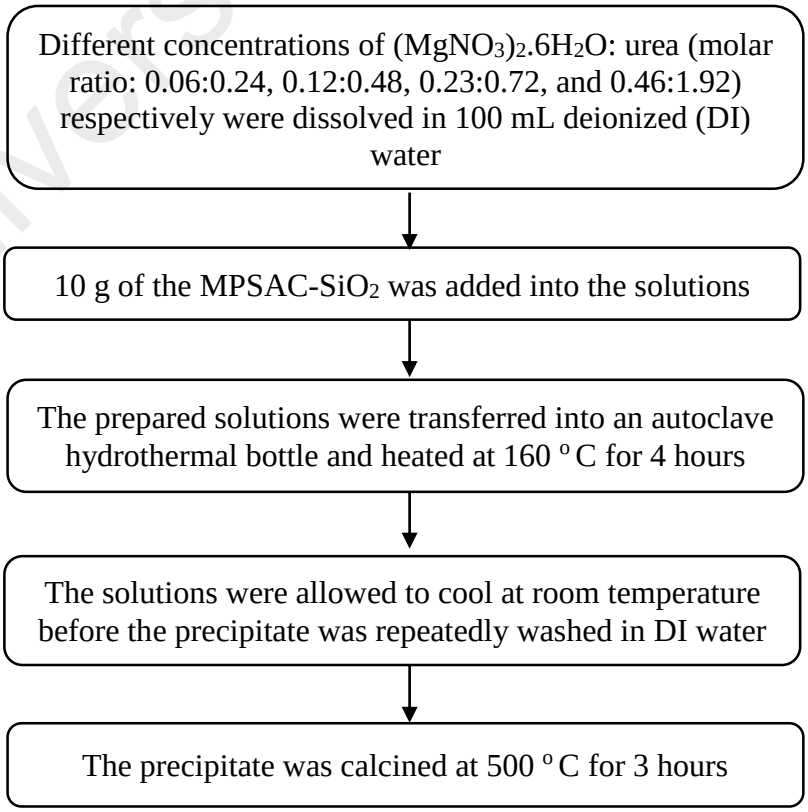

University of Malaya

3.4 Arsenic removal batch adsorption experiments

3.4.1 Adsorption isotherms

Arsenate stock solution (1,000 mg L^{-1}) was prepared by dissolving 4.165 g of $Na_2HAsO_4 \cdot 7H_2O$ into 1 L DI water. Then, AC, MPSAC, MPSAC-La (0.08), MPSAC-La (0.16), MPSAC-La (0.32) and MPSAC-La (0.64) adsorbents (0.025 g) respectively were added to 25 mL arsenate solution (with a concentration between 10 mg L^{-1} and 350 mg L^{-1}) in a 50 mL centrifuge tube. The initial pH of the solution was adjusted to pH 6 ± 0.1 and final pH was measured. The conical flasks were agitated on an orbital shaker for 24 hours at 150 rpm and room temperature (26 ± 1°C). After 24 hours, the final pH was measured and 10 mL of the suspension was filtered out using a 0.45 µm–pore filter, and the arsenate concentration of the filtrate was analyzed using the inductively coupled plasma optical emission spectrometry (ICP–OES, Optima 5300V, Perkin Elmer).

The equilibrated adsorption capacity was calculated using the following equation:

$$Q_{eq} = (C_0 - C_{eq}) \times \frac{V}{M}, \tag{3.1}$$

where, Q_{eq}, C_o, and C_{eq} are the adsorption capacity (mg g^{-1}), initial concentration (mg L^{-1}), and final concentration (mg L^{-1}), respectively. V and M are the volume of the solution (L) and mass of adsorbent (g), respectively. The isotherm data were well–fitted using the Langmuir and Freundlich isotherm models.

University of Malaya

3.4.2 Adsorption kinetics

Arsenate stock solution (1,000 mg L^{-1}) was prepared by dissolving 4.165 g of $Na_2HAsO_4 \cdot 7H_2O$ into 1 L DI water. Then, MPSAC and MPSAC-La (0.64) adsorbents (0.025 g) respectively (0.5 g) was added to 500 mL arsenate solution with an initial concentration, 350 mg L^{-1} in 1 L conical flask. The pH and solution temperature were maintained at pH 6 ± 0.1 and 26 ± 1°C, and the conical flask was shaken at 150 rpm for 5 hours. At predetermined intervals, 5 mL of the sample suspensions were filtered out using a 0.45 µm–pore filter, and the arsenate concentration of the filtrate was analyzed using the inductively coupled plasma optical emission spectrometry (ICP–OES, Optima 5300V, Perkin Elmer).

The equilibrated adsorption capacity was calculated using the following equation:

$$Q_{eq} = (C_0 - C_{eq}) \times \frac{V}{M}, \tag{3.2}$$

where, Q_{eq}, C_o, and C_{eq} are the adsorption capacity (mg g^{-1}), initial concentration (mg L^{-1}), and final concentration (mg L^{-1}), respectively. V and M are the volume of the solution (L) and mass of adsorbent (g), respectively. All of the kinetic data were fitted using the pseudo–second order kinetic and intra particle diffusion models.

University of Malaya

3.4.3 pH effects

Arsenate stock solution (1,000 mg L^{-1}) was prepared by dissolving 4.165 g of $Na_2HAsO_4 \cdot 7H_2O$ into 1 L DI water. Then, MPSAC and MPSAC-La (0.64) adsorbents (0.025 g) respectively were added to 25 mL of arsenate solution with a concentration 350 mg L^{-1} in a 50 mL centrifuge tube. The initial pH of the solutions was adjusted to pH 2 to pH 10 with interval of pH 1. The conical flasks were agitated on an orbital shaker for 24 hours at 150 rpm and room temperature (26 ± 1°C). After 24 hours, the final pH for each solution with different pH were measured and 10 mL of the suspension was filtered out using a 0.45 µm–pore filter, and the arsenate concentration of the filtrate was analyzed using the inductively coupled plasma optical emission spectrometry (ICP–OES, Optima 5300V, Perkin Elmer).

The equilibrated adsorption capacity was calculated using the following equation:

$$Q_{eq} = (C_0 - C_{eq}) \times \frac{V}{M}, \tag{3.3}$$

where, Q_{eq}, C_o, and C_{eq} are the adsorption capacity (mg g^{-1}), initial concentration (mg L^{-1}), and final concentration (mg L^{-1}), respectively. V and M are the volume of the solution (L) and mass of adsorbent (g), respectively. All of the pH data were recorded and presented as the graph of arsenate adsorption capacity (mg g^{-1}) versus final pH.

University of Malaya

3.4.4 Temperature effect

Arsenate stock solution (1,000 mg L^{-1}) was prepared by dissolving 4.165 g of $Na_2HAsO_4 \cdot 7H_2O$ into 1 L DI water. Then, MPSAC and MPSAC-La (0.64) adsorbents (0.025 g) respectively (0.5g) was added to 500 mL arsenate solution with an initial concentration of 350 mg L^{-1} in 1 L conical flask. Three sets of solution were prepared and for each set, the pH and solution temperature were maintained at pH 6 ± 0.1 and the solution temperatures were set to 288 K, 298 K, and 308 K respectively. The conical flask was shaken at a rate of 150 rpm for 5 hours. At predetermined intervals, 5 mL sample suspensions were filtered out using a 0.45 µm–pore filter, and the arsenate concentration of the filtrate was analyzed using the inductively coupled plasma optical emission spectrometry (ICP–OES, Optima 5300V, Perkin Elmer).

The equilibrated adsorption capacity was calculated using the following equation:

$$Q_{eq} = (C_0 - C_{eq}) \times \frac{V}{M}, \tag{3.4}$$

where, Q_{eq}, C_o, and C_{eq} are the adsorption capacity (mg g^{-1}), initial concentration (mg L^{-1}), and final concentration (mg L^{-1}), respectively. V and M are the volume of the solution (L) and mass of adsorbent (g), respectively. All of the temperature data were recorded and presented as the graph of arsenate adsorption capacity (mg g^{-1}) versus final pH. Then, the kinetic data were fitted into the pseudo-second order kinetic model and thermodynamic model studies.

University of Malaya

3.4.5 Competition effects

Arsenate stock solution (1,000 mg L^{-1}) was prepared by dissolving 4.165 g of $Na_2HAsO_4 \cdot 7H_2O$ into 1 L DI water. Then, MPSAC and MPSAC-La (0.64) adsorbents (0.03 g) were added into the arsenate solution (30 mL), with initial concentration of 50 mg L^{-1} and 350 mg L^{-1} in a 50 mL centrifuge tube. Sodium salts (2.5 mmol L^{-1} of NO_3^-, Cl^-, HCO_3^-, or SO_4^{2-}) were also added to the solution. As a reference, a set of arsenate solutions without competing anions was also prepared to compare the sorption capacities. The pH and solution temperatures were maintained at pH 6 ± 0.1 and 26 ± 1°C, respectively. The suspensions were then agitated at 150 rpm for 24 hours.

After 24 hours, the final pH was measured and 10 mL of the suspension was filtered out using a 0.45 µm–pore filter, and the arsenate concentration of the filtrate was analyzed using the inductively coupled plasma optical emission spectrometry (ICP–OES, Optima 5300V, Perkin Elmer).

The equilibrated adsorption capacity was calculated using the following equation:

$$Q_{eq} = (C_0 - C_{eq}) \times \frac{V}{M}, \tag{3.5}$$

where, Q_{eq}, C_o, and C_{eq} are the adsorption capacity (mg g^{-1}), initial concentration (mg L^{-1}), and final concentration (mg L^{-1}), respectively. V and M are the volume of the solution (L) and mass of adsorbent (g), respectively. Then, the competition effect data were presented as the graph of arsenate adsorption capacity (mg g^{-1}) versus solution containing the competing anion.

University of Malaya

3.5 Regeneration

Three cycles of adsorption and desorption were carried out to investigate the reusability of MPBAC–La (0.36) that exhibited the highest sorption capacity in previous tests. The adsorption tests were carried out using a 0.2 g of adsorbent in a 350 mg L^{-1} arsenate solution. The suspensions were agitated for 24 hours at 150 rpm. The adsorbents were separated from the solution using a magnet and dried at 105°C for 1 hour. The adsorption capacity was measured for each cycle. Desorption tests were conducted by stirring the dried adsorbent into a 100 mL NaOH solution (0.5 M) at 150 rpm for 6 hours. Then, the adsorbents were washed with distilled water and dried in a vacuum oven under the same conditions as described above prior to the re–adsorption tests.

3.6 Characterization analysis

The X-ray diffraction spectra for AC, MPSAC, MPSAC-La (0.28), MPSAC-La (0.36) before and after adsorption test were obtained using the X-ray diffractometer with Cu K radiation at 40 kV and 50 mA to determine the present phases (amorphous or crystalline). The spectra were recorded from 20^o to 80^o at a scan rate of 1.2^o min^{-1}. Fourier Transform Infrared (FT-IR) spectra of the adsorbents were recorded in the range of 500-4000 cm-1 on an FT-IR system to investigate the positions and numbers of the functional groups that are available for the adsorbates binding. The surface morphology of the adsorbents was visualized via a Field Emission Scanning Electron Microscope (FESEM) operated at the accelerating voltafe of 20 keV and elemental mapping under high resolutions via the Energy Dispersive X-ray. The Burnauer-Emmett-Teller (BET) surface area (S_{BET}), and pore structural of the adsorbents was detected using the Micrometrics (TriStar II 3020) Surface Area and Porosity Analyzer. All the adsorbent samples were de-gassed at 200°C for 4 hours, prior to adsorption-desorption experiments. The BET surface area was calculated by the Brunauer-Emmett-Teller (BET) equation, micropore volume (Vmi) and

University of Malaya

micropore specific area (Smi) were obtained using the t-plot. The total pore volume (Vt) was obtained by converting the nitrogen adsorption amount at a relative preassure (P/PO) of 0.98 to the liquid nitrogen volume. The mesopore volume (Vme) was calculated by subtracting Vmi from Vt. The burn-off weight percentage, Pb for SAS was determined and was used to measure the degree of activation process. It is defined as the ratio of percentage weight loss of the material during the preparation to the original weight of the raw material. It is mathematically expressed as:

$$p_b = \frac{w_o - w_f}{w_o} x100 \tag{3.6}$$

University of Malaya

3.7 Dye removal batch adsorption experiments

3.7.1 Adsorption isotherms

Dye (Methylene Blue [MB] and Methyl Orange [MO]) stock solution (1,000 mg L^{-1}) was prepared by dissolving 0.5 g of the MB and MO into 0.5 L DI water. PSAC, MPSAC-SiO_2@$MgNO_3$(0.06), MPSAC-SiO_2@$MgNO_3$ (0.12), MPSAC-SiO_2@$MgNO_3$ (0.23) and MPSAC-SiO_2@$MgNO_3$ (0.46) adsorbents (0.03 g) were added to 30 mL dye solution (with a concentration between 50 mg L^{-1} and 1000 mg L^{-1}) in a 50 mL centrifuge tube respectively. The initial pH of the solution was adjusted to pH 6 ± 0.1 and the final pH was measured. The conical flasks were agitated on an orbital shaker for 24 hours at 200 rpm and room temperature (26 ± 1°C). After 24 hours, the final pH was measured and the final concentration for both MB and MO were determined by a UV–visible spectrophotometer (Spectroquant® Pharo300) at an absorbance wavelength of 655 nm for MB and 464 nm for MO. The equilibrated adsorption capacity was calculated using the following equation:

$$Q_{eq} = (C_0 - C_{eq}) \times \frac{V}{M}, \tag{3.7}$$

where, Q_{eq}, C_o, and C_{eq} are the adsorption capacity (mg g^{-1}), initial concentration (mg L^{-1}), and final concentration (mg L^{-1}), respectively. V and M are the volume of the solution (L) and mass of adsorbent (g), respectively. The isotherm data were well–fitted using the Langmuir and Freundlich isotherm models that are explained further in the next section.

University of Malaya

3.7.2 Adsorption kinetics

Dye (Methylene Blue (MB) (500 mg L^{-1}) and Methyl Orange (MO) (1,300 mg L^{-1}) stock solution was prepared by dissolving 0.5 g of MB and 0.75 g of MO into 0.5 L DI water. PSAC and MPSAC-SiO_2@$MgNO_3$ (0.46) adsorbents were added in a 1 L conical flask with 500 mL dye solution (500mg L^{-1} initial concentration for MB and 1300 mg L^{-1} for MO). The pH and solution temperature were maintained at pH 6 ± 0.1 and 26 ± 1°C, and the conical flask was shaken at a rate of 200 rpm for 8 hours. At predetermined intervals, 5 mL of the sample suspensions were taken out and measured using the UV–visible spectrophotometer (Spectroquant® Pharo300) at an absorbance wavelength of 655 nm for MB and 464 nm for MO.

The equilibrated adsorption capacity was calculated using the following equation:

$$Q_{eq} = (C_0 - C_{eq}) \times \frac{V}{M}, \tag{3.8}$$

where, Q_{eq}, C_o, and C_{eq} are the adsorption capacity (mg g^{-1}), initial concentration (mg L^{-1}), and final concentration (mg L^{-1}), respectively. V and M are the volume of the solution (L) and mass of adsorbent (g), respectively. All of the kinetic data were fitted using pseudo–second order kinetic and intra particle diffusion models.

University of Malaya

3.7.3 pH effects

Dye (Methylene Blue (MB) (500 mg L^{-1}) and Methyl Orange (MO) (1,300 mg L^{-1}) stock solution was prepared by dissolving 0.5 g of MB and 0.75 g of MO into 0.5 L DI water. PSAC and MPSAC-SiO_2@$MgNO_3$ (0.46) adsorbents were added in a 1 L conical flask with 500 mL dye solution (500mg L^{-1} initial concentration for MB and 1300 mg L^{-1} for MO). The initial pH of the solutions was adjusted to pH 2 to pH 10 with interval of pH 1. The conical flasks were agitated on an orbital shaker for 24 hours at 200 rpm and room temperature (26 ± 1°C). After 24 hours, the final solution of the pH was recorded, and the remaining dye concentrations were measured. At predetermined intervals, 5 mL of the sample suspensions were taken out and measured using the UV–visible spectrophotometer (Spectroquant® Pharo300) at an absorbance wavelength of 655 nm for MB and 464 nm for MO.

The equilibrated adsorption capacity was calculated using the following equation:

$$Q_{eq} = (C_0 - C_{eq}) \times \frac{V}{M}, \tag{3.9}$$

where, Q_{eq}, C_o, and C_{eq} are the adsorption capacity (mg g^{-1}), initial concentration (mg L^{-1}), and final concentration (mg L^{-1}), respectively. V and M are the volume of the solution (L) and mass of adsorbent (g), respectively. All of the pH data were recorded and presented as the graph of MB and MO adsorption capacity (mg g^{-1}) versus the final pH.

University of Malaya

3.7.4 Ionic Strength

Dye (Methylene Blue (MB) (500 mg L^{-1}) and Methyl Orange (MO) (1,300 mg L^{-1}) stock solution was prepared by dissolving 0.5g of MB and 0.75g of MO into 0.5 L DI water respectively. 0.5 g of PSAC and MPSAC-SiO_2@$MgNO_3$ (0.46) adsorbents were added in a 1 L conical flask with 500 mL of the dye solution (500mg L^{-1} initial concentration for MB and 1300 mg L^{-1} for MO).

Sodium Chloride (NaCl) at different initial concentrations (0.1M-0.5M) were added to the solution. As a reference, a set of MB and MO solutions without NaCl were also prepared to compare sorption capacities. The pH and solution temperatures were maintained at pH 6 ± 0.1 and 26 ± 1°C, respectively. The suspensions were then agitated at 200 rpm for 24 hours. After 24 hours, the final pH was measured and the final concentration for MB and MO were determined by a UV–visible spectrophotometer (Spectroquant® Pharo300) at an absorbance wavelength of 655 nm for MB and 464 nm for MO. The equilibrated adsorption capacity was calculated using the following equation:

$$Q_{eq} = (C_0 - C_{eq}) \times \frac{V}{M}, \tag{3.10}$$

where, Q_{eq}, C_o, and C_{eq} are the adsorption capacity (mg g^{-1}), initial concentration (mg L^{-1}), and final concentration (mg L^{-1}), respectively. V and M are the volume of the solution (L) and mass of adsorbent (g), respectively.

University of Malaya

3.8 Regeneration

Four cycles of the adsorption-desorption were carried out to investigate the reusability of MPSAC-SiO_2@$MgNO_3$ (0.46) that exhibited the highest sorption capacity in previous tests. The adsorption tests were carried using 0.6 g of adsorbent in a 1300 mg L^{-1} MO solution. The suspensions were agitated for 24 hours at 200 rpm. The adsorption capacity was measured for each cycle. The adsorbents were separated from the solution using a magnet and desorption tests were conducted by washing the used adsorbent using distilled water until the orange color is lessen. Then, the washed adsorbent was oven-dried at 105°C for 1 hour followed by the calcination at 500˚C for 2 hours. Lastly, re-adsorption test was conducted.

3.9 Characterization analysis

The X-ray diffraction spectra for PSAC, MPSAC, and MPSAC-SiO_2@$MgNO_3$ (0.46) before and after adsorption test were obtained using the X-ray diffractometer with Cu K radiation at 40 kV and 50 mA to determine the present phases (amorphous or crystalline). The spectra were recorded from 20^o to 80^o at a scan rate of 1.2^o min^{-1}. Fourier Transform Infrared (FT-IR) spectra of the adsorbents were recorded in the range of 500-4000 cm-1 on an FT-IR system to investigate the positions and numbers of functional groups available for the adsorbates binding. The surface morphology of the adsorbents was visualized via a Field Emission Scanning Electron Microscope (FESEM) operated at the accelerating voltafe of 20 keV and elemental mapping under high resolutions via the Energy Dispersive X-ray. The Burnauer-Emmett-Teller (BET) surface area (S_{BET}) and pore structural of the adsorbents were detected using the Micrometrics (TriStar II 3020) Surface Area and Porosity Analyzer. All of the adsorbent samples were de-gassed at 200°C for 4 hours, prior to adsorption-desorption experiments. The BET surface area was calculated by the Brunauer-Emmett-Teller (BET) equation, micropore volume (Vmi) and

University of Malaya

micropore specific area (Smi) were obtained using the t-plot. The total pore volume (Vt) was obtained by converting the nitrogen adsorption amount at a relative pressure (P/PO) of 0.98 to the liquid nitrogen volume. The mesopore volume (Vme) was calculated by subtracting the Vmi from Vt. The burn-off weight percentage, Pb for SAS was determine and it measures the degree of activation process. It is defined as the ratio of percentage weight loss of the material during preparation of the original weight of the raw material. It is mathematically expressed as:

$$p_b = \frac{w_o - w_f}{w_o} x100 \tag{3.11}$$

University of Malaya

CHAPTER 4: RESULTS & DISCUSSION

Chapter summary

This chapter was divided based on the removal studies, Sub-Chapter 4.1 – Sub-Chapter 4.7 are the results and discussions of the batch experimental and characterization analysis on the arsenate removal studies, while Sub-Chapter 4.8 – Sub-Chapter 4.13 are the results and discussions of the batch experimental and characterization analysis on the Methyl Orange and Methylene Blue dyes removal.

University of Malaya

4.1 Arsenate isotherms Studies

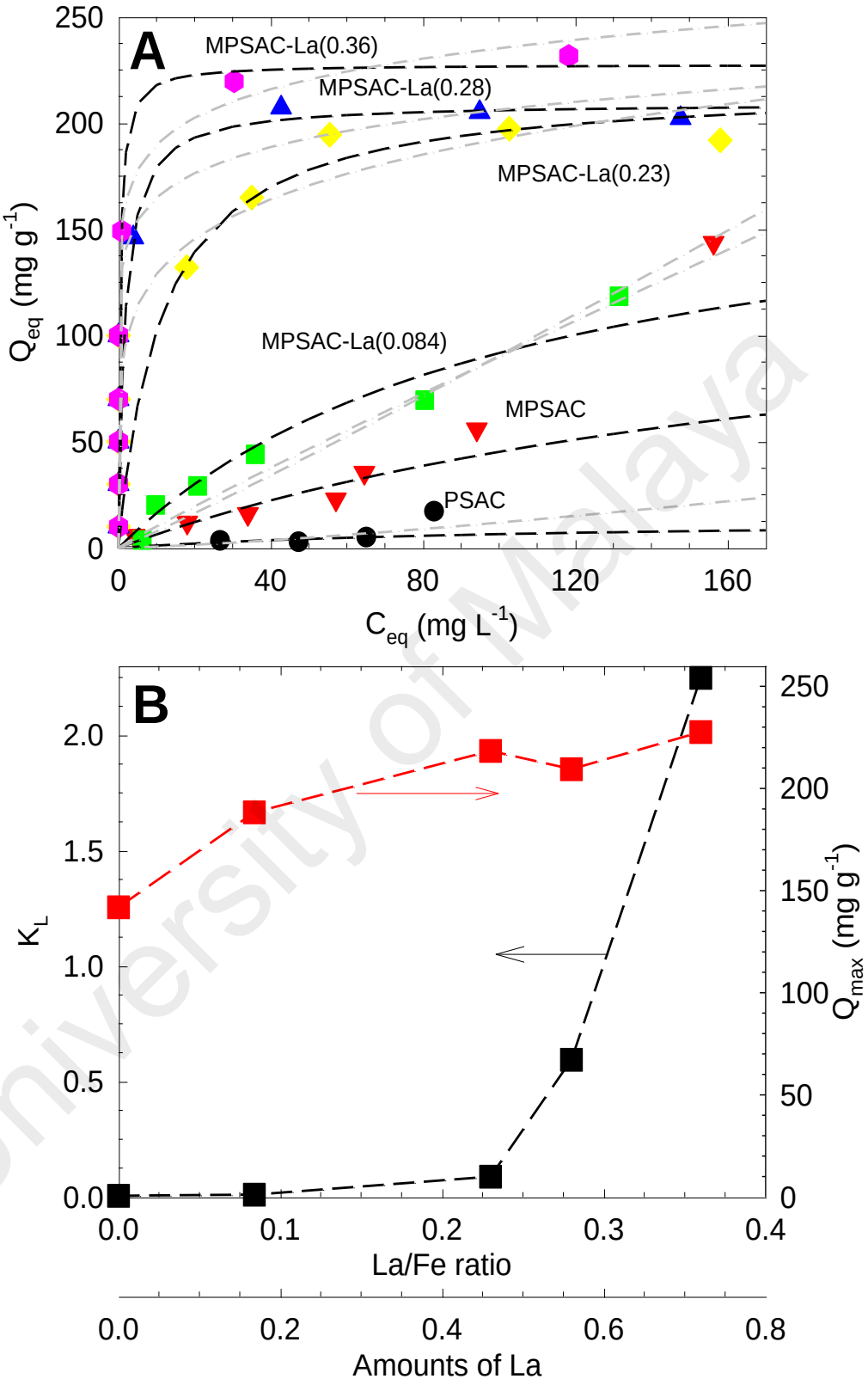

Figure 4.1 (A) Adsorption isotherm of arsenate on the PSAC, MPSAC and MPSAC impregnated with different amounts of lanthanum at pH 6, C_i = 10 ~ 350 mg L^{-1} and 1 g L^{-1} of adsorbent. Black color fit lines are the Langmuir and gray color fit lines are the Freundlich isotherm model (B) Q_{max} and K_L values vs. the ratio of La/Fe or the amounts of La.

University of Malaya

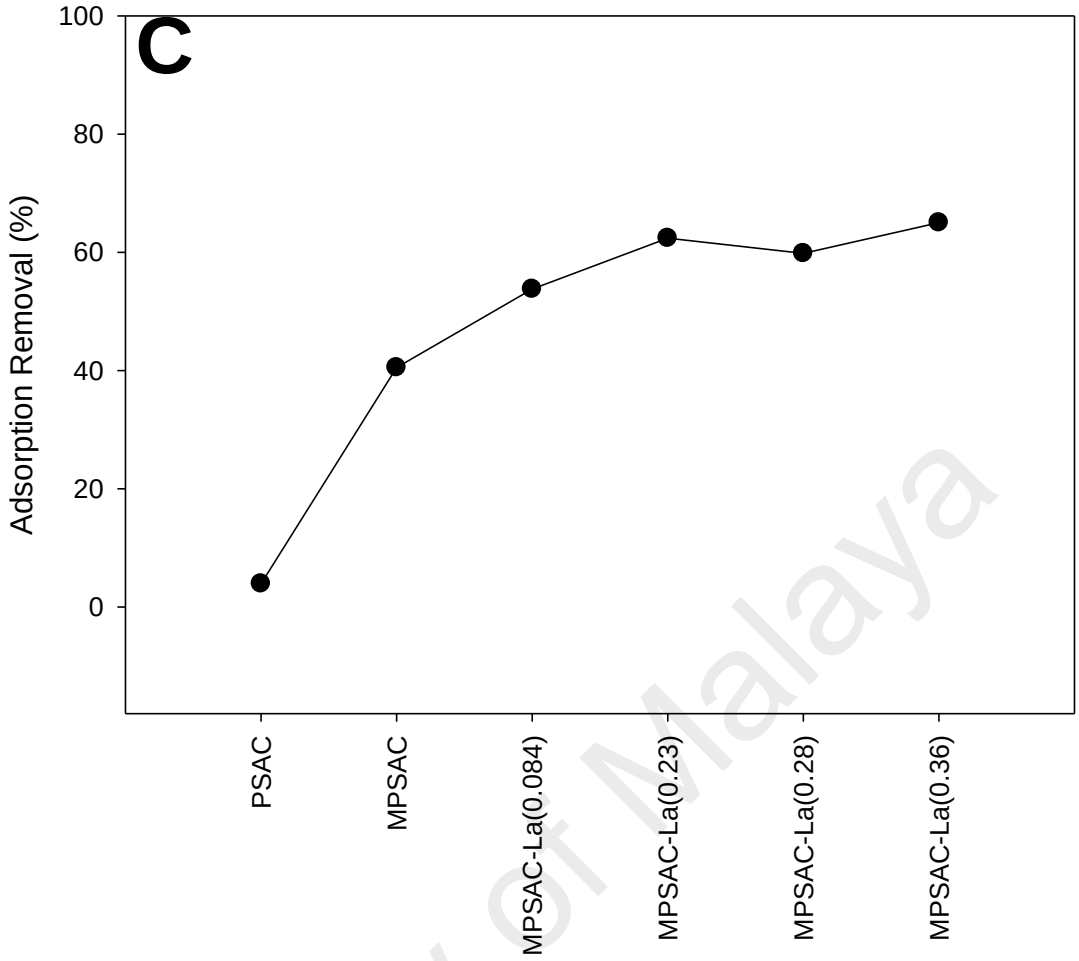

Figure 4.1 (C) Percentage removal of arsenate removal

The arsenate adsorption isotherms for the various samples at the initial arsenate concentrations (10 mg L^{-1} to 350 mg L^{-1}) are illustrated in Figure 4.1(A)., which showed that the samples had different adsorption trends. At 90 mg L^{-1} of C_{eq}, PSAC, MPSAC, and MPSAC–La (0.084) achieved approximately 20 mg g^{-1}, 40 mg g^{-1}, and 70 mg g^{-1} adsorption capacities (q_{eq}), respectively. At the same point of C_{eq}, MPSAC–La (0.23), MPSAC–La (0.28), and MPSAC–La (0.36) had adsorption capacities of 170 mg g^{-1}, 190 mg g^{-1}, and 220 mg g^{-1}, respectively.

Isotherm data were fitted using two isotherm models; Langmuir and Freundlich. Table 4.1 shows that Langmuir represented the isotherm data more accurately (except for PSAC), because its determination coefficients ($R^2 > 0.92$) were higher than those R^2 (> 0.77) for MPSAC and MPSAC–La (0.084–0.36) fit by Freundlich. The lowest q_{max} value

University of Malaya

for PSAC was only 13.8 mg g^{-1}, but MPSAC–La (0.36) had the highest q_{max} of 227.6 mg g^{-1}. Thus, surface modification by the dual impregnation of Fe and La [MPSAC–La (0.36)] increased the adsorption capacity by 16.5 times that of the unmodified PSAC. Although MPSAC–La (0.36) had a q_{max} 1.6 times greater than that of MPSAC (141.8 mg g^{-1}), its Langmuir constant (K_L = 2.25) was 230 times greater than that of MPSAC (0.01) (see Figure 4.1(B)).

Limousin et al. (2007) specified four main types of Langmuir isotherm. La–impregnated media (La/Fe mass ratio greater than 0.23) can be classified as an H–type Langmuir isotherm, indicating a high affinity. The other media are L–type Langmuir isotherms, as they have an adsorption capacity on arsenate concentration and active site on adsorbent surface (Limousin et al., 2007).

Table 4.1(A) Langmuir and Freundlich isotherm parameters for arsenate adsorption onto PSAC, MPSAC and MPSAC impregnated with different amount of lanthanum (III) at pH 6, Ci (350 mg L-1)

adsorbent type	Langmuir isotherm				Freundlich isotherm		
	R^2	K_L	q_{max}		R^2	K_f	1/n
PSAC	0.387	0.009	13.8		0.553	0.03	0.768
MPSAC	0.921	0.005	141.8		0.859	0.67	1.065
MPSAC-La(0.084)	0.987	0.010	188.3		0.822	1.14	1.055
MPSAC-La(0.23)	0.947	0.088	218.4		0.770	86.36	5.744
MPSAC-La(0.28)	0.989	0.594	209.4		0.863	131.88	10.296
MPSAC-La(0.36)	0.995	2.248	227.6		0.975	153.27	10.757

University of Malaya

Based on Table 4.1, it was observed that the K_L values significantly increased as the impregnated amount of La increased. The higher value of K_L, the stronger sorption affinity between adsorbate and adsorbent can be obtained (Apostol, Mamasakhlisi, & Subotta, 2015). The Fe-La composite hydroxide synthesized by Zhang et al. (2014) also showed that the larger K_L and q_{max} values were obtained with the higher ratio of La/Fe (in the range of 1/3~1/0). In an interesting aspect, MPSAC–La (0.36) had a much higher q_{max} than Fe–La composite [La/Fe (1/3), 116 mg g^{-1}], which had a similar La/Fe ratio. This might happened due to the structural differences since MPSAC–La has a sequence of Fe and La at the inner and outer layers, respectively, while Fe-La composite has a mixed matrix.

The following experiments were conducted using the MPSAC and MPSAC–La (0.36) because the MPSAC–La (0.36) had the highest K_L and q_{max}. The MPSAC was chosen as a comparative media to find out the influence of La for the efficiency of arsenate removal.

University of Malaya

4.2 Arsenate Kinetics

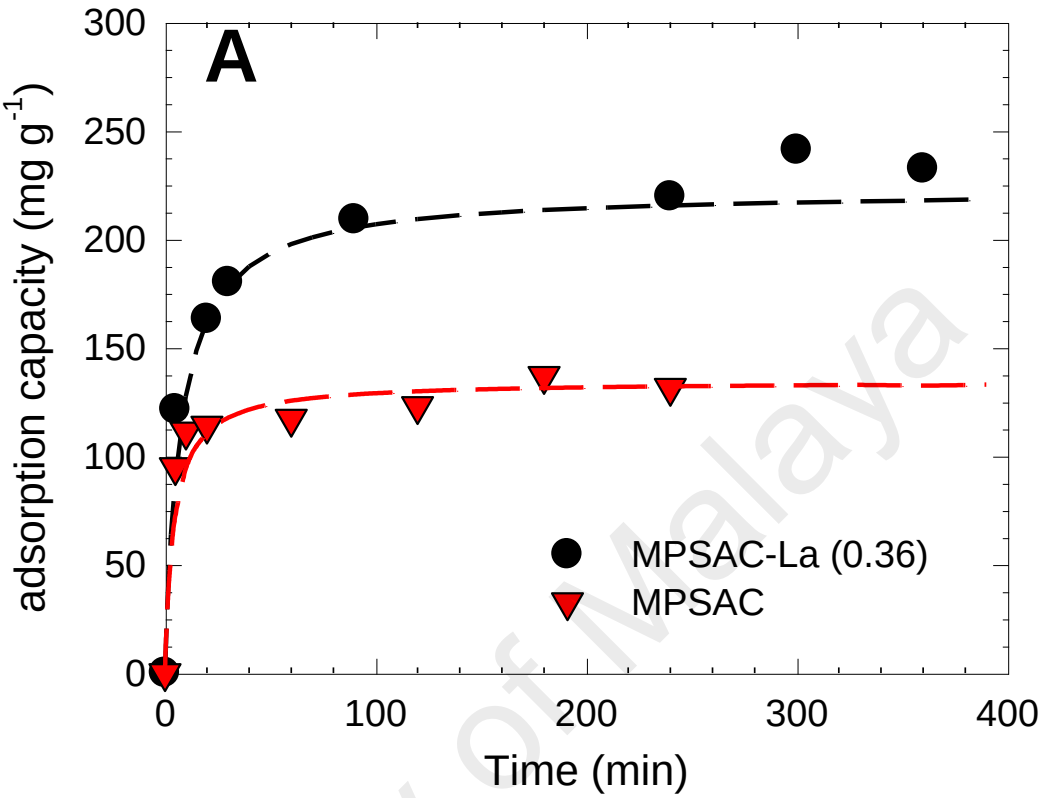

Figure 4.2 (A) kinetics of arsenate removal by MPSAC-La (0.36) for the removal of arsenate at pH 6, C_i = 350 mg L^{-1}, 1.0 g L^{-1} of adsorbent

University of Malaya

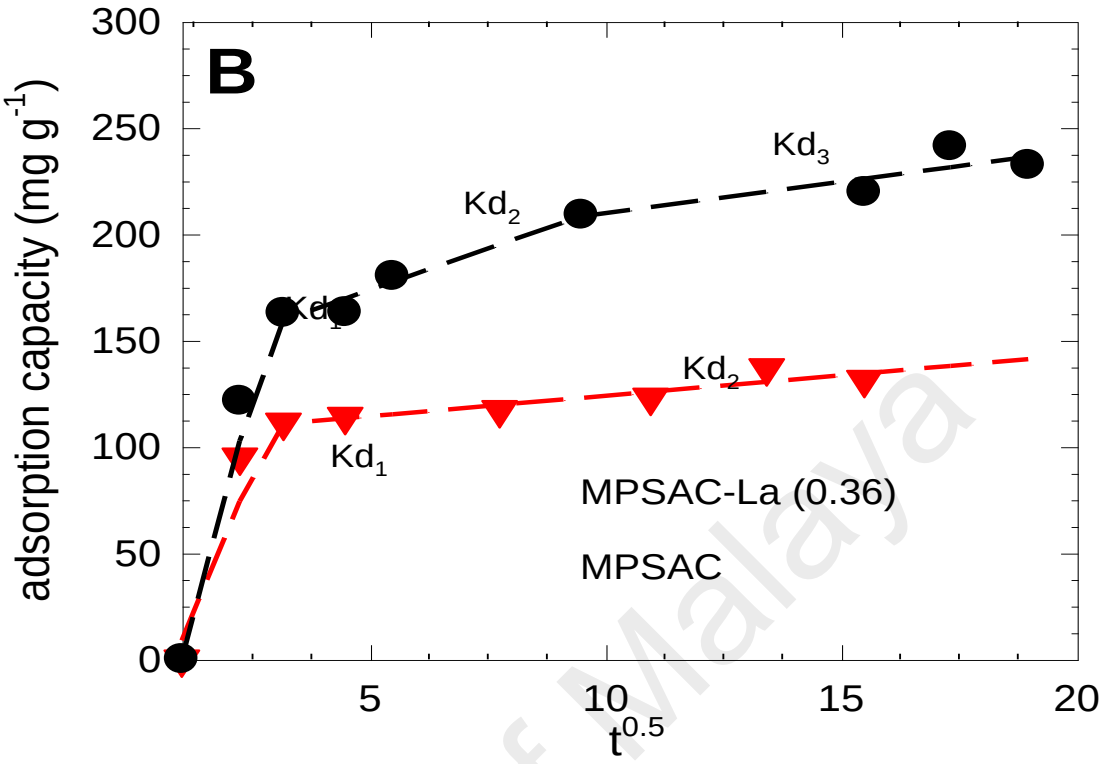

Figure 4.2 (B) intra-particle diffusion modelling of MPSAC-La (0.36) for the removal of arsenate at pH 6, C_i = 350 mg L^{-1}, 1.0 g L^{-1} of adsorbent

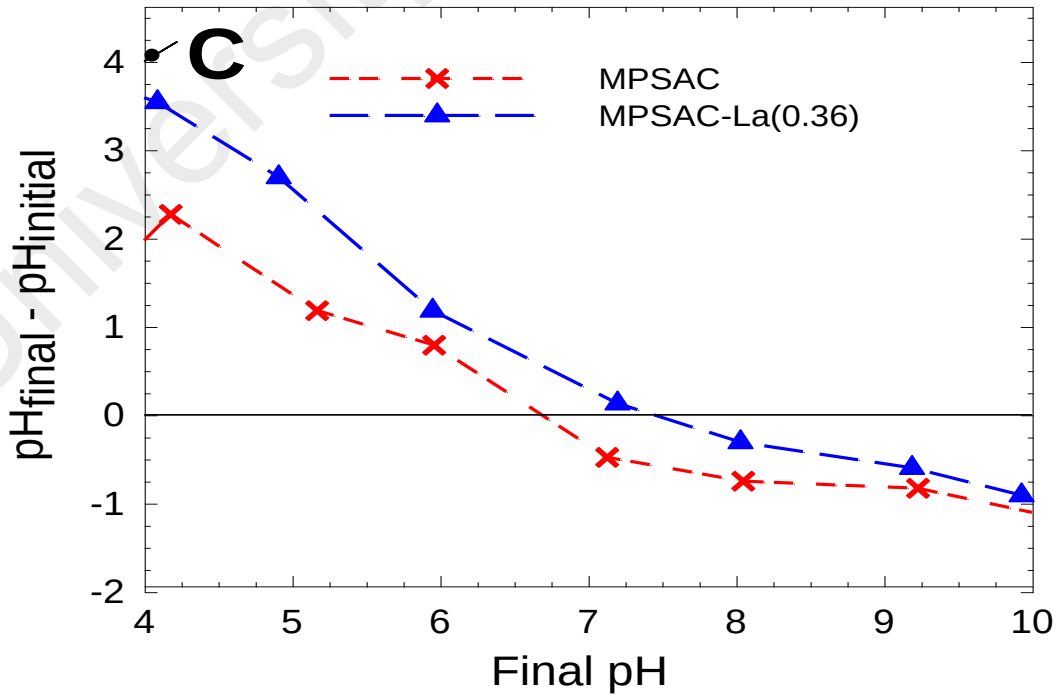

Figure 4.2 (C) pH_{PZC} of MPSAC-La (0.36)

University of Malaya

Figure 4.2 (A) shows the kinetic data of MPSAC and MPSAC–La (0.36), as well as the fit lines of the pseudo–second order kinetic model ($R^2 > 0.98$). The adsorption trend shows two patterns, which are the fast and slow rates. At the first ~30 minutes, MPSAC–La (0.36) and MPSAC had fast sorption speeds with 78% and 87% arsenate removal percentages over the equilibrated capacity (q_{eq}), respectively. The q_{eq} of the MPSAC and MPSAC–La (0.36) were 134.5 mg g^{-1} and 240.6 mg g^{-1}, which are almost similar to the q_{eq} of previous isotherm tests at the same condition. So, this proves that the performed batch tests were reliable. To investigate the adsorption rate and removal mechanism of arsenate by the MPSAC–La (0.36) and MPSAC, the pseudo first-order and pseudo second-order kinetic models were utilized. By comparing their R^2 values (Table 4.2), the pseudo first-order kinetic model for MPSAC-La (0.36) had a higher value (0.994) than the pseudo second-order kinetic model (0.988). Thus, it can be deduced that the physical-sorption (precipitation) is an influenced removal mechanism by the MPSAC-La (0.36). Meanwhile, the pseudo first-order kinetic model shown by the MPSAC is lower than the pseudo second-order kinetic model, which means that there is no physical-sorption influenced removal mechanism. In addition, the intra particle diffusion model was also plotted to prove the diffusion mechanism.

Figure 4.2 (B) shows the kinetic data and fit lines using the IPD model. The linearized curves for both media did not pass through the origin, proving that IPD is not the only affecting factor (Yürüm, Kocabaş-Ataklı, Sezen, Semiat, & Yürüm, 2014). Generally, adsorption can be affected by three steps: film and bulk boundary diffusion (k_{d1}), intra particle diffusion (k_{d2}) and physical or chemical binding at the active sites (k_{d3}) (K. Wu et al., 2013). Lately, Liu et al. (2015) reported that the predominant formation of the bidentate binuclear corner-sharing inner-sphere complexes between the arsenate and the nano–magnetite is based on their spectroscopic analyses (C.-H. Liu et al., 2015). Through XPS analyses, Zhang et al. (2009) also conveyed the nano–magnetite doped on the

University of Malaya

activated carbon fiber had a major role to eliminate arsenate with the mechanism of inner-sphere complexation (S. Zhang, Li, & Chen, 2009). Based on those evidences, further tests were conducted to prove the removal mechanism of arsenate by the MPSAC–La (0.36).

Table 4.2 Parameters of the pseudo-first and pseudo-second order kinetic models for arsenate adsorption by MPSAC–La (0.36) and MPSAC

Adsorbent	Pseudo first order kinetic model			Pseudo second order kinetic model			
	q_e (mg g^{-1})	K_{ad} (min^{-1})	R^2	q_e (mg g^{-1})	k_2 (g mg^{-1} min^{-1})	v_0 (mg g^{-1} min^{-1})	R^2
MPSAC	167.4	0.005976	0.407	134.5	0.0017	6.7	0.997
MPSAC–La (0.36)	265.2	0.0038	0.994	240.6	0.0003	20.8	0.988

Table 4.3 Comparison of sorption capacities and speed with other references

Adsorbent	Pseudo second order kinetic model					
	Initial arsenate concentration (mg L^{-1})	**Final pH**	**q_e (mg g^{-1})**	**v_0 (mg g^{-1} min^{-1})**	**R^2**	**reference**
[1]MPSAC-La (0.36)	350	6.0	240.60	20.8	0.988	This study
[2]Low-cost MFD	50	6.0	71.23	5.90	-	(Hao, Liu, Li, Du, & Wang, 2014)
[3]NZVI–RGO	7	7.0	17.00	0.04	0.999	(C. Wang et al., 2014)
$NiFe_2O_4$	10	7.0	14.46	0.25	-	(Y. Liu et al., 2015)
Fe–La (3:1)	15	7.0	77.80	0.0005	0.945	(W. Zhang et al., 2014)
Fe–La (1:3)	30	7.0	153.00	0.00013	0.963	(W. Zhang et al., 2014)
[4]p(APTMACl) microgels	250	N/A*	131.57	0.026	0.9989	(Rehman et al., 2016)

[1]MPSAC-La (0.36) (La–impregnated, magnetized PSAC
[2]Low-cost MFD (Modified Sawdust)
[3]NZVI–RGO (Nanoscale zero valent iron-reduce graphite oxide)
[4]p (APTMACl) microgels (cationic 3-Acrylamidopropyl)-trimethyl ammonium chloride microgels)
*N/A: not available

University of Malaya

Table 4.2 shows the kinetic parameters of MPSAC and MPSAC–La (0.36), as well as their comparison with other references in Table 4.3. Accordingly, MPSAC–La (0.36) had about 3.1 times higher initial sorption rate (v_0) than MPSAC. Table 4.3 shows that MPSAC–La (0.36) had the highest v_0 (20.8 mg g^{-1} h^{-1}). In fact, faster adsorption rate might occur when a higher amount of positive charge of sorbent is available (Serizawa, Kamimura, & Akashi, 2000) due to the electrostatic interaction with the arsenate oxyanion (Pierce & Moore, 1982; W. Zhang et al., 2014).

To prove the electrostatic characteristics of the media, pH_{PZC} was measured and the data were presented as shown in Figure 4.2(C). Consequently, MPSAC–La (0.36) had a higher pH_{PZC} (7.4) than MPSAC (6.8). At pH < pH_{PZC}, the positive charges will dominate and increase the attraction effect with the arsenate oxyanion (Y. Liu et al., 2015; W. Zhang et al., 2014), increasing the adsorption velocity. Thus, at the same pH condition, MPSAC–La (0.36) has a higher amount of positive charge than MPSAC and eventually gives a higher arsenate removal speed.

University of Malaya

4.3 Arsenate pH effects

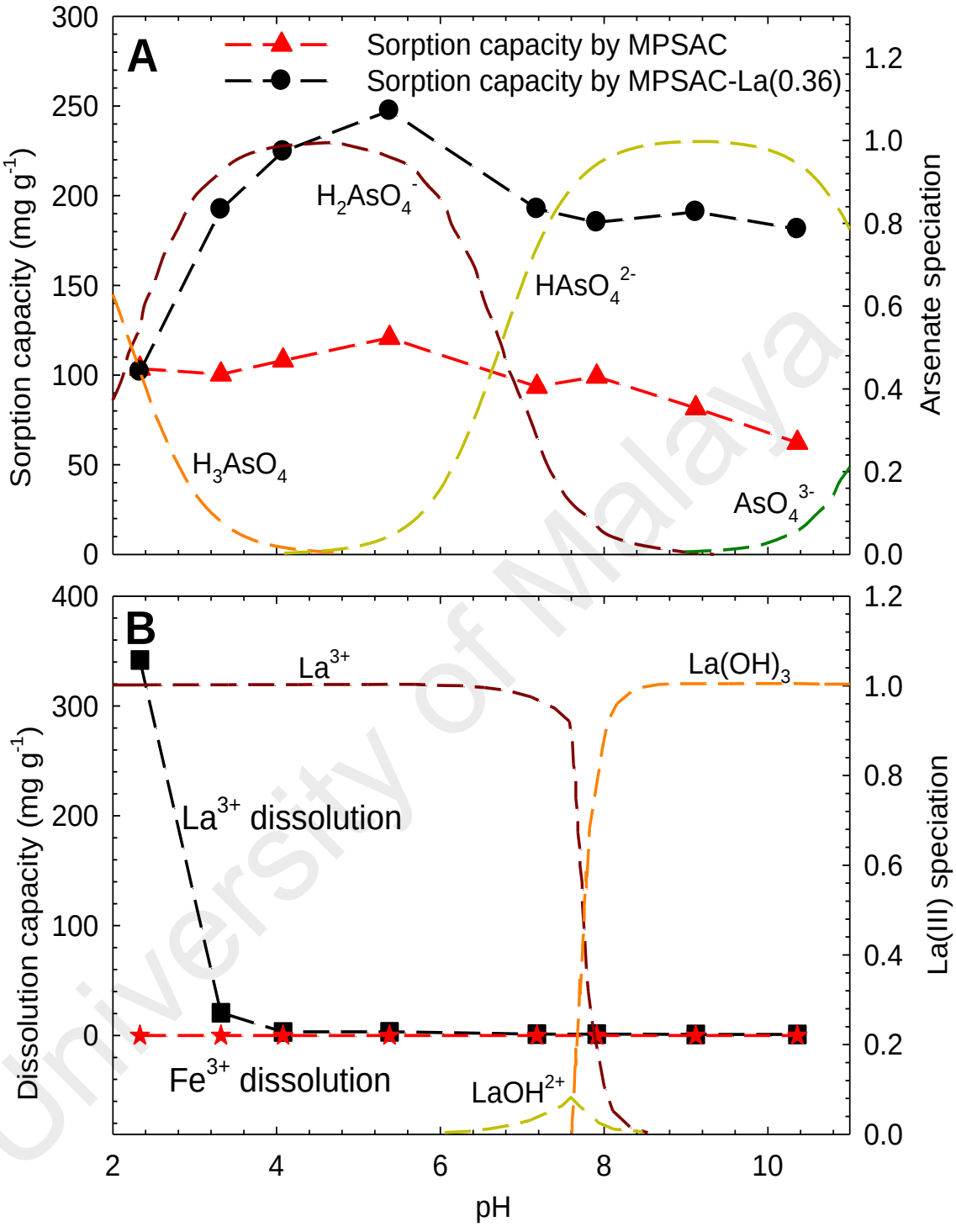

Figure 4.3 (A) arsenate speciation and sorption capacity by MPSAC-La (0.36) at different pH and (B) La^{3+} speciation and leaching concentrations of La^{3+} and Fe^{3+} ions

University of Malaya

Figure 4.3(A) shows arsenate speciation and equilibrated sorption capacity (q_{eq}) by MPSAC and MPSAC–La (0.36) at different pH. MPSAC–La (0.36) had higher sorption capacities than MPSAC at most pH range. The highest sorption capacities for MPSAC–La (0.36) and MPSAC were 247.3 and 120.7 mg g^{-1}, respectively, at pH 5.4. These values are well matched to the results of the isotherms and the kinetics conducted at pH 6, revealing reliable experiments. As pH was lower than 5, q_{eq} of MPSAC–La (0.36) was reduced significantly and was even similar to that of MPSAC at pH 2.3. Figure 4.3 (B) shows La^{3+}/Fe^{3+} dissolution and La speciation according to pH. The dissolved concentration of La^{3+} ions exponentially increased as the pH reduced. Zhang et al. (2014) also measured the dissolution of La with various La–Fe composite by pH. As a result, the La dissolution increased when the La/Fe increased. For example, La/Fe (1/3) started to dissolve La at pH < 7, while La/Fe (1/0) had La dissolution at pH < 9. In this study, however, MPSAC–La (0.36) (La/Fe, 0.36/1) had La dissolution occurred at pH < 4. Accordingly, as shown at Zhang et al. (2014), this demonstrates that heterogeneous metal oxide might have a particular stabilization effect on La dissolution, inferring that nano–magnetite might have a strong binding strength to stabilize La.

The highest La^{3+} ion dissolution, 340 mg g^{-1} was obtained at pH 2.3 and this value was equivalent to 94% of La amounts that were incorporated into the media. Thus, it can be deduced that most La coated on media was dissolved out into the solution at acidic condition. This minimized sorption capacity might be due to the dissolution of La^{3+}, which does not participate in the arsenate removal as a precipitation agent (N. Haque, Morrison, Cano-Aguilera, & Gardea-Torresdey, 2008). Due to this fact, MPSAC–La (0.36) had the same sorption capacity to MPSAC at pH 2.3. For all ranges of pH, Fe^{3+} was not dissolved due to the La coating and low solubility of magnetite (Cornell & Schwertmann, 2003).

University of Malaya

The sorption capacities of arsenate were gradually reduced from pH 5.4 to 8 and they were stable to be about ~ 190 mg g^{-1} at pH > 8. In this study, the chemical equilibrium-modeling program, 'Medusa/Hydra', was applied to generate the soluble and solid complexes.

Table 4.3: Mixed metal ions complexes (soluble and solids species) for Medusa

Metals	Soluble and Solid Complexes	Species	Reactions	Log K
La(III)	Soluble complexes	$La(OH)_2^+$	$La^{3+} = 2H^+ + La(OH)_2^+$	-18.14
		$La(OH)_3$	$La^{3+} = 3H^+ + La(OH)_3$	-27.91
		$La(OH)_4^-$	$La^{3+} = 4H^+ + La(OH)_4^-$	-40.86
		$La_5(OH)_9^{6+}$	$5La^{3+} = 9H^+ + La_5(OH)_9^{6+}$	-71.2
		$LaOH^{2+}$	$La^{3+} = 2H^+ + LaOH^{2+}$	-8.66
		OH^-	$H^+ + OH^-$	-14.00
	Solid complexes	$La(OH)_{3\ (C)}$	$La^{3+} = 3H^+ + La(OH)_{3\ (C)}$	-20.30
As(V)	Soluble complexes	$H_2AsO_4^-$	$2H^+ + AsO_4^{3-} = H_2AsO_4^-$	18.354
		H_3AsO_4	$3H^+ + AsO_4^{3-} = H_3AsO_4$	20.597
		$HAsO_4^{2-}$	$H^+ + AsO_4^{3-} = HAsO_4^{2-}$	11.596
	Solid complexes	$As_2O_{5\ (C)}$	$6H^+ + 2AsO_4^{3-} = As_2O_{5\ (C)}$	13.90

Table 4.3 shows the soluble and solid species of individual metals, terms of reaction, and equilibrium constants (log K). The La speciation shows that La^{3+} exists dominantly as cationic species at pH < 8 and La $(OH)_3$ is prevalent at pH > 8. Based on this speciation, therefore, arsenate is dominantly removed by precipitation at pH < 8 while it complexes on the surface of La $(OH)_3$ at pH > 8. Soluble La^{3+} ions are expected to react with arsenate to form $LaAsO_4$ precipitate (W. Zhang et al., 2014). There are two available precipitation reactions as shown below:

$$La^{3+} + H_2AsO_4^- \rightarrow LaAsO_4 + 2H^+ \quad (4.1)$$

$$La^{3+} + HAsO_4^- \rightarrow LaAsO_4 + H^+ \quad (4.2)$$

University of Malaya

The maximum sorption capacity was found when the species of $H_2AsO_4^-$ is dominant (Shujuan Zhang, Li, & Chen, 2010). This might happened by the following circumstances; as shown by the above precipitation reactions, R1 releases the double hydrogen ions (H^+) of R2 and soluble H^+ ions help to further solubilize La $(OH)_3$ to release La^{3+} for precipitation. Along with the stability of La phase, dissolved La^{3+} was not detected because it was involved in the precipitation reaction at $4 < pH < 8$. When pH is less than 4, however, H_3AsO_4, non-ionic prevalent species, does not react with La^{3+} ion to form precipitate. The dissolution trend of La^{3+} was reversely related to the speciation fraction of H_3AsO_4. Meanwhile, arsenate (as $HAsO_4^{2-}$ species) might be mainly removed by the inner-sphere complexation (W. Zhang et al., 2014) onto the surface of La $(OH)_3$ under alkaline condition ($pH > 8$).

University of Malaya

4.4 Mechanism of arsenate removal by MPSAC–La

In order to elucidate the arsenate removal mechanism, spectroscopic analyses such as XRD, SEM–EDS, N_2 gas isotherm and FT–IR were performed for the prepared media and arsenate retained media.

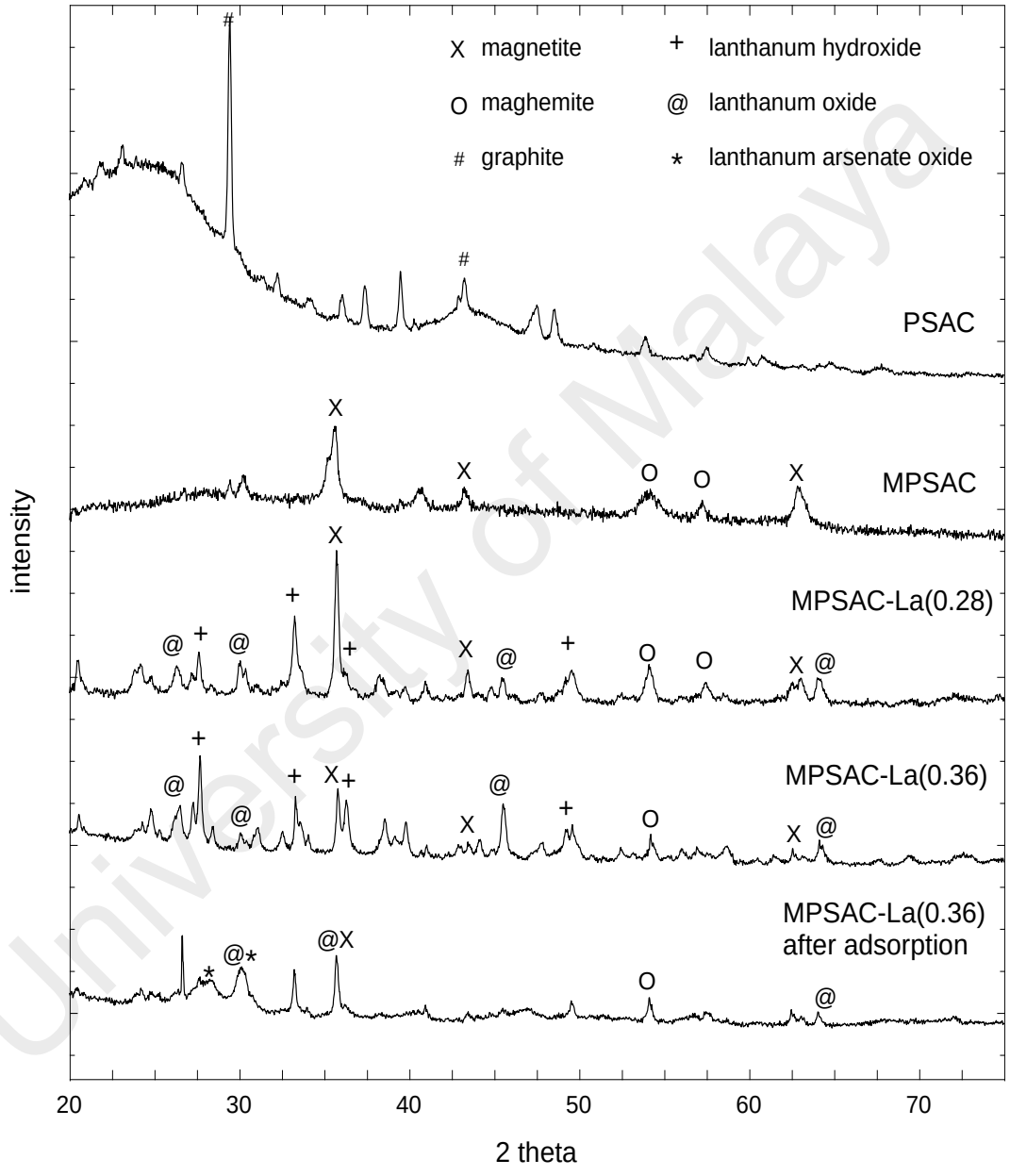

Figure 4.4 XRD results of PSAC, MPSAC, MPSAC-La (0.28), MPSAC-La (0.36) and MPSAC-La (0.36) after adsorption at pH 6, C_i = 350 mg L^{-1}, 1 g L^{-1} of adsorbent.

University of Malaya

Figure 4.4 shows the XRD results of PSAC, MPSAC, MPSAC–La (0.28), MPSAC–La (0.36) and arsenate retained MPSAC–La (0.36) at pH 6. PSAC has significant graphite peaks of (002) and (100) at 28^{o} and 43^{o}, respectively. The magnetic materials coated on the surface of MPSAC were identified as magnetite and maghemite. Three broad peaks at 37^{o}, 43^{o} and 62^{o} of the 2 theta were corresponding to (311), (400) and (440) planes of magnetite [JCPDS : 19–0629] (Maity, Kale, Kaul-Ghanekar, Xue, & Ding, 2009) while the two broad peaks at 53^{o} and 56^{o} were identified as (422) and (511) planes of maghemite [JCPDS:39-1346] (Kim et al., 2012). Although the magnetization properties between the magnetite and maghemite are similar (S. R. Chowdhury, Yanful, & Pratt, 2011), the oxidation of magnetite might lead to the formation of maghemite during the drying process of MPSAC. Once Lanthanum was incorporated into MPSAC with a ratio of 0.28:1 (La:Fe), the peaks of lanthanum oxide (LO) phase were shown at 27^{o}, 30^{o}, 47^{o} and 64^{o} on (100), (101), (110), and (202) planes, while the phase of lanthanum hydroxide (LH) was emerged at 28^{o}, 33^{o}, 37 and 49^{o} on (110), (101), (200), (111), and (300) planes, respectively. However, it still has the magnetite and maghemite peaks. As for MPSAC–La (0.36), the phase of LH increased more than LO, and magnetite and maghemite phases still existed, but reduced significantly. The peaks of LO and LH were determined to refer to La_2O_3 [JCPDS: 05–0602] and La $(OH)_3$ [JCPDS:36-1481]. The XRD pattern for arsenate retained MPSAC–La (0.36) showed the formation of $LaAsO_4$ phase [JCPDS:15-756] at 28^{o} and 30^{o} which are the plane of (120) and (012), correspondingly. The results exhibited that the arsenate was dominantly removed by the precipitation mechanism (W. Zhang et al., 2014). In addition, as the LO peaks still existed, the disappearance of LH peaks revealed that LH was leached away and $LaAsO_4$ layer was covered on the LO phase during the removal of arsenate from liquid phase.

University of Malaya

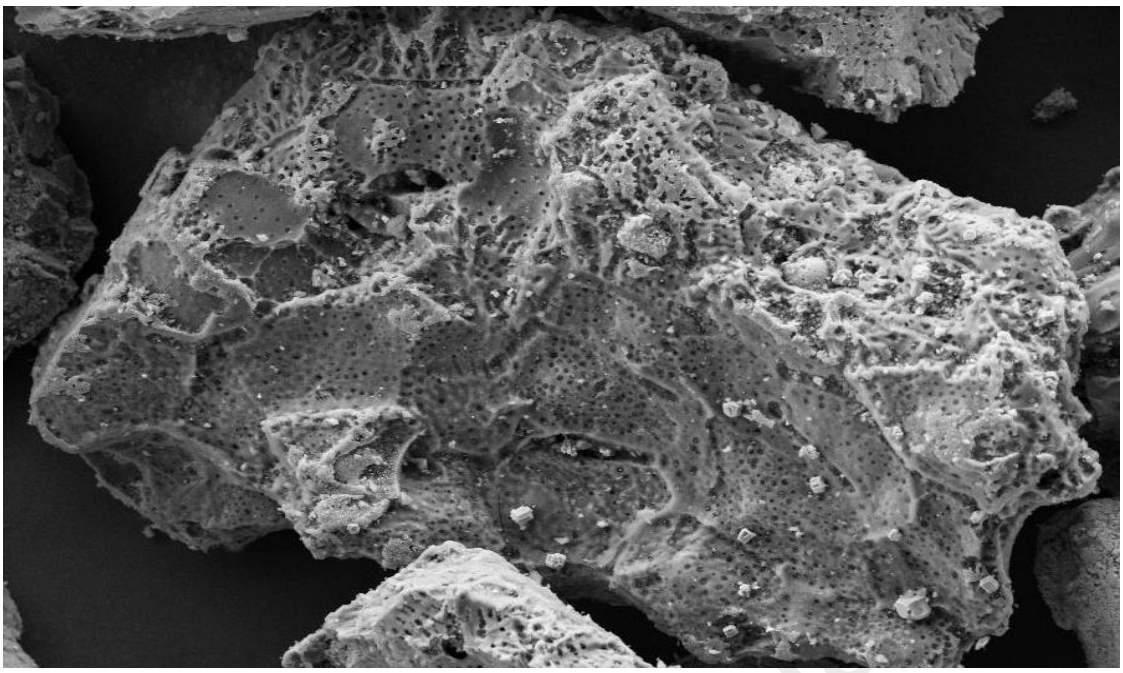

Figure 4.5 (A) FESEM for PSAC

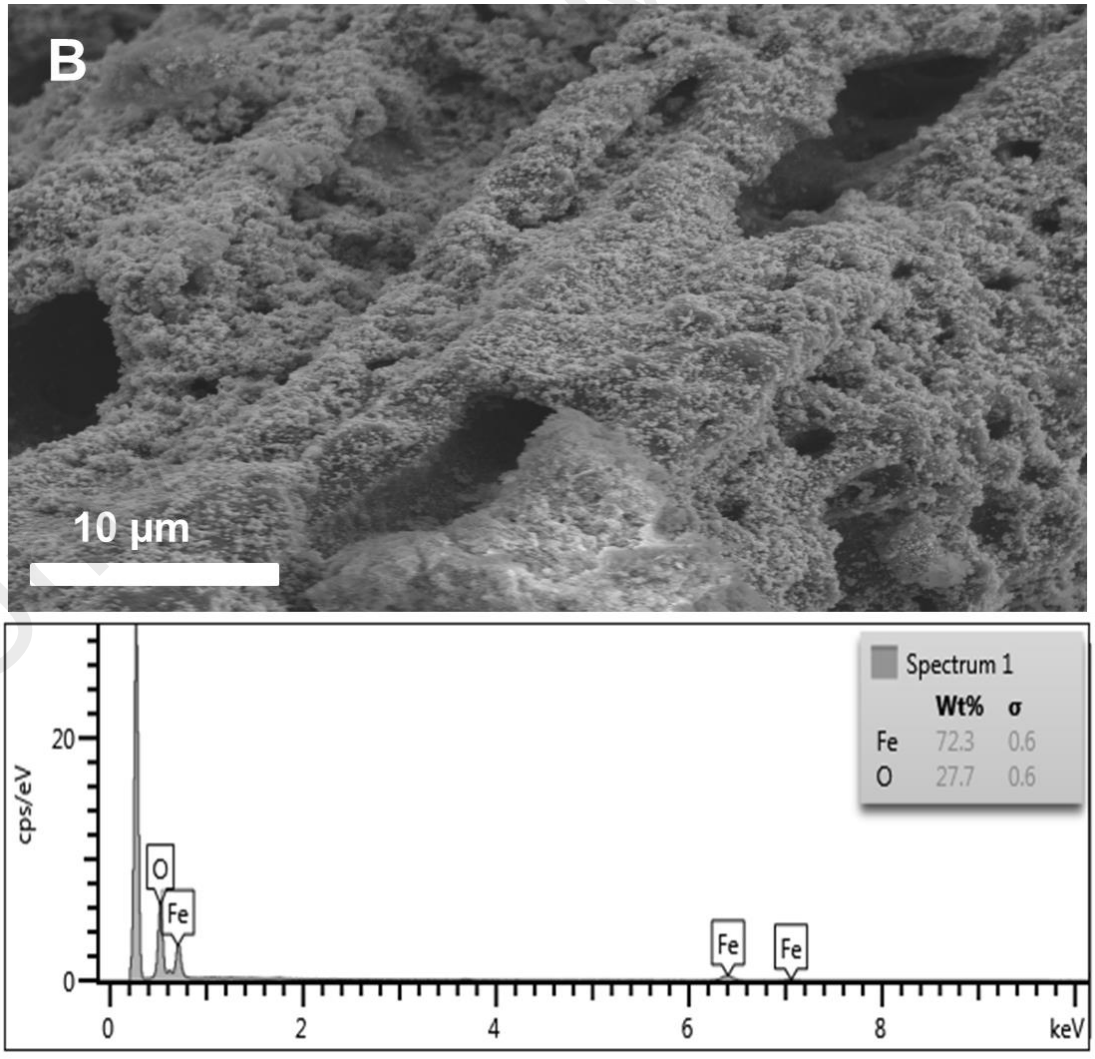

Figure 4.5 (B) FESEM+EDX for MPSAC

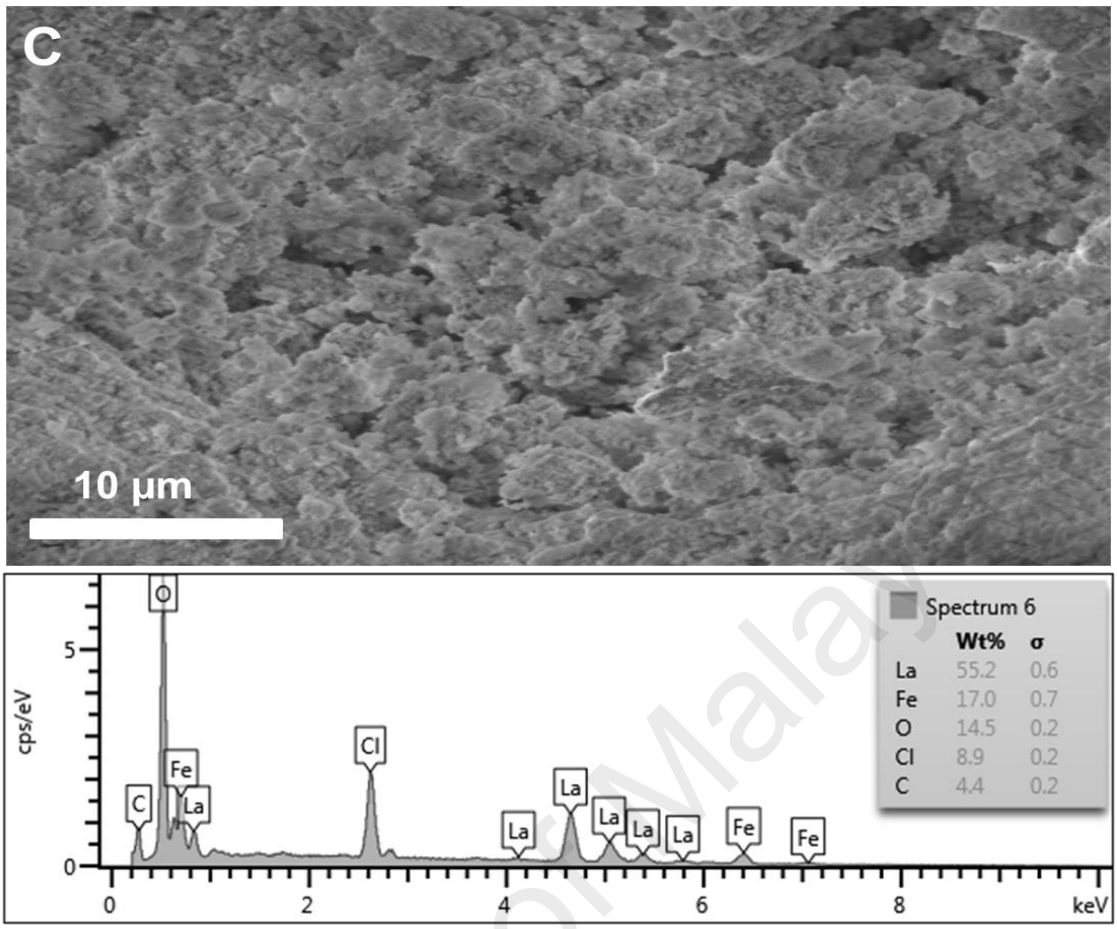

Figure 4.5 (C) FESEM+EDX for MPSAC-La (0.36)

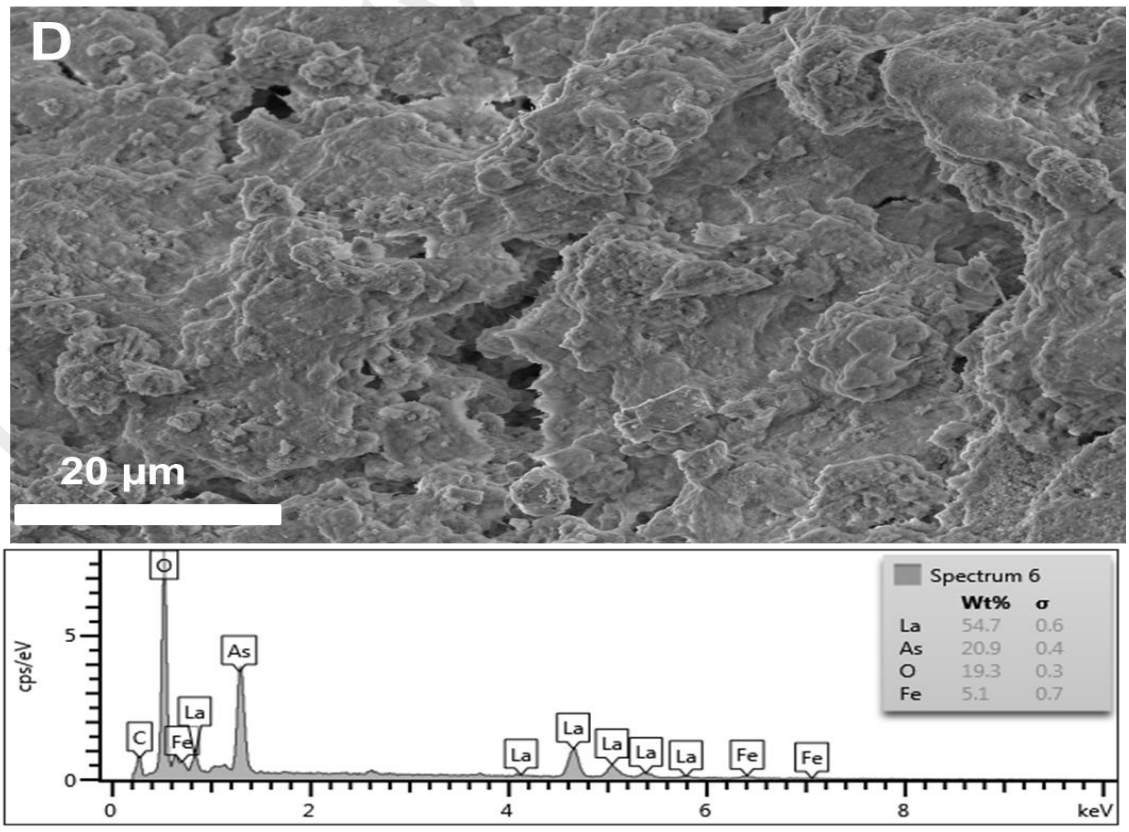

Figure 4.5 (D) FESEM+EDX for arsenate retained MPSAC-La (0.36) with the condition: pH 6, C_i = 350 mg L^{-1}, 1 g L^{-1} of adsorbent.

The morphology of PSAC, MPSAC, MPSAC–La (0.36) and arsenate retained MPSAC-La (0.36) at pH 6 were analyzed using the FESEM–EDX. Figure 4.5A show the morphological structures of the PSAC, in which outer pores were highly developed. Figure 4.5B shows the morphology of MPSAC and ball-like nanoparticles on the surface, although the outer pores were still found. The EDX shows that MPSAC contained 72.3% of Iron and 27.7% of Oxygen. Through the molecular weight calculation, the iron oxide deposited on the PSAC was identified as a dominant phase of magnetite (Fe_3O_4). Figure 4.5C shows the morphological structure of MPSAC–La (0.36), in which the nano-particles of magnetite and maghemite disappeared. Instead, a 3-Dimensional (3D) nano plate-like and hexagonal layered structures of LO/LH were dominantly coated on the surface (Y. Guo, Zhu, Qiu, & Zhao, 2012). The EDS analysis shows the MPSAC-La (0.36) contained 55.2% of Lanthanum and 17% of Iron. It shows that the surface of MPSAC-La (0.36) was not fully covered by LO/LH as shown in XRD results.

Figure 4.5D shows the dissolution-precipitation caused morphological changes of arsenate retained MPSAC-La (0.36) that formed large plate-like and hexagonal layered structure. Grover et al. (2010) suggested that the arsenate reacts with dissolved layered double hydroxide (LDH) and formed small particles. However, the formed precipitates had large morphological structures for the case of MPSAC–La (0.36). The EDS data shows that 54.7%, 5.1% and 20.9% of Lanthanum, Iron and Arsenic weight percentages, respectively. Thus, the weight ratio (2.62) of Lanthanum to Arsenic is higher than the theoretical ratio (1.85) for $LaAsO_4$ which was seen at XRD. This result is well matched to the finding of XRD, in which LO and $LaAsO_4$ phases were co-existed.

University of Malaya

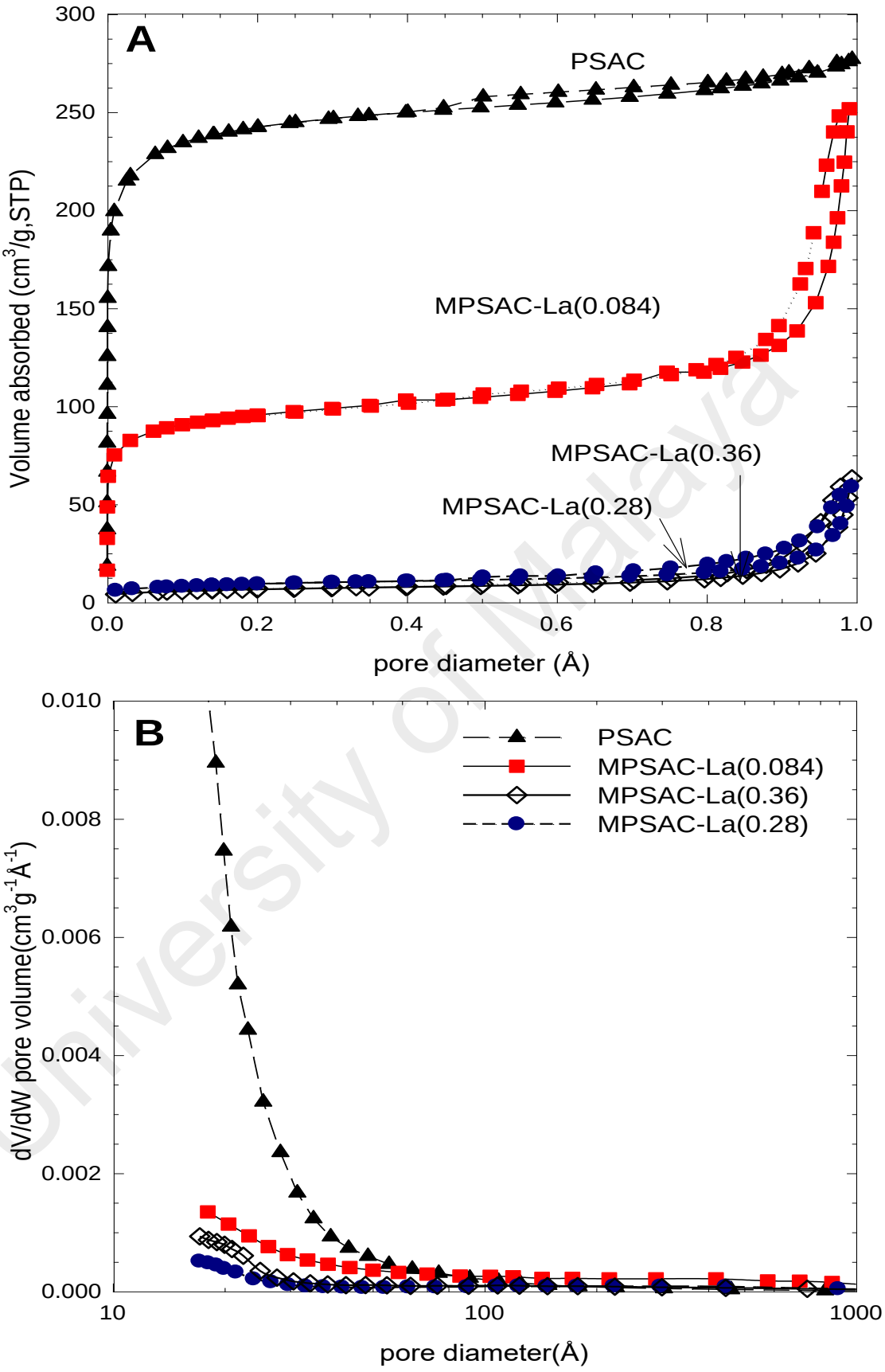

Figure 4.6 (A) N2 adsorption and desorption isotherms (B) pore size distribution (BJH) curve of MPSAC, MPSAC-La (0.084), MPSAC-La (0.28) and MPSAC-La (0.36) at pH 6, Ci = 350mg L-1, 1 g L-1 of adsorbent.

University of Malaya

Figure 4.6 shows N_2 gas isotherm and BJH pore size distribution of various media. According to the IUPAC standard classification, PSAC shows that the type I isotherm curve represents the long horizontal knee feature of the isotherm, predominantly consisting of micropore structures. Meanwhile, others show type IV isotherm curve. Accordingly, with a small incorporation of Lanthanum, micropores largely reduced, instead the meso and macropore structures were developed. However, as the incorporation amount of Lanthanum increased, the microporous structure completely disappeared and the meso and macropores also reduced. Based on those results, it can be inferred that the meso and macropores were created by the inter-spaces of the nano-magnetite and maghemite. However, incorporated LH/LO is glued between the nano-particles to eliminate most pore structures.

Table 4.4 Porosity characterization of PSAC, MPSAC, MPSAC–La (0.084), MPSAC–La (0.28), MPSAC–La (0.36)

Samples	**Molar ratio of La: Fe**	**BET surface area (m^2g^{-1})**	**total pore volume (cm^3g^{-1})**	**Micro - pore Area (m^2g^{-1})**	**Volume (cm^3g^{-1})**	**primary mesopore**		
						Area (m^2g^{-1})	Volume (cm^3g^{-1})	Size (W_{KJS},Å)
PSAC	NA*	842.5	0.428	777.8	0.428	153.1	0.116	18.4
MPSAC –La (0.084)	0.17:1	332.3	0.389	247.6	0.389	109.1	0.389	43.7
MPSAC –La (0.28)	0.56:1	23.0	0.098	3.1	0.001	20.0	0.095	169.7
MPSAC –La (0.36)	0.72:1	32.7	0.091	6.0	0.003	26.8	0.087	111.34

*not available

Based on Table 4.4, PSAC has the highest BET surface area (842.5 m^2 g^{-1}) and micropore area (777.8 m^2 g^{-1}) so that micropores were dominant. Meanwhile, PSAC–La (0.28) had the lowest BET surface area (23 m^2 g^{-1}) and micropore area (3.1 m^2 g^{-1}). About 99.6% of the micropores were disappeared with Lanthanum incorporation, indicating that most pores were clogged by LO/LH.

University of Malaya

Table 4.5 Comparison of maximum adsorption capacities and sorption densities of various media

Adsorbents	BET surface area (m^2 g^{-1})	Maximum arsenate adsorption capacity (q_{max})	Sorption density (mg m^{-2})	pH	references
Fe–La (3:1)	224.5	116	0.52	7	(W. Zhang et al., 2014)
Fe–La (1:3)	54.8	235.4	4.3	7	(W. Zhang et al., 2014)
MPBAC–La (0.36)	32.7	227.6	6.9	6	This study
MPBAC	842.5	141.1	0.17	6	This study
La_{50}SBA–15	184.7	124.4	0.67	7.2	(Jang et al., 2004)
Cu/Mg/Fe/La LDH	241	43.5	0.18	6	(Y. Guo et al., 2012)
Mg–Fe–Al–LDH	63.6	18.4	0.29	6	(J. Hong, Zhu, Lu, & Qiu, 2014)

Table 4.5 shows the comparison of q_{max} and sorption densities with other references. MPSAC–La (0.36) had a comparable q_{max} (227.6 mg g^{-1}) to Fe–La (1:3) composite (hydr) oxides (235.4 mg g^{-1}) (W. Zhang et al., 2014). As shown in this study, Zhang et al. (2014) presented that arsenate adsorption capacity is increased as Lanthanum amount is increased. As a remarkable result, MPSAC–La (0.36) had a higher sorption density (6.9 mg m^{-2}) than La–Fe (3:1) (4.3 mg m^{-2}) (W. Zhang et al., 2014), even though it has a smaller ratio of Lanthanum to Iron (0.36:1). Other than having a high sorption capacity, MPSAC–La (0.36) has advantages in the physical aspects such as the granular-size and its magnetism, while Fe:La (1:3) has a fine size and is non-magnetic.

University of Malaya

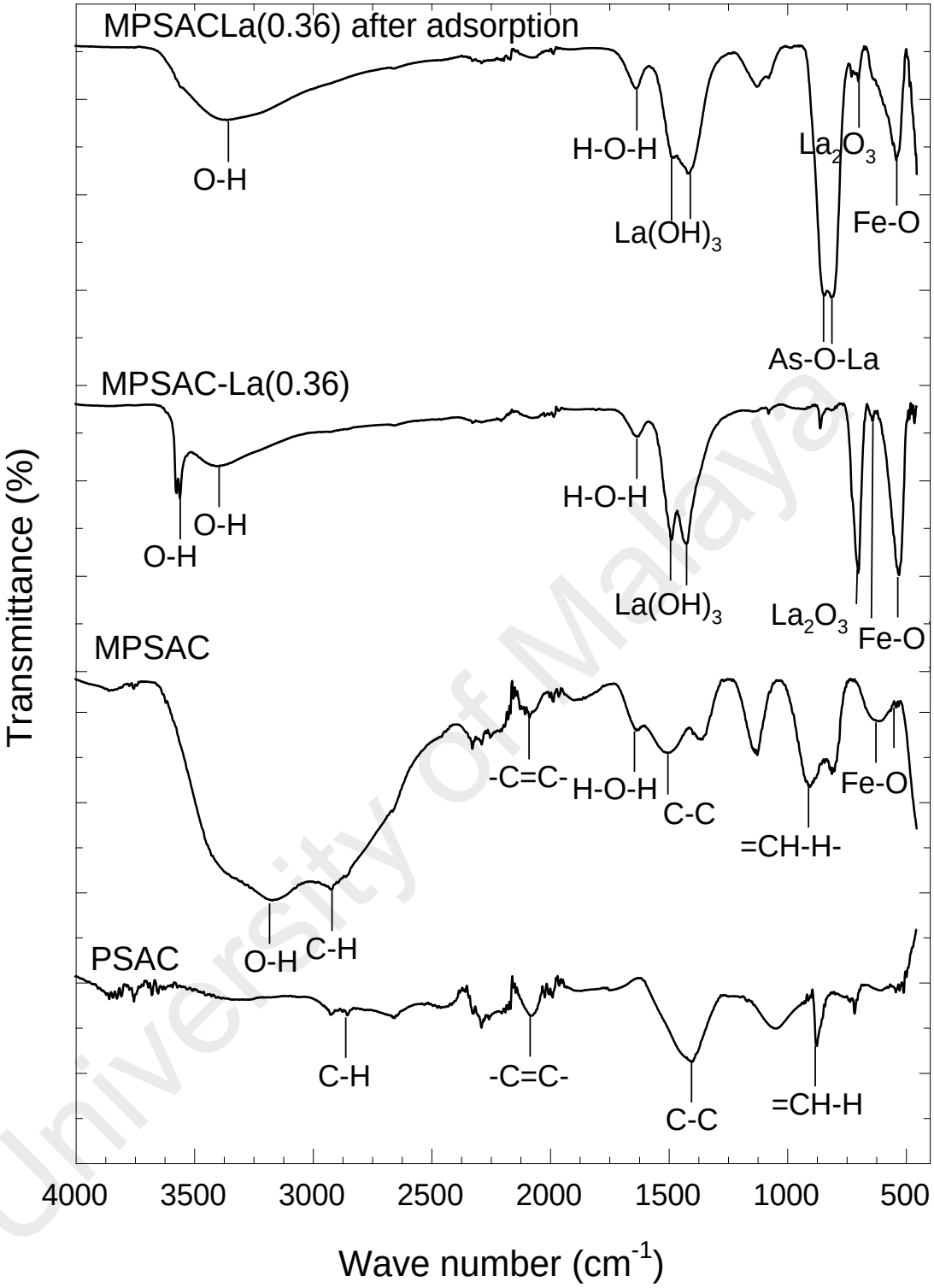

Figure 4.7 FT-IR spectra of MPSAC, MPSAC-La (0.36) and MPSAC-La (0.36) after adsorption at pH 6, C_i = 350mg L^{-1}, 1 g L^{-1} of adsorbent.

University of Malaya

The FT–IR spectra for PSAC, MPSAC, MPSAC–La (0.36) and arsenate retained MPSAC-La (0.36) were illustrated in Figure 4.7. The peaks at 2915/2917, 2074/2100 and 1409/1499 cm^{-1} in the IR spectra of PSAC/MPSAC, were indicated to C–H, –C=C– (carbonyl) and C–C aromatic stretching, respectively. The peak at 612 cm^{-1} for MPSAC is assigned to Fe–O stretching. The difference between PSAC and MPSAC is the OH peak which can be seen at 3000 ~ 3500 cm^{-1}. This difference shows that MPSAC media was coated with the magnetite and maghemite.

When Lanthanum is impregnated, new IR peaks at 3395 and 3556 cm^{-1} were emerged to indicate O–H stretching group of LH (Aghazadeh, Golikand, Ghaemi, & Yousefi, 2011). The peak at 1629 cm^{-1}, H–O–H was observed to be the deformation of water molecules by forming physi-sorbed water on the oxide. The IR peak at 1484 and 1423 cm^{-1} is attributed from the reaction of LH with CO_2 (Aghazadeh et al., 2011). The IR peak at 698 cm^{-1} is the characteristic of LO (Méndez et al., 2010). When arsenate is retained at MPSAC–La (0.36), the peaks of O–H and LO/LH at 3556, ~1400, 500–700 cm^{-1} were significantly reduced and new peaks at 808 and 839 cm^{-1} were assigned to As–O–La precipitate as $LaAsO_4$ (W. Zhang et al., 2014). Thus, these facts can infer that LO/LH were utilized to form arsenate precipitate. Overall, scheme 1 presents MPSAC–La (0.36) preparation and arsenate removal mechanism.

University of Malaya

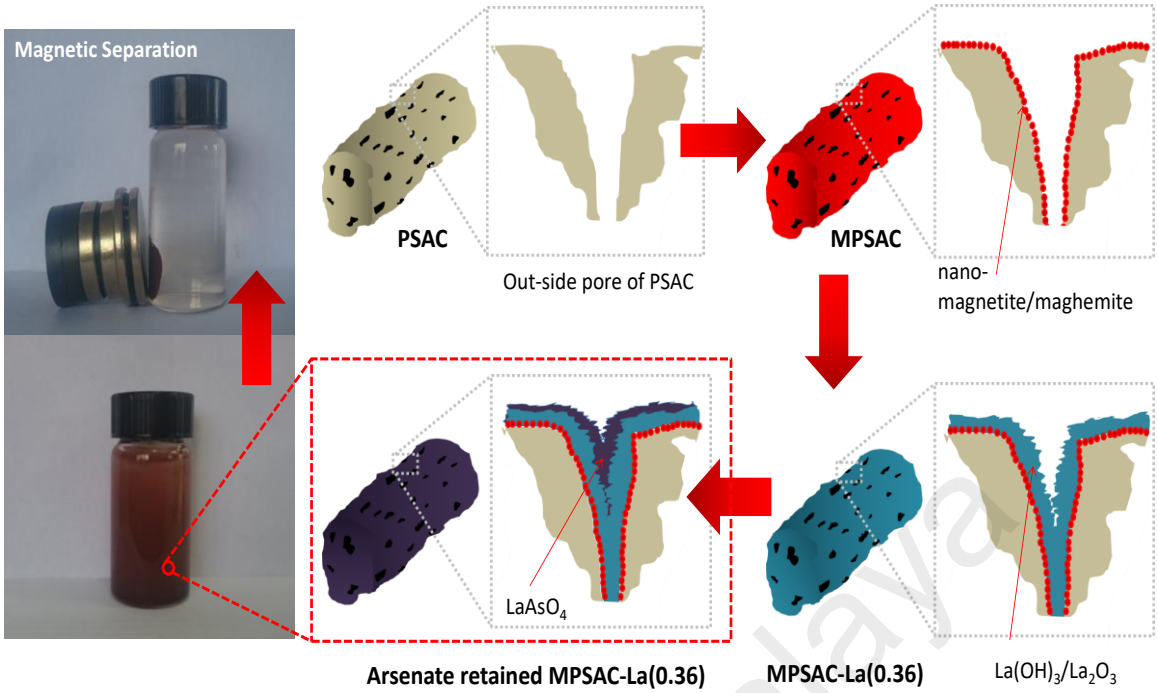

Scheme 1 Schematics of MPSAC–La (0.36) preparation and arsenate removal mechanism

University of Malaya

4.5 Arsenate Thermodynamics

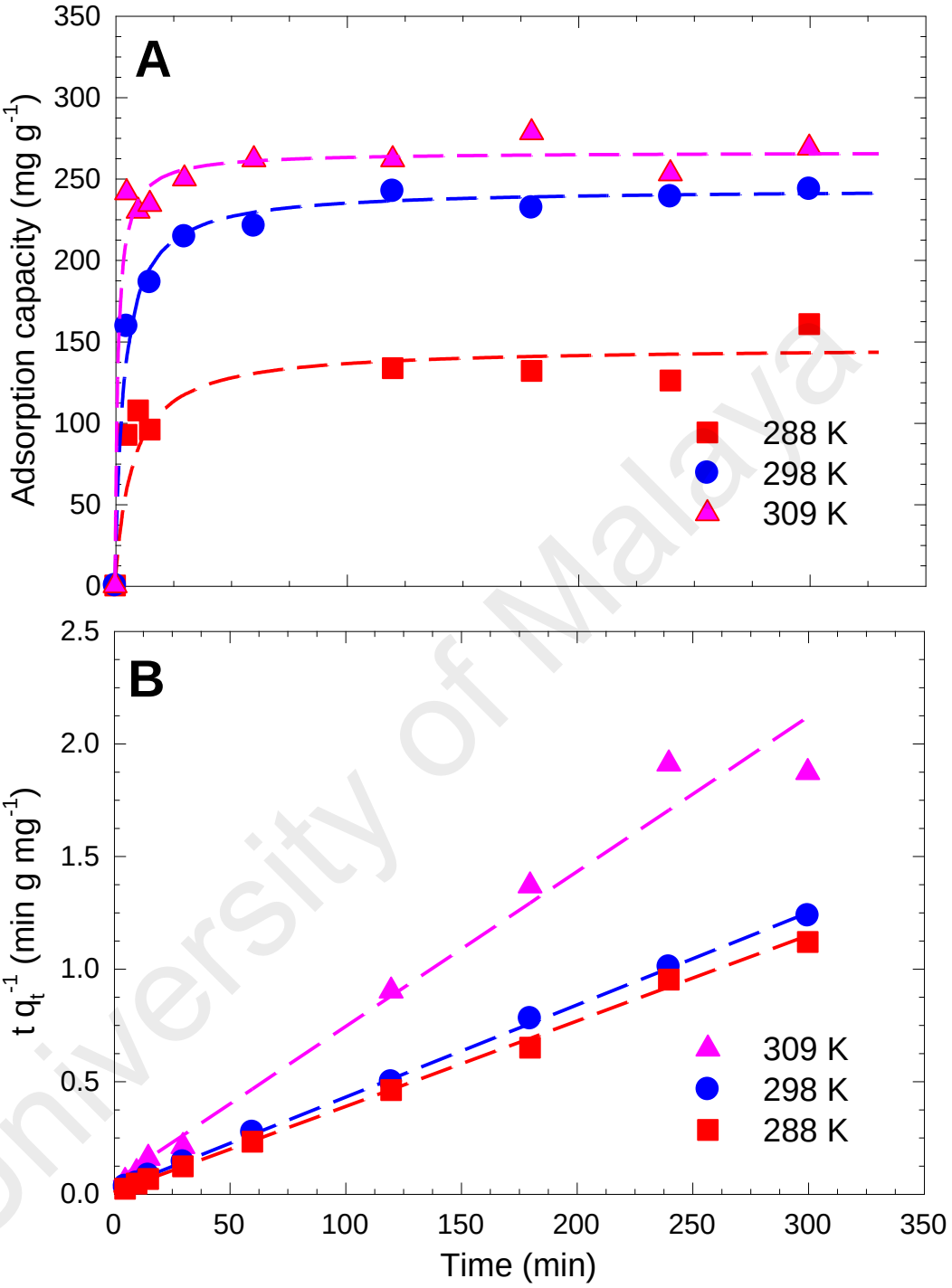

Figure 4.8 (A) temperature effect on arsenate adsorption capacity of MPSAC–La (0.36), (B) pseudo second order kinetic model at pH 6 C_i = 350 mg L^{-1}, 1 g L^{-1} of adsorbent.

University of Malaya

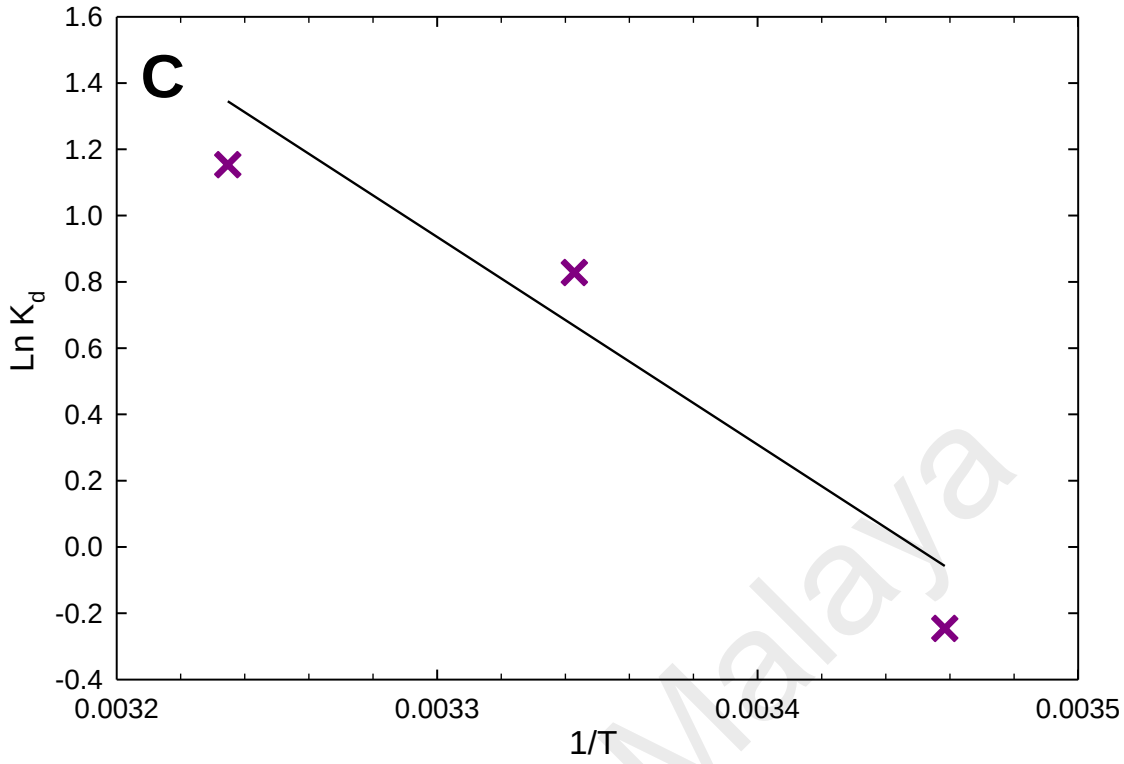

Figure 4.8 (C) thermodynamics curve at pH 6 C_i = 350 mg L^{-1}, 1 g L^{-1} of adsorbent.

Temperature is one of the factor to affect adsorption capacity of arsenate by media in liquid-solid medium. In this study, the temperature effect was studied at 289, 299 and 309 K. Figure 4.8 (A) shows that the arsenate adsorption capacity increased from 146 to 266 mg g^{-1} as temperature increased from 289 to 309 K, indicating endothermic nature and chemisorption process (Al-Degs, El-Barghouthi, El-Sheikh, & Walker, 2008). The kinetic data was fitted by pseudo-second order kinetic model as shown in Figure 4.8 (B). The increment in temperature caused not only an increment of the driving force between arsenate and MPSAC–La (0.36), but also a decrement of the energy barrier. Thermodynamics curve was constructed in Figure 4.8 (C) and analysis was conducted by evaluating the changes of enthalpy (ΔS°), entropy (ΔH°), and Gibbs free energy (ΔG°).

University of Malaya

Based on the following equations, $\ln(mq_{eq}/C_{eq})$ vs. 1/T was plotted.

$$\ln\left(\frac{mq_{eq}}{C_{eq}}\right) = \frac{\Delta S^o}{R} - \frac{\Delta H^o}{RT} \tag{4.3}$$

$$\Delta G^o = -RT\ln\left(\frac{mq_{eq}}{C_{eq}}\right) \tag{4.4}$$

Where m is the dosage of MPSAC–La (0.36) (g L^{-1}), A is the Arrhenius factor and R (8.314 J/mol/K) and T are the gas constant and temperature in K, respectively.

Table 4.6 Thermodynamic parameters of arsenate adsorption by MPSAC–La (0.36)

T (K)	Δ Gº (kJ/mol)	Δ Hº (kJ/mol)	ΔSº (J/mol K)
298	11.48	55.46	190.12
308	–29.79		
318	–42.90		

Thermodynamics constants were tabulated in Table 4.6. The positive values of ΔH° (55.46 kJ/mol) and ΔS° (190.12 J/mol K) indicate that the adsorption is endothermic and there are some structural disturbances of the MPSAC–La (0.36) during the adsorption process (S. Hong, Wen, He, Gan, & Ho, 2009; Kong et al., 2014). This structural disturbance was also proven by the results of SEM–EDS, XRD and FT–IR analyses. Since the ΔG° values show an increase of negative value with the increase of temperature, the arsenate adsorption by MPSAC–La (0.36) is efficient at higher temperature.

University of Malaya

4.6 Competition effect and regeneration

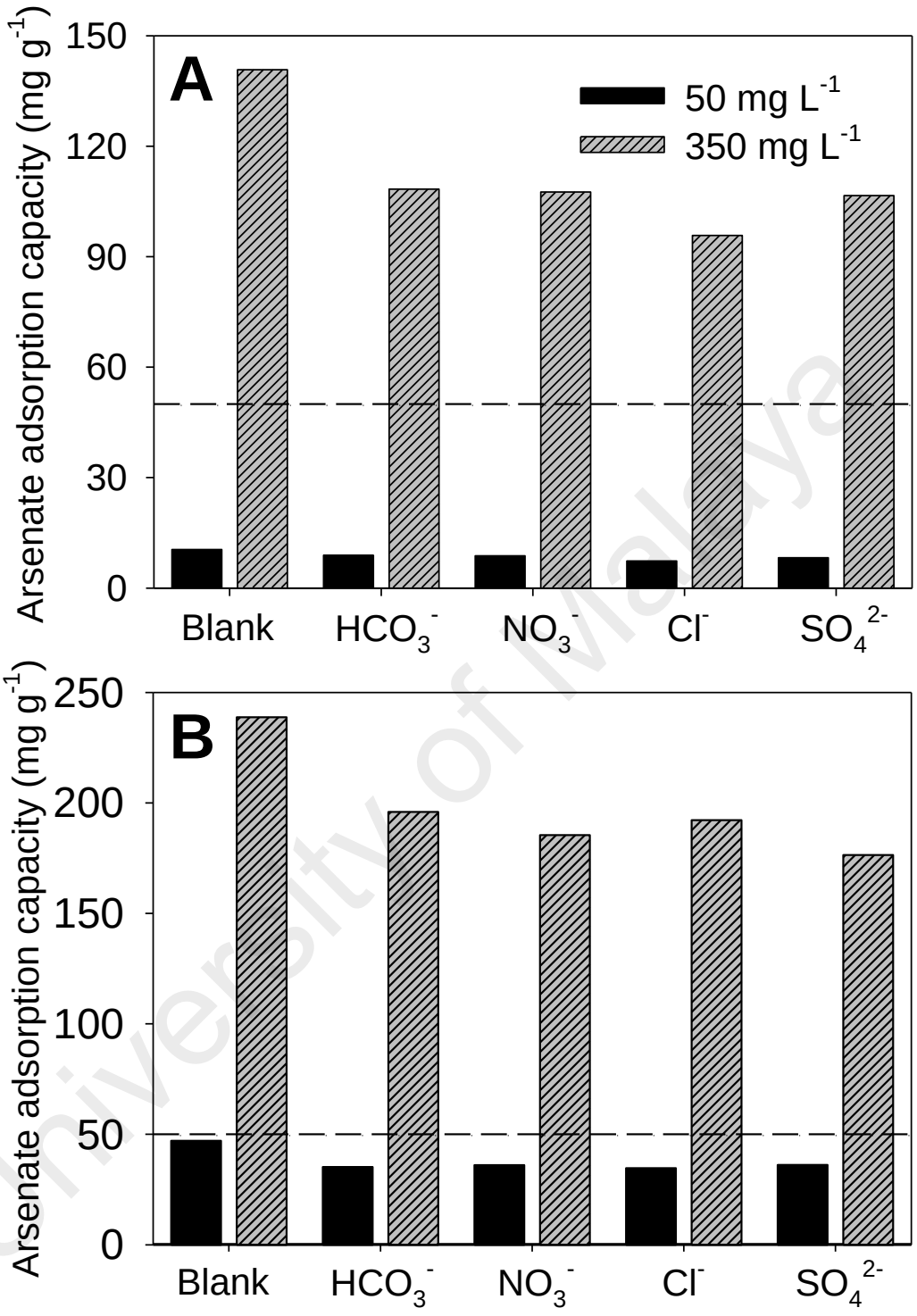

Figure 4.9(A) MPSAC and (B) MPSAC–La (0.36) competition effect of arsenate with 2.5 mmol L^{-1} of coexisting anion at pH 6, C_i = 50 and 350 mg L^{-1}, 1 g L^{-1} of adsorbent

University of Malaya

The coexisting anion (HCO^{3-}, NO^{3-}, Cl^- and SO_4^{2-}) in sodium salt compound were selected as competitive anion in this study because it were commonly found in groundwater and surface water (Patnaik, 2017). The effect of co-existing anions towards arsenate adsorption capacity was illustrated in Fig 4.9 with fixed coexisting anions concentration at 2.5 mmol L^{-1}, and two different concentrations of arsenate were chosen to simulate a wide range of contamination level at groundwater, acid mine drainage and industrial wastewater. As a result, the adsorption capacities of arsenate by MPSAC were reduced to more than 30% with the addition of Cl^- at C_i = 350 mg L^{-1} (Fig. 4.9A), while those of MPSAC–La (0.36) were less than 30% for all co-existing anions (Fig. 4.9B). Accordingly, the adsorption of arsenate to both media were interfered by anion (HCO_3^-, SO_4^{2-}, NO_3^-, Cl^-) (Liu, Zhou, Chen, Zhang, & Chang, 2013). However, MPSAC–La (0.36) has less sensitivity to anionic competition than MPSAC.

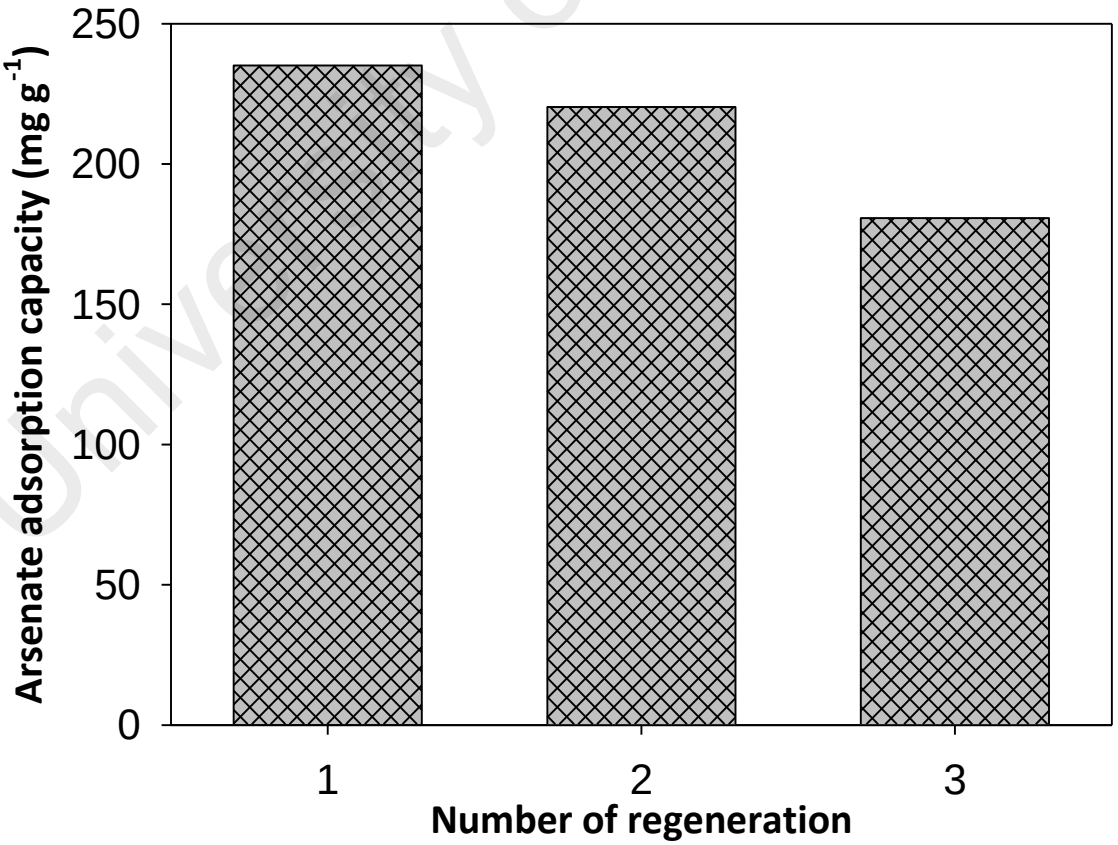

Figure 4.10 Regeneration effect for MPSAC–La (0.36) at pH 6, C_i = 350 mg L^{-1}, 1 g L^{-1} of adsorbent

University of Malaya

Figure 4.10 shows the regeneration effect for MPSAC-La (0.36) and up to three cycles of adsorption and desorption were carried out with success to examine the reusability of MPSAC–La (0.36). Once arsenate adsorption was completed, used MPSAC–La (0.36) was regenerated using 0.5 M NaOH solution. As a result, MPSAC–La (0.36) had approximately 75% of the first arsenate adsorption capacity at the third cycle. As per the analogous case, Zhang et al. (2014) reported that Fe–La composite hydroxide achieved a 75% adsorption rate at the fourth re-adsorption cycle. Presumably, the NaOH solution provides an alkaline condition either to desorb complexed arsenate due to the Donnan exclusive effect (Donnan, 1995; S. Sarkar et al., 2010) or to refresh the surface of LO in order to detach the precipitates $LaAsO_4$ and create a fresh surface of LH. Thus, it can be summarized that MPSAC–La (0.36) can be recycled effectively using NaOH solution, providing an economic advantage.

University of Malaya

4.7 Dye Isotherm Studies

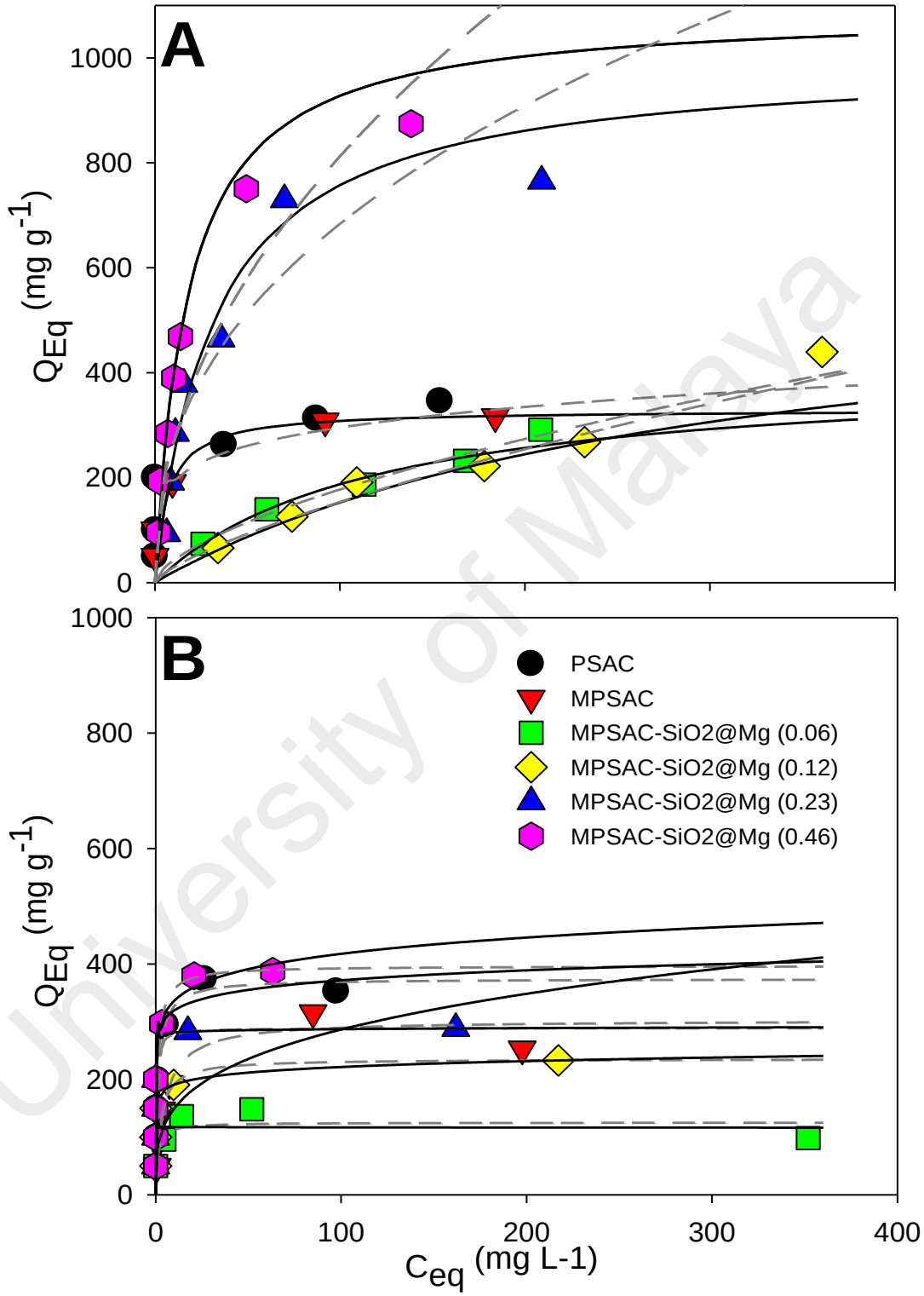

Figure 4.11 (A) adsorption isotherm of Methyl Orange, C_i = 50 ~ 1000 mg L^{-1} (B) adsorption isotherm of Methylene Blue, C_i = 50 ~ 500 mg L^{-1} on PSAC, MPSAC and MPSAC-SiO_2 impregnated with different amount of $MgNO_3$ at pH 6 and 1 g L^{-1} of adsorbent. The black color fit line is Langmuir and the gray color fit line is Freundlich isotherm model

University of Malaya

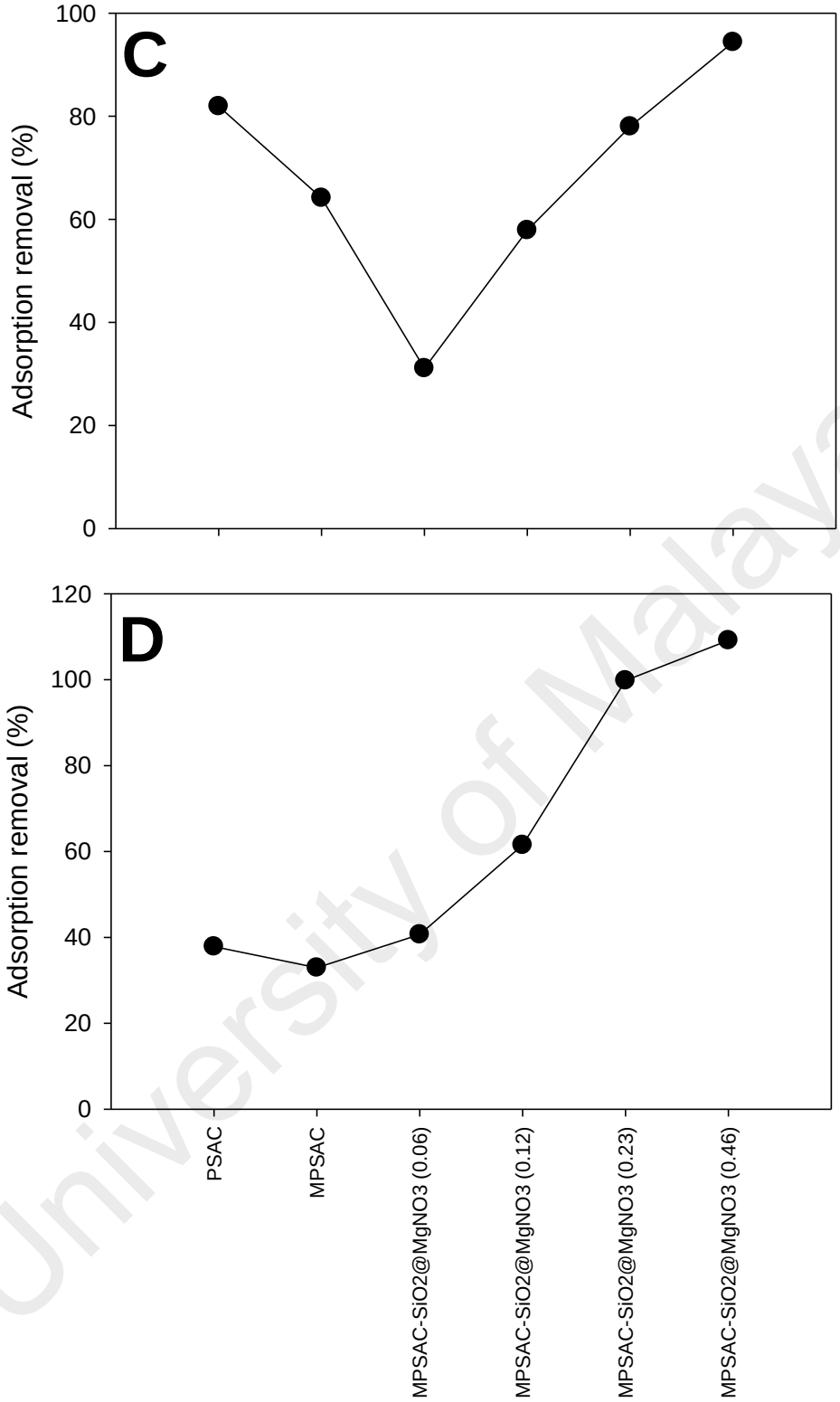

Figure 4.11 (C) Percentage removal of Methylene Blue dye removal (D) Percentage removal of Methyl Orange dye

University of Malaya

The isotherm studies show the initial concentrations were between 50 to 1000 mg L^{-1} for Methyl Orange and between 50 to 500 mg L^{-1} for Methylene Blue. The maximum initial concentration for Methyl Orange was double than Methylene Blue because MPSAC-SiO_2@$MgNO_3$ (0.23) and MPSAC-SiO_2@$MgNO_3$ (0.46) adsorbent show that Methyl Orange removal percentage is more than 90% removal at the initial concentration of 500 mg L^{-1}.

Based on Figure 4.11 (A), it shows that the Methyl Orange adsorption isotherm studies at C_{eq}, 200 mg L^{-1} for MPSAC, PSAC, MPSAC-SiO_2@$MgNO_3$ (0.23) and MPSAC-SiO_2@$MgNO_3$ (0.46) approximately achieved the removal capacities at 240 mg g^{-1}, 260 mg g^{-1}, 820 mg g^{-1}, and 994 mg g^{-1}. While at the same C_{eq} point, MPSAC-SiO_2@$MgNO_3$ (0.08) and MPSAC-SiO_2@$MgNO_3$ (0.12) show the removal capacities at 220 mg g^{-1} and 240 mg g^{-1} respectively.

Figure 4.11(B) were plotted to show the Methylene Blue adsorption isotherm studies at 200 mg L-1 of C_{eq}, MPSAC, PSAC and MPSAC-SiO_2@$MgNO_3$ (0.46) approximately achieved 320 mg g^{-1}, 380 mg g^{-1}, and 430 mg g^{-1} removal capacities. Meanwhile, for MPSAC-SiO_2@$MgNO_3$ (0.06), MPSAC-SiO_2@$MgNO_3$ (0.12), and MPSAC-SiO_2@$MgNO_3$ (0.23) achieved 100mg g^{-1}, 220 mg g^{-1}, and 280 mg g^{-1} respectively.

University of Malaya

Table 4.7 Langmuir and Freundlich isotherm parameters for Methyl Orange adsorption onto PSAC, MPSAC an and MPSAC-SiO_2 impregnated with different amount of $MgNO_3$ at pH 6, C_i (1000 mg/L)

adsorbent type	Langmuir isotherm			Freundlich isotherm		
	R^2	K_L	q_{max}	R^2	K_f	1/n
PSAC	0.991	0.0601	378.371	0.998	129.824	5.120
MPSAC	0.999	0.145	329.354	0.968	128.698	5.541
MPSAC-SiO_2@$MgNO_3$ (0.06)	0.995	0.009	406.651	0.989	9.978	1.600
MPSAC-SiO_2@$MgNO_3$ (0.12)	0.994	0.004	614.751	0.9727	5.424	1.377
MPSAC-SiO_2@$MgNO_3$ (0.23)	0.946	0.0315	997.806	0.877	103.188	2.435
MPSAC-SiO_2@$MgNO_3$ (0.46)	0.956	0.057	1091.614	0.937	87.449	2.066

Table 4.8 Langmuir and Freundlich isotherm parameters for Methylene Blue adsorption onto PSAC, MPSAC an and MPSAC-SiO_2 impregnated with different amount of $MgNO_3$ at pH 6, C_i (500 mg/L)

adsorbent type	Langmuir isotherm			Freundlich isotherm		
	R^2	K_L	q_{max}	R^2	K_f	1/n
PSAC	1	0.681	409.547	1	342.062	27.702
MPSAC	0.999	0.204	320.746	0.840	75.987	0.307
MPSAC-SiO_2@$MgNO_3$ (0.06)	0.978	0.361	155.430	0.643	94.961	0.089
MPSAC-SiO_2@$MgNO_3$ (0.12)	1	0.198	289.362	1	142.466	7.848
MPSAC-SiO_2@$MgNO_3$ (0.23)	1	0.040	389.959	1	142.658	5.893
MPSAC-SiO_2@$MgNO_3$ (0.46)	1	0.198	471.821	1	258.303	7.888

The isotherm data for both Methyl Orange and Methylene Blue dyes removal were plotted using the Langmuir and Freundlich Isotherm Model and the model's constants were calculated and tabulated in Table 4.7 and Table 4.8 for Methyl Orange and Methylene Blue dyes removal, respectively. In Table 4.7, all adsorbents show that the Langmuir determination coefficient (R^2> 0.94) are higher than the Freundlich

University of Malaya

determination coefficient (R^2 > 0.87), which indicated that Methyl Orange removal isotherm studies were best fitted using the Langmuir Isotherm Model. Next, in Table 4.8, Langmuir and Freundlich models constant for Methylene Blue dye removal were compared and showed that all of the Langmuir and Freundlich determination coefficient for all adsorbents show R^2=1, except for MPSAC and MPSAC-SiO_2@$MgNO_3$ (0.06) adsorbent that showed the Langmuir determination coefficient as R^2>0.97, which were higher than the Freundlich determination coefficient (R^2>0.64). From these observation, Methylene Blue dye removal isotherm studies were found to be best fitted isotherm studies using the Langmuir isotherm model, which is similar to Methyl Orange removal isotherm studies.

To further confirm that the adsorption of both dyes were best fitted with Langmuir isotherm model, a dimensionless constant separation factor, K_L was used to determine the Langmuir Isotherm characteristics. Different values of R_L represent different types of isotherms: irreversible (K_L=0), favorable (0<K_L<1), or unfavorable (K_L>1). The calculated K_L values for all adsorbent in both dye removal shows K_L values were between 0 and 1. Thus, it proved Langmuir Isotherm Model was favorable (H. Wang et al., 2014).

The q_{max} value for Methyl Orange removal by unmodified PSAC was 378.37 mg g^{-1}, but the highest removal was achieved by modified adsorbent with the highest $MgNO_3$ content, MPSAC-SiO_2@$MgNO_3$ (0.46) at 1019.61 mg g^{-1}, which was 2.7 times higher than that unmodified PSAC. However, the q_{max} value for Methylene Blue removal by unmodified PSAC was 409.54 mg g^{-1} and still MPSAC-SiO_2@$MgNO_3$ (0.46) was achieved at the highest removal capacity at 471.82 mg g^{-1}, which was only 1.15 times higher than unmodified PSAC. The unmodified PSAC was recorded to have significant removal capacity for Methylene Blue, which might be due to its fine particle size (~0.074mm). Rahman et al. (2012) stated in his batch test study on Methylene Blue

University of Malaya

removal by using the Activated Carbon at different particle sizes that the removal efficiency is influenced by the adsorbent's particle size due to the fact that with a smaller particle size, the surface area of adsorbent were increased and eventually provide a greater number of active sites for the adsorption to occur (Rahman, Amin, & Alam, 2012). On the other hand, the modified adsorbent, MPSAC-SiO_2@$MgNO_3$ (0.46) show a very significant removal capacity for Methyl Orange due to the cationic charges that acts as additional properties that were carried by $MgNO_3$ (Mg^{2+}) and have electrostatic attraction forces between the Methyl Orange (anionic dye). However, it is less efficient in Methylene Blue dye because both carry the same charges. Therefore, in the next batch test experiment, unmodified PSAC was used to compare its efficiency with the modified adsorbent MPSAC-SiO_2@$MgNO_3$ (0.46).

University of Malaya

4.8 Dyes Kinetic Studies

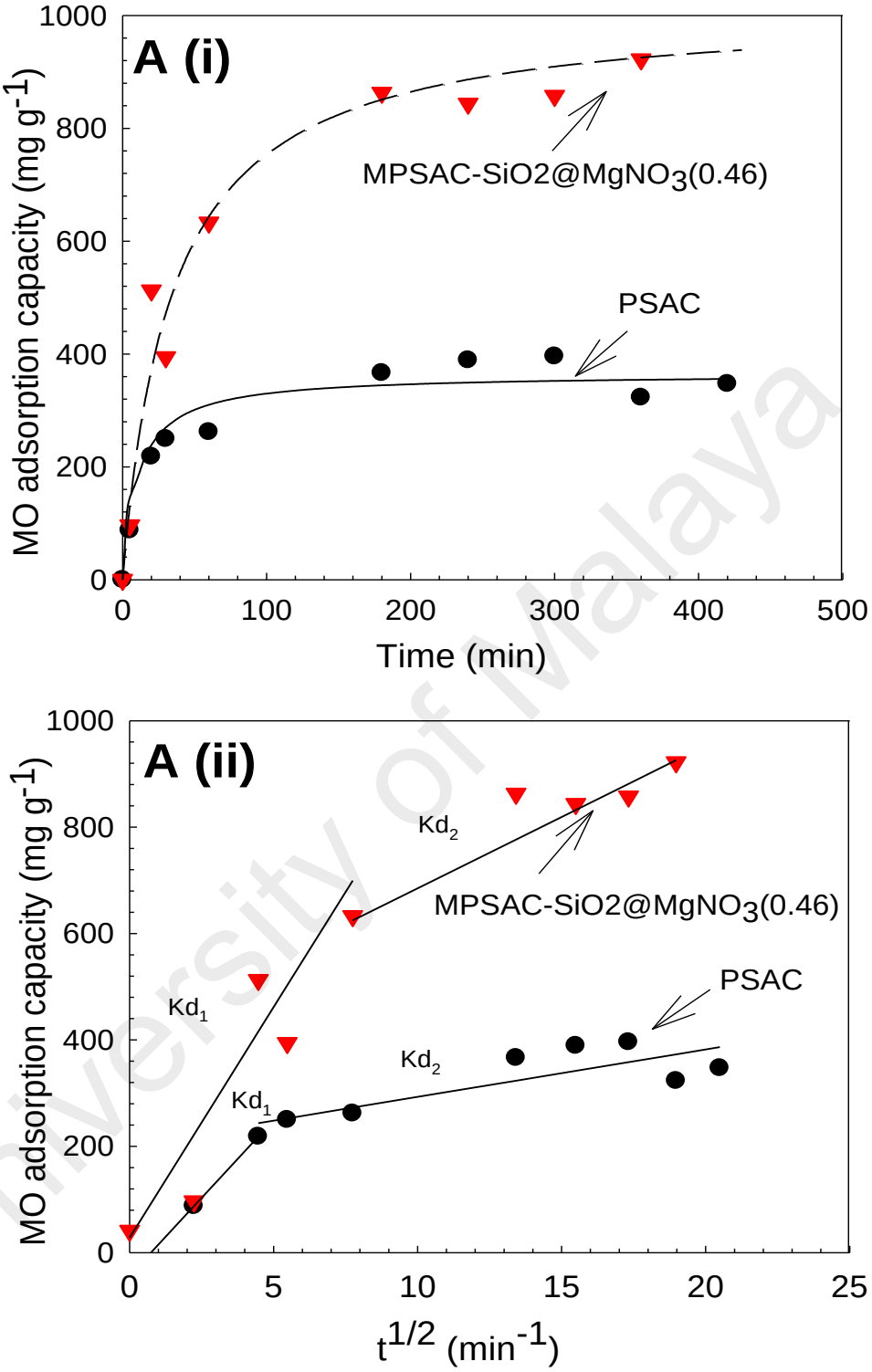

Figure 4.12 (A) (i) kinetics of Methyl Orange dye removal at pH 6, C_i = 1300 mg L^{-1}, 1.0 g L^{-1} of adsorbent, (ii) intra particle diffusion kinetic model for Methyl Orange dye removal

University of Malaya

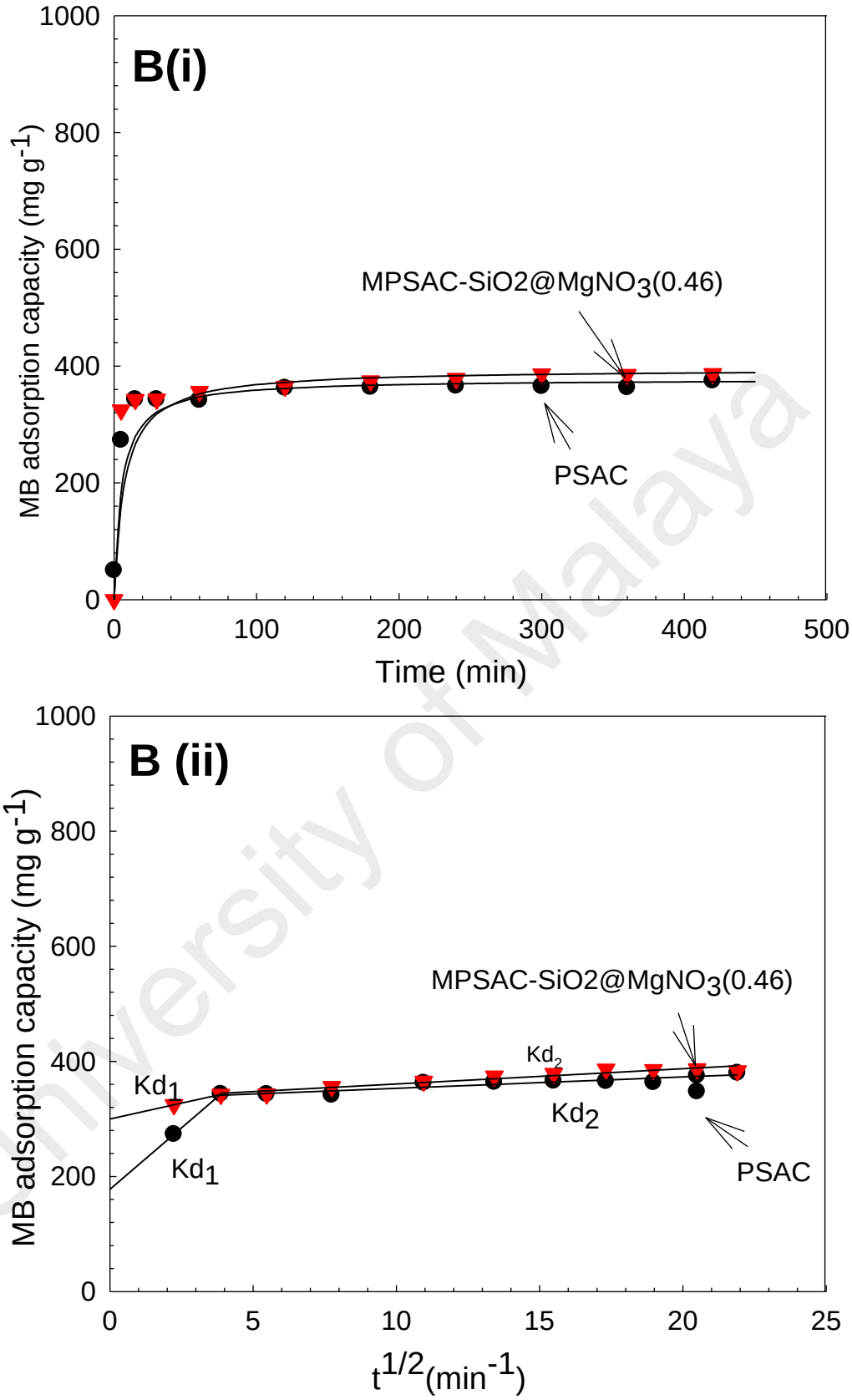

Figure 4.12 B (i) kinetics of Methylene Blue dye removal at pH 6, C_i = 1300 mg L^{-1}, 1.0 g L^{-1} of adsorbent by PSAC and MPSAC-SiO_2@$MgNO_3$ (0.46) (ii) intra particle diffusion kinetic model for Methylene Blue dye removal

University of Malaya

Figure 4.12 shows the kinetic data and pseudo-second order kinetic model of (A) Methyl Orange dye and (B) Methylene Blue dye removal by using the synthesized material, MPSAC-SiO_2@$MgNO_3$ (0.46*)* and unmodified PSAC adsorbent to compare the adsorption kinetic pattern. Based on both figures, all of the kinetic data were best fitted using the pseudo second order kinetic model with $R^2 > 0.98$. In figure 4.12 (A), Methyl Orange dye kinetic data was observed to have a moderate adsorption rate for MPSAC-SiO_2@$MgNO_3$ (0.46), but a slow adsorption rate for the unmodified PSAC. This phenomenon can be explained through the percentage removal comparison, whereby at first 30 minutes, MPSAC-SiO_2@$MgNO_3$ (0.46*)* and the unmodified PSAC shows the percentage removal of 30% and 19% of methyl orange adsorbed over the equilibrated capacity (q_{eq}), respectively. Then, at 180 minutes, the percentage removal for MPSAC-SiO_2@$MgNO_3$(0.46) was significantly increased up to 83%, while a slow increase was observed for the unmodified PSAC of only 28%. Based on the pseudo-second order kinetic model, the q_{eq} of MPSAC-SiO_2@$MgNO_3$(0.46*)* and the unmodified PSAC are 1042.47 mg g^{-1} and 364.64 mg g^{-1}, respectively. As in previous isotherm studies, the adsorption isotherm capacity ratio for MPSAC-SiO_2@$MgNO_3$ (0.46*)* and the unmodified PSAC are 2.7:1, while based on the kinetic studies, the adsorption capacity ratio is 2.9:1, which is almost similar to previous studies that proved the batch experimental tests data were reliable.

Subsequently, figure 4.12(B) shows the methylene blue dye removal kinetic data by MPSAC-SiO_2@$MgNO_3$ and the unmodified PSAC, which shows a fast and slow adsorption rate for both adsorbents. Again, this phenomenon can be described through the percentage removal comparison, whereby at the first 30 minutes, MPSAC-SiO_2@$MgNO_3$ (0.46*)* and the unmodified PSAC show the percentage removal of 68.6% and 68.4% of methylene blue adsorbed over the equilibrated capacity (q_{eq}), respectively. Then at 180 minutes, the percentage removal for both adsorbent increased to 73%

University of Malaya

removal, which is approximately only 4% increment. Based on the pseudo-second order kinetic model, the q_{eq} of MPSAC-SiO_2@$MgNO_3$ (0.46*)* and the unmodified PSAC are 395.05 mg g^{-1} and 377.84 mg g^{-1}, respectively. As in previous isotherm studies, the adsorption isotherm capacity ratio for MPSAC-SiO_2@$MgNO_3$ (0.46*)* and the unmodified PSAC are 1.15:1. Meanwhile, based on the kinetic studies, the adsorption capacity ratio is 1.05:1, which is almost similar to the previous studies that represent the reliability of the batch experimental tests data.

To further investigate the adsorption rate and removal mechanism of Methyl Orange and Methylene Blue dyes, both pseudo-first order pseudo-second order kinetic models were compared. Based on the data tabulated in Table 4.9, unmodified PSAC adsorbent showed that the pseudo-first order kinetic model, R^2=0.496, which is less than the pseudo-second order kinetic model, R^2=0.982. Meanwhile, MPSAC-SiO_2@$MgNO_3$ (0.46*)* showed pseudo-first order kinetic model (R^2=0.739) is less than the pseudo-second order kinetic model (R^2=0.988) for Methyl Orange dye. On the other hand, the data for Methylene Blue dye removal was tabulated in Table 4.10 proved the same case happened for both adsorbents. The pseudo-first order kinetic model for PSAC (R^2=0.605) is less than the pseudo-second order kinetic model (R^2=0.999) and the pseudo-first order kinetic model for MPSAC-SiO_2@$MgNO_3$ (0.46) (R^2=0.707) is less than the pseudo-second order kinetic model (R^2=0.999). Based on these comparisons, all cases showed the R^2 value for the pseudo-second order kinetic model is significantly higher than the pseudo-first order kinetic model, which proved that chemisorption influenced the removal mechanism (Y. Ho & G. McKay, 1998).

University of Malaya

To further investigate, intra particle diffusion (IPD) model were calculated based on the equation below:

$$q_t = K_{diff} t^{1/2} + C$$

Where K_{diff} is intra particle diffusion rate constant (mg g^{-1} min^{-1}) and C is the intercept.

The intra particle diffusion models were then plotted as shown in figure 4.12(A) (ii) and 4.12 (B) (ii). The values of intercept, C can be used to determine the thickness of boundary layer because the larger the intercept, the greater the influenced surface sorption in the rate-controlling step (Demirbas & Nas, 2009; Kavitha & Namasivayam, 2007). Based on the intra particle diffusion illustrated figures, MPSAC-SiO_2@$MgNO_3$ (0.46) adsorbent showed a higher C value than the unmodified PSAC adsorbent for both Methyl Orange and Methylene Blue dye removals, which proved the surface sorption has a greater influence in the dye removal using MPSAC-SiO_2@$MgNO_3$ (0.46) adsorbent.

As described in previous studies, intra particle diffusion model is plotted to determine the diffusion mechanism. When the linearized curve did not intersect at the origin, it showed that the intra particle diffusion is not the only limiting rate. Based on the plotted graph, it showed that all of the IPD kinetic model did not intersect at origin, which proved that the intra particle diffusion is not the only limiting rate and external mass transfer mechanism, such as surface sorption may have happened. Further batch test and characterization analysis were conducted to strengthen the data analysis.

University of Malaya

Table 4.9 Parameters of pseudo–first and pseudo–second order kinetic models for Methyl Orange dye adsorption by MPSAC-SiO_2@$MgNO_3$ (0.46) and PSAC.

Adsorbent	Pseudo first order kinetic model			Pseudo second order kinetic model			
	q_e (mg g^{-1})	K_{ad} (min^{-1})	R^2	q_e (mg g^{-1})	k_2 (g mg^{-1} min^{-1})	v_0 (mg g^{-1} min^{-1})	R^2
PSAC	503.10303	0.001988	0.496	364.744	0.0003	34.50	0.982
MPSAC-SiO_2@$MgNO_3$ (0.46)	408.564	0.002448	0.739	1042.474	0.00002	26.062	0.988

Table 4.10 Parameters of pseudo–first and pseudo–second order kinetic models for Methylene Blue dye adsorption by MPSAC-SiO_2@$MgNO_3$ (0.46) and PSAC.

Adsorbent	Pseudo first order kinetic model			Pseudo second order kinetic model			
	q_e (mg g^{-1})	K_{ad} (min^{-1})	R^2	q_e (mg g^{-1})	k_2 (g mg^{-1} min^{-1})	v_0 (mg g^{-1} min^{-1})	R^2
PSAC	343.839	0.0029	0.605	377.838	0.0005	71.577	0.999
MPSAC-SiO_2@$MgNO_3$ (0.46)	422.037	0.0023	0.707	395.045	0.0003	54.320	0.999

University of Malaya

Table 4.11 Comparison of Methyl Orange sorption capacities and speeds with other references

Adsorbent	Pseudo second order kinetic model						
	Initial Methyl Orange concen-tration (mg L^{-1})	**Adsorbent dosage (g L^{-1})**	**Final pH**	**q_e (mg g^{-1})**	**v_0 (mg g^{-1} min^{-1})**	**R^2**	**reference**
[1]MPSAC-SiO_2@MgNO_3 (0.46)	1300	1.0	6.0	1042.47	26.062	0.988	This study
[2]FAC	450	0.4	7.0	862.25	0.184	0.999	(Gong et al., 2013)
[3]MOF-235	40	0.1	5.6	477	0.0009	0.998	(E. Haque, Jun, & Jhung, 2011)
[4] CS/Mt-OREC	40	0.12	3.0	5.11	0.01957	0.995	(Zeng et al., 2015)
[5]MIL-101 MOFs	30	1.0	*	8.85	0.028	0.995	(Shen, Luo, Zhang, & Luo, 2015)
[6]CNTs-A	150	0.75	*	161.3	0.002	0.999	(Ma et al., 2012)

[1] MPSAC-SiO_2@$MgNO_3$(0.46)-$MgNO_3$ with silica coated magnetically palm shell waste-based activated carbon, 0.46:192, MgNO3: urea
[2] FAC-Finger-Citron-Residue-Based Activated Carbon
[3]MOF-235metal-organic framework material, iron terephthalate
[4] CS/Mt-OREC-Chitosan/organic rectorite-Fe_3O_4
[5]MIL-101 MOFs-Hierarchically mesostructured MIL-101 metal–organic frameworks with different mineralizing agents
[6]CNTs-A-Activated carbon nanotubes
*Not Available

University of Malaya

Table 4.12 Comparison of Methylene Blue sorption capacities and speeds with other references

Adsorbent	Pseudo second order kinetic model						
	Initial Methyl Orange concen-tration (mg L^{-1})	**Adsorbent dosage (g L^{-1})**	**Final pH**	**q_e (mg g^{-1})**	**v_0 (mg g^{-1} min^{-1})**	**R^2**	**reference**
[1]MPSAC-SiO2@MgNO3 (0.46)	500	1.0	6.0	395.04	54.320	0.988	This study
[2]FAC	450	0.4	7	548.17	0.396	0.999	(Gong et al., 2013)
[3]MOF-235	40	0.1	5.6	187	0.00022	0.998	(E. Haque et al., 2011)
[4] CS/Mt-OREC	40	0.12	6.0	9.89	0.0322	0.999	(Zeng et al., 2015)
[5]MIL-101 MOFs	30	1.0	*	67.4	-0.02	0.992	(Shen, Luo, et al., 2015)
[6]CNTs-A	300	0.75	*	454.5	0.0007	0.999	(Ma et al., 2012)

[1] MPSAC-SiO_2@$MgNO_3$(0.46)-$MgNO_3$ with silica coated magnetically palm shell waste-based activated carbon, 0.46:192, MgNO3:urea
[2] FAC-Finger-Citron-Residue-Based Activated Carbon
[3]MOF-235metal-organic framework material, iron terephthalate
[4] CS/Mt-OREC-Chitosan/organic rectorite-Fe_3O_4
[5]MIL-101 MOFs-Hierarchically mesostructured MIL-101 metal–organic frameworks with different mineralizing agents
[6]CNTs-A-Activated carbon nanotubes
*Not Available

University of Malaya

4.9 Dyes pH effects

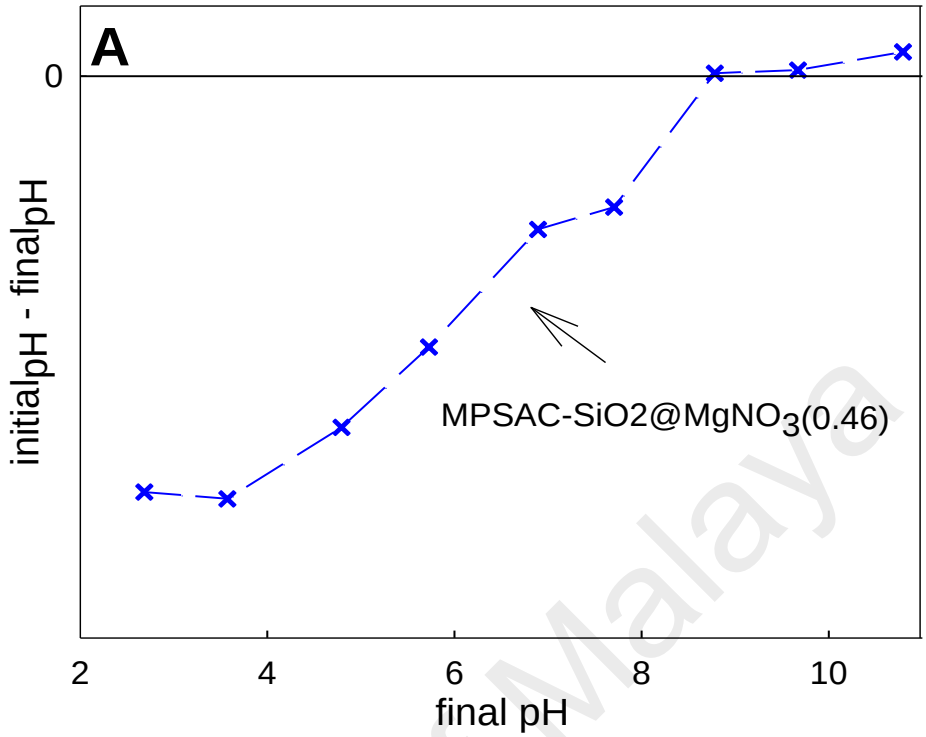

Figure 4.13 (A) pHpzc MPSAC-SiO_2@$MgNO_3$(0.46)

Figure 4.13 (A) illustrated pHpzc for MPSAC-SiO_2@$MgNO_3$ (0.46) adsorbent to prove the influenced of electrostatic attraction force mechanism between adsorbent and dye ion. The pH_{pzc} for MPSAC-SiO_2@$MgNO_3$ (0.46) was 8.87. The pH_{pzc} reported by previous research on LDH (Layered Double Hydroxide) was between 6.8 to 8.9 and consistent with the current study (Das, Das, & Parida, 2003; Yang, Shahrivari, Liu, Sahimi, & Tsotsis, 2005). At pH < pH_{pzc}, the adsorbent surface will be dominated by the positive charged ion due to the presence of Fe^{2+} (nano-magnetite), Silica, Si^{2+} and Magnesium, Mg^{2+} ion. Thus, at pH lower than pHpzc, Methyl Orange dye (anionic dye) will be adsorbed at a higher rate because of the electrostatic attraction forces effect between the anionic dye onto the positive charge on adsorbent surfaces (Reddy, Krushnamurty, Mahammadunnisa, Dayamani, & Subrahmanyam, 2015). Unfortunately, it gives disadvantage to the Methylene Blue dye (cationic dye) due to the repulsion effect between similar charge ions.

University of Malaya

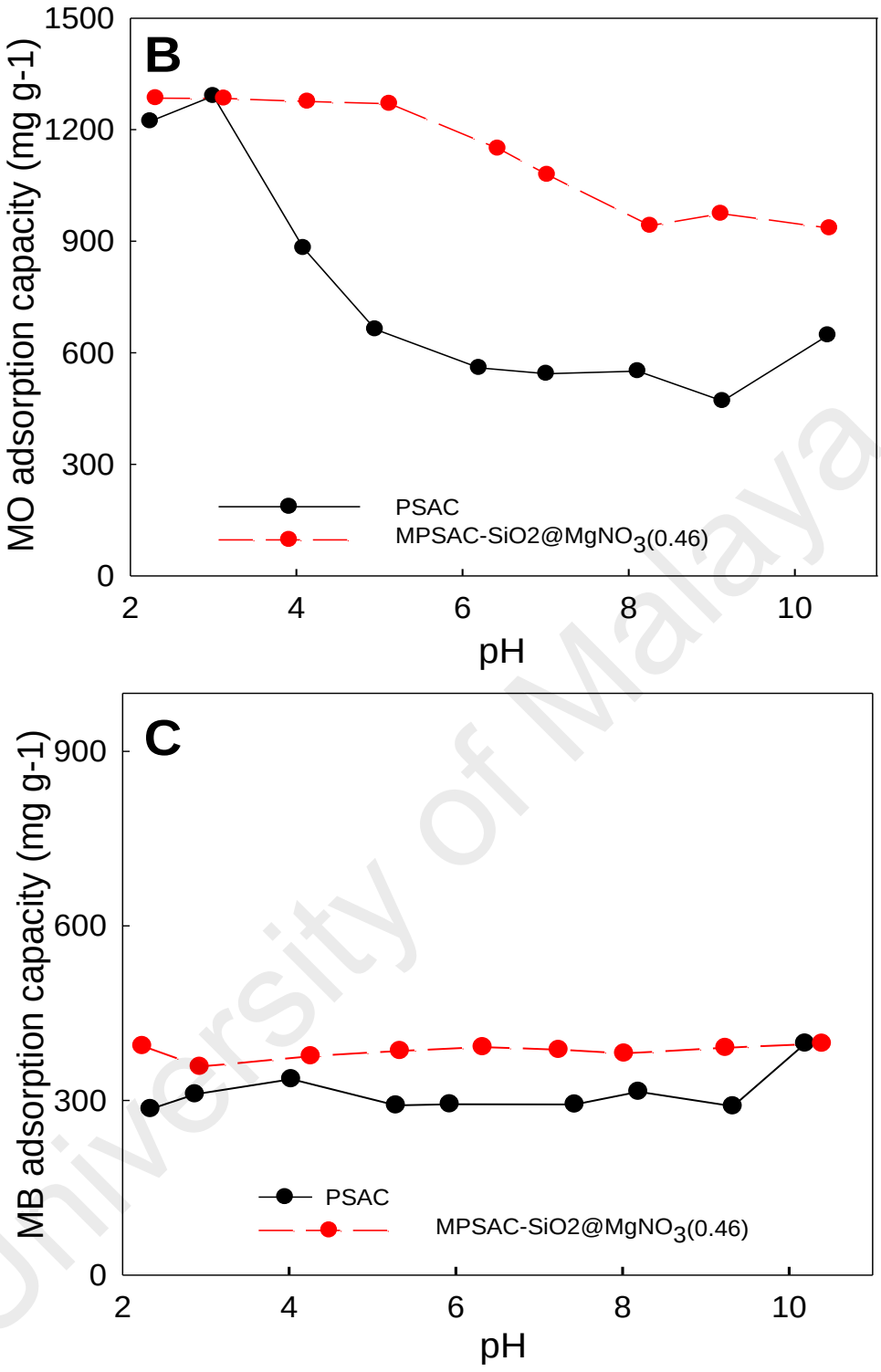

Figure 4.13 (B) pH effect studies for Methyl Orange dye, C_i=500 mg L^{-1} (C) pH effect studies for Methylene Blue dye, C_i=1300 mg L^{-1}

University of Malaya

Figure 4.13 (B) shows Methyl Orange dye removal pH studies by using the unmodified PSAC and MPSAC-SiO_2@$MgNO_3$(0.46) adsorbents. Approximately at pH ~2 to ~5, MPSAC-SiO_2@$MgNO_3$ (0.46) adsorbent is able to remove Methyl Orange dye at the highest capacity of 1280 mg g^{-1} and made it decreased to 1270 mg g^{-1}, where the adsorption capacity continually decreased steadily at pH ~6 to ~7 with the adsorption capacity of 1150 mg g-1 to 1080 mg g-1. As previous pH batch tests were kept constant at pH~6. The adsorption capacity obtained from pH studies at pH ~6 to ~7 for Methyl Orange is reliable as it is almost similar to the value of q_{max} during the isotherm studies (1091 mg g^{-1}). The Methyl Orange adsorption capacities were observed to further decrease at pH~ 8, but a slight increment of adsorption capacity was observed as the pH increased up to pH 10 proving that other mechanisms like π-π electron donor acceptor and pore filling might have happened during the adsorption process (Ma et al., 2012).

The same phenomenon was observed when the unmodified PSAC was used to remove Methyl Orange, whereby the highest capacity of 1290 mg g-1 was recorded at pH~3, but decreased significantly when pH is more than 3.The same pattern were observed by Ghasemian et al. (2016) using synthesized SiCNP-AC and Ai et al. (2011) using Mg-Al double Hydroxide to remove Methyl Orange dye (Ai, Zhang, & Meng, 2011; Ghasemian & Palizban, 2016). To explain this phenomena, Chen et al. (2010) stated that Methyl Orange has chromophores with two different chemical structures, which are azo bond and anthraquinone that are influenced by the pH of solution. The chemical structures are illustrated below:

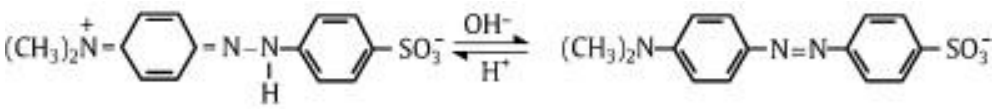

University of Malaya

On the other hand, H^+ ions are available in abundance on both adsorbent surfaces in acidic condition to help attract Methyl Orange anionic molecules. Eventually, available H^+ ions were less in alkaline condition, but OH^- ions were available in abundance that caused repulsion between the OH^- anion and Methyl Orange anionic molecules (Hamdaoui & Naffrechoux, 2007). However, MPSAC-SiO_2@$MgNO_3$ (0.46) surface contained Mg^{2+}, Si^{2+}, Fe^{2+} that provide more cationic molecule along a wide pH in order to help enhance the ability of Methyl Orange adsorption. Thus, the removal capacity recorded by MPSAC-SiO_2@$MgNO_3$ (0.46) at most pH range are much higher than the unmodified PSAC adsorbent.

Figure 4.13 (C) shows Methylene Blue dye removal in pH studies using the unmodified PSAC and MPSAC-SiO_2@$MgNO_3$ (0.46) adsorbents. Based on the illustrated figure, ~pH 2, MPSAC-SiO_2@$MgNO_3$ (0.46) showed the adsorption capacity of 393.5 mg g^{-1} that decreased when pH > ~2 and there is no significant reduction or increment observed at pH > ~3 to pH < ~10. The highest adsorption capacity of 397.7 mg g^{-1} was recorded at pH 10.4. Meanwhile, the unmodified PSAC's adsorption capacity at pH~2 to pH~4 had a slight increment from 285.4 mg g^{-1} to 336.9 mg g^{-1} and decreased at pH > ~4 while remaining constant until pH~9, but significantly increased when pH achieved 10.4 with adsorption capacity of 397.9 mg g^{-1}. The same phenomenon was observed by Said et al. (2012) using sugarcane bagasse modified with propionic acid where it stated that Methylene Blue dye removal was not influenced by pH of solution. The other reason to support this phenomenon is that Methylene Blue carried cationic properties in which at acidic condition, the H^+ ion and other cations available caused repulsion and competition effect between the Methylene Blue dye molecules and did not aid in the removal process. The highest adsorption capacity recorded for both adsorbents is at pH 10.4. Due to the abundance availability of OH^- in alkaline condition, Methylene Blue dye removal performance was improved.

University of Malaya

4.10 Dyes Competition Anion Studies

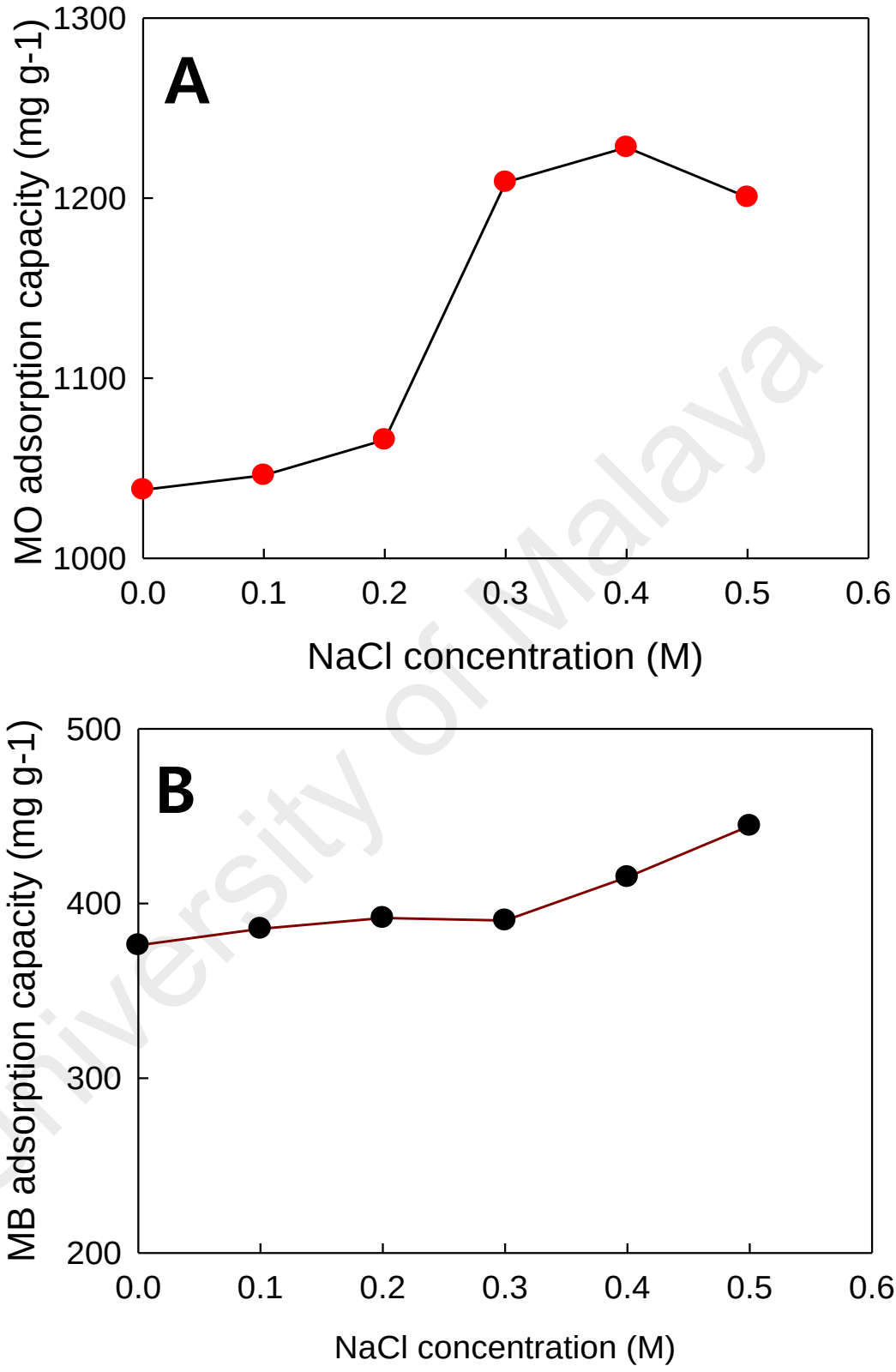

Figure 4.14 Effect of ionic strength (NaCl) on (A) Methyl Orange, C_i=1300 mg L^{-1} and (B) Methylene Blue dye, C_i=500mg L^{-1} adsorption by MPSAC-SiO_2@$MgNO_3$ (0.46) at pH 6, 1.0 g L^{-1} of adsorbent

University of Malaya

Commonly, Sodium Chloride (NaCl) salt is used as a stimulator in dyeing process. Thus, NaCl solution was used as a competing anion to observe its effect in Methyl Orange and Methylene Blue dye removal. Figure 4.14 (A) showed Methyl Orange dye adsorption capacity at 0 M- 0.5 M NaCl concentration, whereby 0 M NaCl concentration was set up as controlled variable. Based on the plotted graph, Methyl Orange adsorption capacity showed a slight increment from 0 M NaCl (1038 mg g^{-1}) to 0.2 M NaCl (1065.8 mg g^{-1}) and is significantly increased to 1208.8 mg g^{-1} at 0.3 M NaCl with the highest adsorption capacity recorded at 0.4 M NaCl (1228 mg g^{-1}) was introduced. Eventually, the adsorption capacity decreased to 1200 mg g^{-1} when 0.5 M NaCl was used. Meanwhile, Figure 4.10 (B) showed Methylene Blue dye adsorption capacity was at the same NaCl concentration range. From the observation, at 0 M until 0.3 M NaCl concentration introduced, the Methylene Blue adsorption capacity were not much affected and only significantly increased when 0.4 M to 0.5 M NaCl concentration introduced.

Based on the theory, when there is an electrostatic attraction force between the adsorbent and adsorbate, increment of NaCl in solution will cause the adsorption capacity to decrease. In contrast, when the electrostatic attraction forces between adsorbent and adsorbate repelled, increment of NaCl in solution will cause the adsorption capacity to increase (Alberghina, Bianchini, Fichera, & Fisichella, 2000). Supposedly, MPSAC-SiO_2@$MgNO_3$ (carry positive charge) will have attraction force with Methyl Orange (anionic dye) and have repulsion force with Methylene Blue (cationic dye). Interestingly, the experimental result did not support the theories, whereby the Methyl Orange adsorption capacity should decrease, but was observed otherwise, while Methylene Blue adsorption capacity did not show a significant increment when NaCl introduced increased. Ma et al. (2012) also observed the same phenomena using synthesized CNTs-A (carry negative charge) adsorbent, whereby Methyl Orange dye (anionic dye) was well explained using the theory, but Methylene Blue (cationic dye) did not.

University of Malaya

The significant increase in Methyl Orange adsorption capacity when NaCl addition is increased was assumed to happen because of the dimerization of Methyl Orange dye in the solution (Al-Degs et al., 2008). Al degs et al. (2008) also explained the variety of mechanisms that have been proposed to explain this aggregation. These forces can be attributed to ion-dipole forces, dipole-dipole forces, van der Waals forces and dispersion forces arising from delocalized π electrons, which occur between dye molecules in the solution.

University of Malaya

4.11 Dyes Regeneration Effect

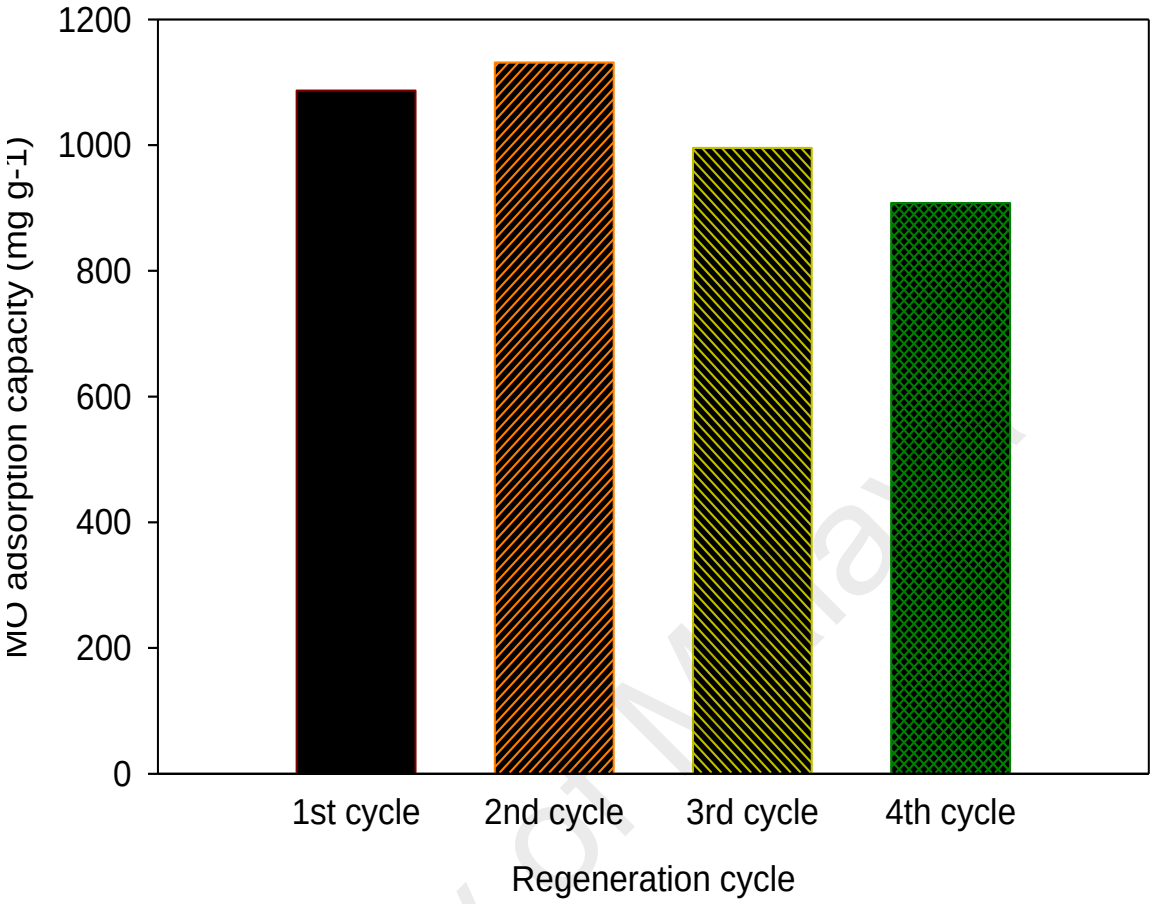

Figure 4.15 Regeneration effect for MPSAC-SiO_2@$MgNO_3$ (0.46) at pH 6, Methyl Orange dye, C_i = 1300 mg L^{-1}, 1 g L^{-1} of adsorbent

Nowadays, synthesized adsorbent with regeneration ability is a practically important feature to be classified as a green adsorbent. The regeneration studies on MPSAC-SiO2@$MgNO_3$ (0.46) adsorbent were carried out using the used-adsorbent to remove Methyl Orange dye since it has a more significant capability to remove Methyl Orange than Methylene Blue dye.

The used-adsorbent will be washed repeatedly using distilled water to remove Methyl Orange dye until the orange color is lessen followed by the drying process. Then, the dried-used-adsorbent was thermally treated at 500˚C to decompose any methyl orange left on the surface of the adsorbent. Zhu et al. (2005) described in his LDH (Layered Double Hydroxide) study, the LDH surface is capable to be regenerated through calcination due to the "memory effect", which means almost all of the adsorbed organic

pollutant can be eliminated (Zhu, Li, Xie, & Xin, 2005). Figure 4.15 shows the regeneration effect for MPSAC-SiO_2@$MgNO_3$ (0.46) up to four successful cycle adsorption-desorption. After the first regeneration, it was recorded that the adsorption capacity for the second regeneration cycle increased up to 4% and achieved 104% of the first regeneration cycle. However, it decreased down to 8% and achieved 92% of the first regeneration cycle. The adsorption capacity further decreased in the next regeneration cycle and 84% of the first regeneration cycle was obtained at the fourth regeneration cycle. The same phenomenon was also experienced by Zhu et al. (2005) in the regeneration of LDH/CLDHs, that indicated the thermal regeneration (calcination) is only achievable for the first two regeneration cycles and further regeneration cycle will suffer a loss in sorption capacities. Zhu et al. (2005) also described the large loss of sorption capacities might be due to the LDH crystallinity structure, which was reduced because of a certain amount of dye that was incorporated into the adsorbent surface and disturbed the reconstruction of the crystallinity structure during the repeated thermal regeneration. However, based on this study, even though the structural disturbance caused the adsorption capacity to reduce during the thermal regeneration, the newly developed adsorbent still shows a high adsorption capacity at the fourth cycle, which proved that it is competent to be a cost-effective adsorbent.

University of Malaya

4.12 Mechanism of dye removal by MPSAC-SiO_2@$MgNO_3$(0.46) adsorbent

In order to elucidate the Methyl Orange removal mechanism, spectroscopic analyses such as XRD, FESEM–EDX, N_2 gas isotherm and FT–IR were performed for the prepared adsorbent and adsorbent with Methyl Orange loaded.

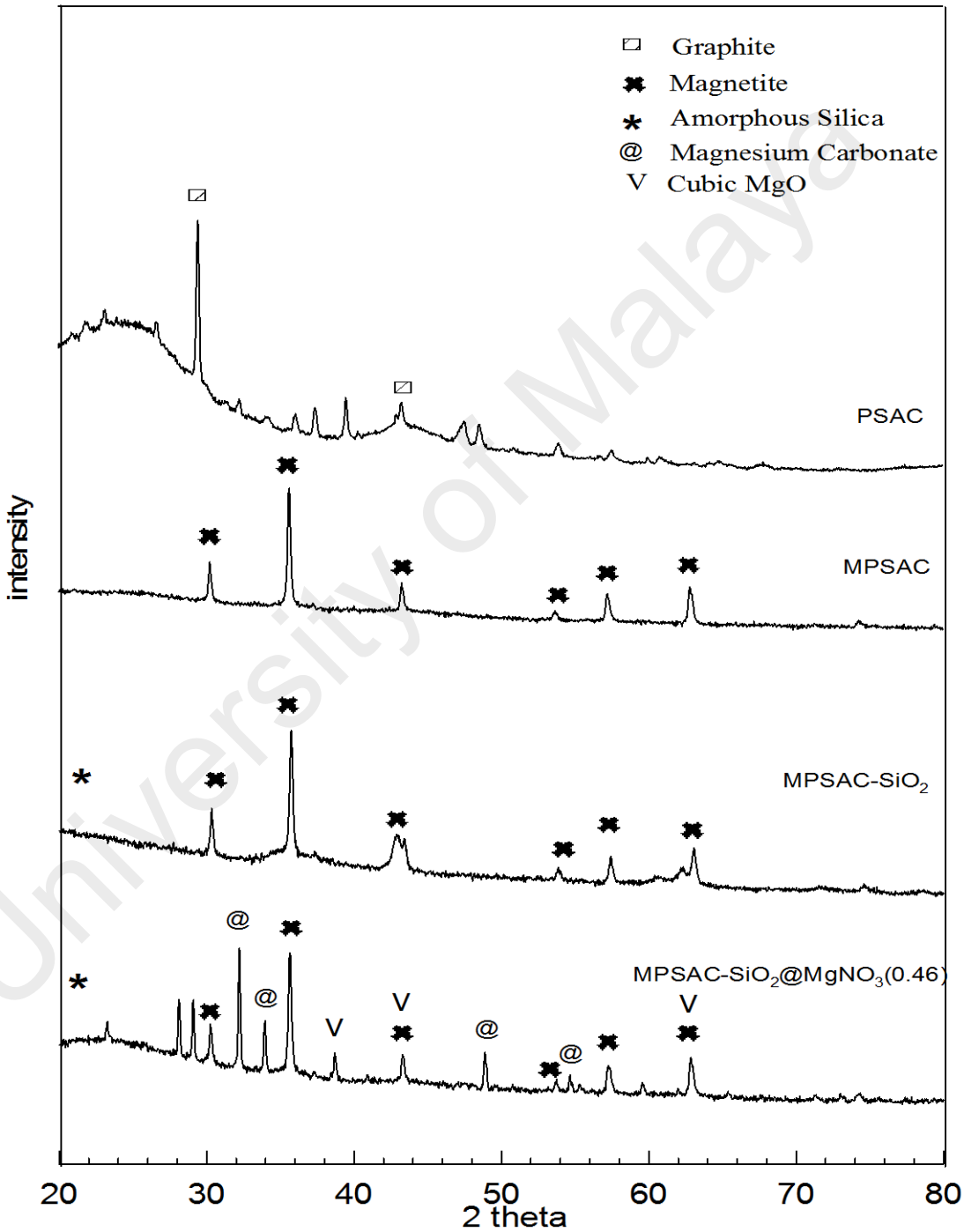

Figure 4.16 XRD results of PSAC, MPSAC, MPSAC-SiO_2, MPSAC-SiO_2@$MgNO_3$(0.46) adsorbents

University of Malaya

Figure 4.16 shows the XRD results of the PSAC, MPSAC, MPSAC-SiO_2 and MPSAC-SiO_2@$MgNO_3$ (0.46). PSAC was observed to have significant graphite peaks at 28˚ and 43˚, respectively. When nano-magnetite was introduced on the surface of MPSAC, new peaks that emerged at 29.5˚, 37˚, 42.5˚, 54.5˚, 56.5˚, 62.5˚ theta were corresponding to (220), (311), (400), (422), (511) and (440) planes of the magnetite based on JCPDS file: 19-0629 (B. Y. Yu & Kwak, 2010). After MPSAC-SiO_2 were coated with silica, the amorphous silica peaks were found at 20˚ to 28˚ (Libera, Elam, & Pellin, 2008) and the magnetite planes were not changed, indicating that the nano-magnetite (Fe_3O_4) were trapped under the SiO_2 nanoparticles coated layer (Feng et al., 2010). The incorporation of $MgNO_3$ caused many new sharp peaks formed at 32˚,34˚ ,42.5˚, 49˚ 55˚ theta and were consistent to the (104) (006) (113) (202) (116) planes of Magnesium Carbonate, $MgCO_3$ (Magnesite) based on JCPDS file: 80-0042 (Gao, Zhang, Li, Lang, & Xu, 2008). Chowdury et al. (2016) described in his study that the formation of Magnesium carbonate instead of Magensium Oxide or Magnesium Hydroxide might be because of the hydrothermal condition, where urea undergoes slow decomposition and formed NH_3 and CO_2 followed by hydrolysis that produced OH^- and HCO_3^- (I. H. Chowdhury, Chowdhury, Bose, Mandal, & Naskar, 2016). The formation mechanism can be expressed by the following equation:

$$CO(NH)_2 + H_2O \rightarrow 2NH_3 + CO_2 \quad (4.5)$$

$$NH_3 + H_2O \rightarrow NH_4^+ + OH^- \quad (4.6)$$

$$CO_2 + H_2O \rightarrow H^+ + HCO_3^- \quad (4.7)$$

$$5Mg(NO_3)_2 + 6OH^- + 4HCO_3- \rightarrow Mg_5(CO_3)_4.4H_2O + 10NO_3^- \quad (4.8)$$

University of Malaya

Still, some of $MgCO_3$ were converted successfully into cubic MgO through the calcination process and its peak can be seen at 38˚, 43˚ and 63˚ theta, which were consistent with (111) (200) and (220) planes based on JCPDS file no. 45-946 (I. H. Chowdhury et al., 2016).

The probable decomposition of $MgCO_3$ crystallization could be explained through the following equations:

$$Mg_5(CO_3)_4(OH)_2.4H_2O \rightarrow Mg_5(CO_3)_4(OH)_2 + 4H_2O \quad (4.9)$$

$$Mg_5(CO_3)_4(OH)_2 \rightarrow 4MgCO_3 + MgO + H_2O \quad (4.10)$$

$$MgCO_3 \rightarrow MgO + CO_2 \quad (4.11)$$

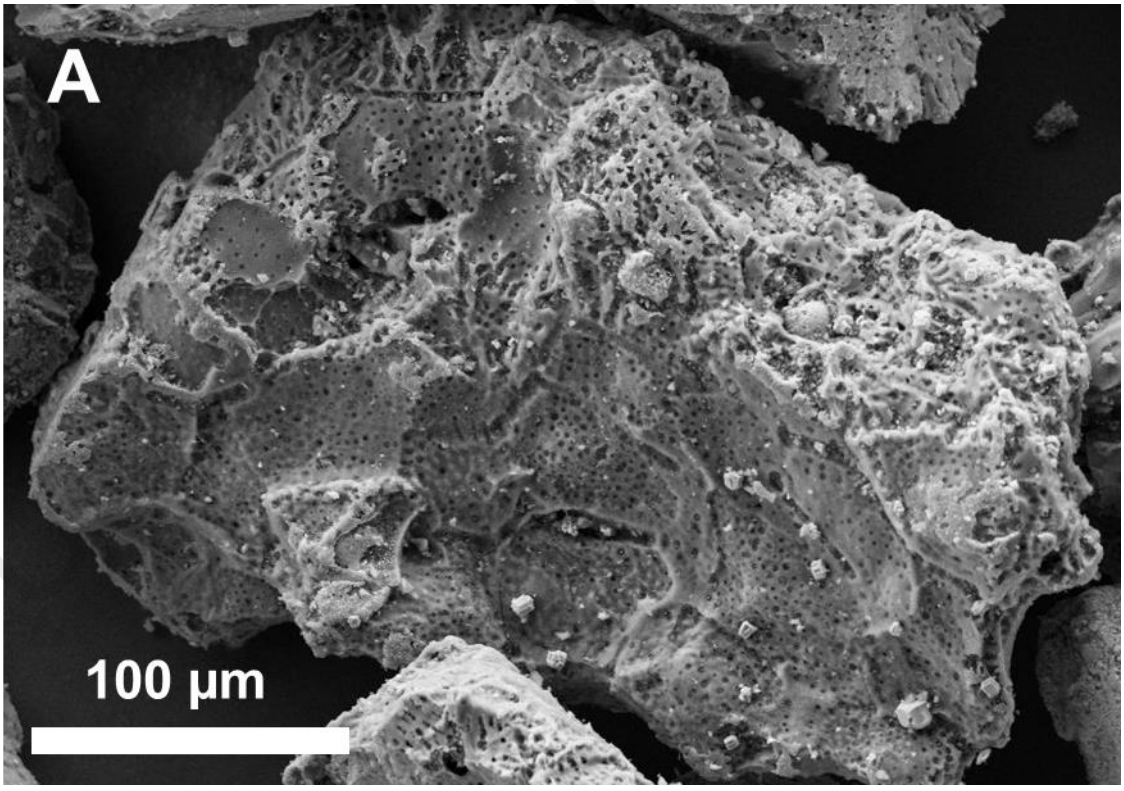

Figure 4.17 (A) FESEM for PSAC

University of Malaya

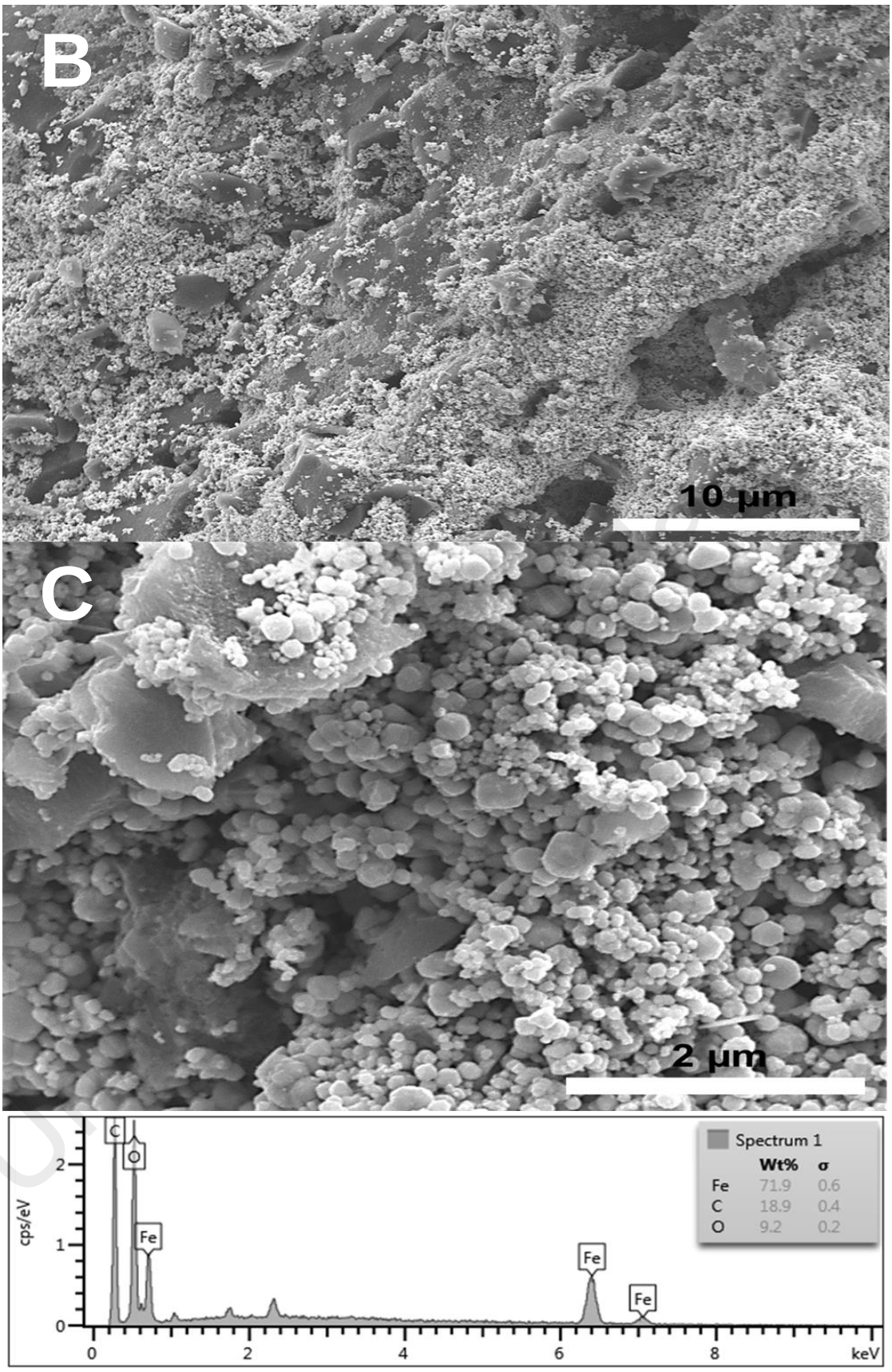

Figure 4.17 (B) FESEM-EDX for MPSAC at low magnification and (C) MPSAC at high magnification

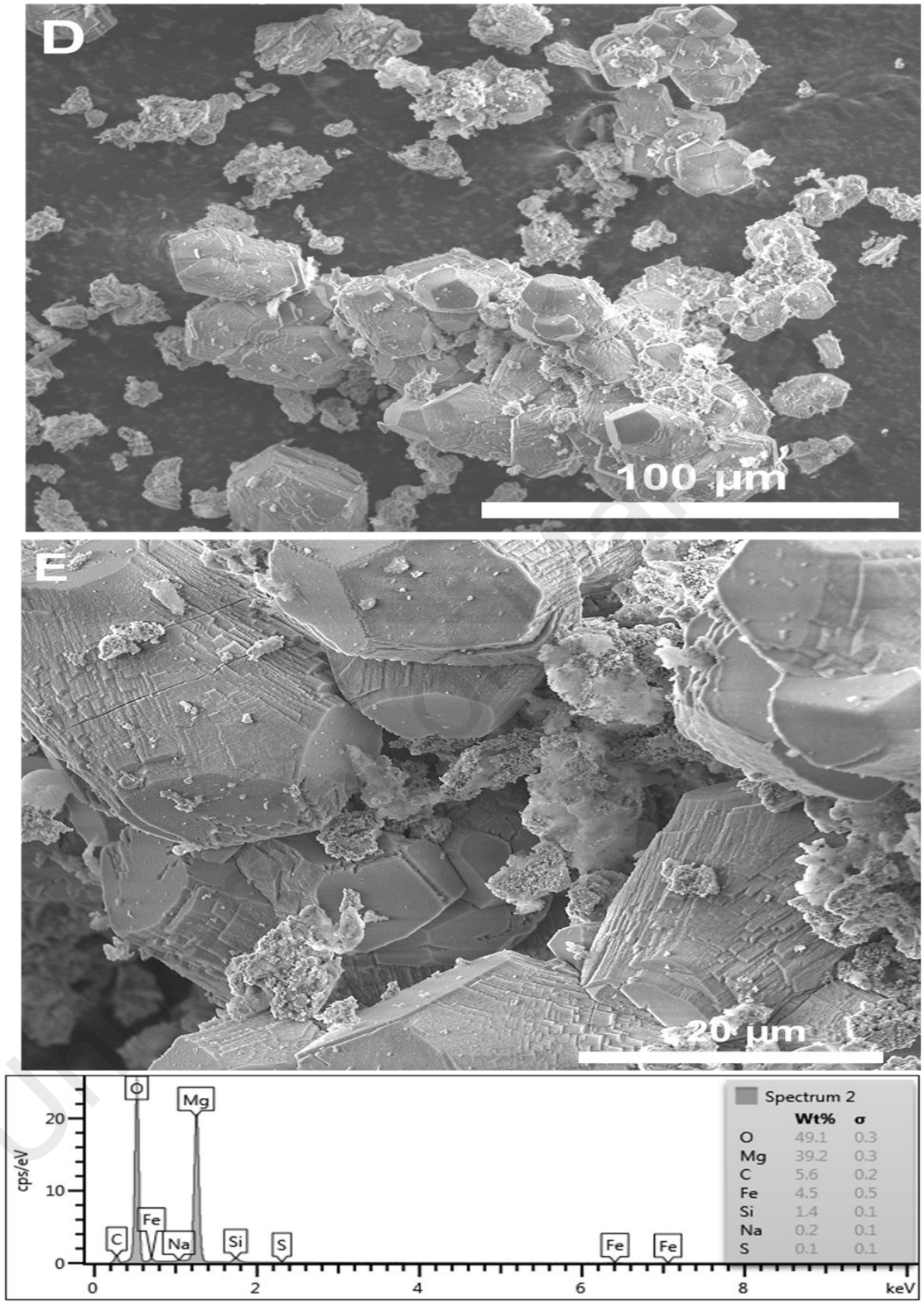

Figure 4.17 (D) FESEM-EDX for MPSAC-SiO_2@$MgNO_3$ at low magnification (E) MPSAC-SiO_2@$MgNO_3$ (0.46) high magnification

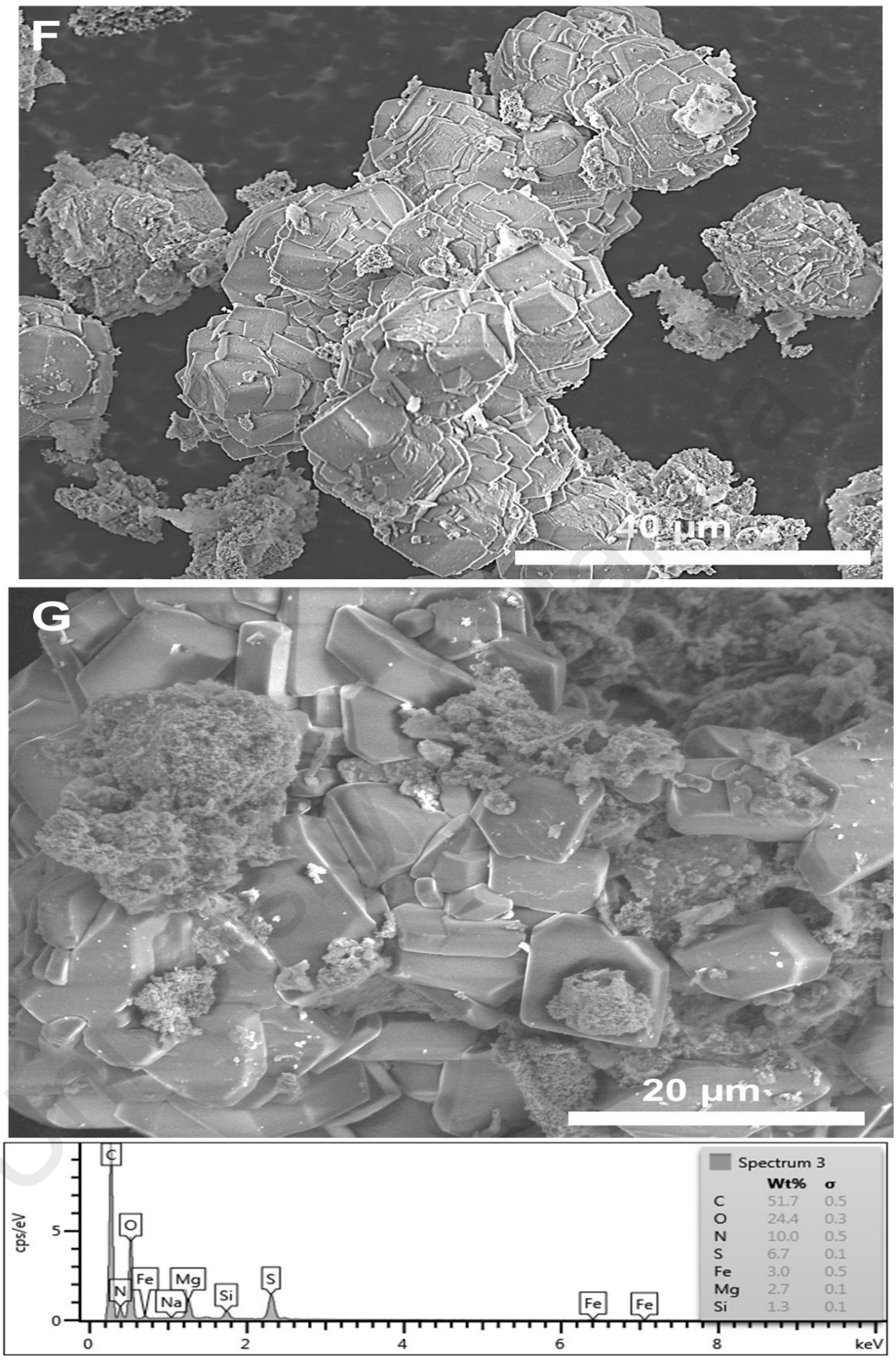

Figure 4.17 (E) FESEM-EDX for MPSAC-SiO_2@$MgNO_3$ (0.46) (F) Methyl Orange loaded MPSAC-SiO_2@$MgNO_3$ (0.46) with the condition: pH 6, C_i = 1300 mg L^{-1}, 1 g L^{-1} of adsorbent.

The morphology of PSAC, MPSAC, MPSAC-SiO_2@$MgNO_3$ (0.46) and Methyl Orange loaded MPSAC-SiO_2@$MgNO_3$ (0.46) at pH 6 were analyzed using the FESEM–EDX. Figure 4.17A shows the morphological structures of PSAC, in which the outer pores were highly developed. When MPSAC were incorporated with the nano-magnetite through film coating method, most of the outer pores surface were covered with ball-like nanoparticles as seen on Figure 4.17B and 4.17C. Based on the EDX graph, it showed that MPSAC adsorbent contained 71.9% of Iron, 18.9% of Carbon and 9.2% of Oxygen. Figure 4.17D shows the morphology of MPSAC-SiO_2@$MgNO_3$ (0.46) adsorbent at low magnification where ball-like nanoparticles of magnetite were totally covered by the Magnesium Carbonate and the outer pores were totally blocked. The Magnesium Carbonate formed a layered like rhombohedra stacked structure giving a 3D architectural structure towards the adsorbent. The same structure was also found by (Gao et al., 2008). Meanwhile, a higher magnification of MPSAC-SiO_2@$MgNO_3$ (0.46) adsorbent in figure 4.17E shows each rhombohedra, which consist of nano-sheet layer forming the rhombohedral 3D structure. The free anions (NO3-) along with OH- and HCO3- anions were adsorbed on the well-arrangement hydroxide surfaces of adsorbent, either through loose coordination with Mg^{2+} or hydrogen bonding. Then, OH^- and HCO_3^- anions were expected to be adsorbed in alternatives ways onto the most crystallographic plane of the hydro magnesium carbonate (hydromagnesite) that produced plate-like or sheet-like nanostructures (Chowdhury et al., 2016). The EDX graph show MPSAC-SiO_2@$MgNO_3$ (0.46) adsorbent contained the highest percentage of Magnesium (39.2%) followed by Oxygen (49.1%), Carbon (5.6%), Iron (4.5%) and Silicon (1.4%), which proved that most of the adsorbent surfaces were covered by Magnesium. However, the morphological structure of MPSAC-SiO_2@$MgNO_3$ (0.46) adsorbent was changed after Methyl Orange was loaded on the surface adsorbent and were observed in Figure4.17F and 4.17G. The rhombohedra structure was changed into a cuboidal block structure and the nano-sheet

University of Malaya

disappeared until a smooth and shiny surface were observed. This may be due to the interaction of MPSAC-SiO_2@$MgNO_3$ (0.46) adsorbent surface and Methyl Orange dye during the adsorption process (Vinod Kumar Gupta, Pathania, Sharma, Agarwal, & Singh, 2013). Sarkar et al. (2015) investigated the cationic and anionic dyes removal and also reported the same observation when the dyes were loaded on the adsorbent surface where the layered particle-like structure was observed to form a smooth and shiny surface, which dominantly because the accumulation of the dyes on the adsorbent surface and suggested it as the physical interaction (A. K. Sarkar, Saha, Panda, & Pal, 2015). Meanwhile, the EDX graph showing the Carbon (51.7 %), Oxygen (24.4 %), Nitrogen (10 %), Sulphur (6.7 %), Na (0.2 %) levels proved that there were Methyl Orange molecule ($C_{14}H_{14}N_3NaO_3S$) that were loaded on the surface.

University of Malaya

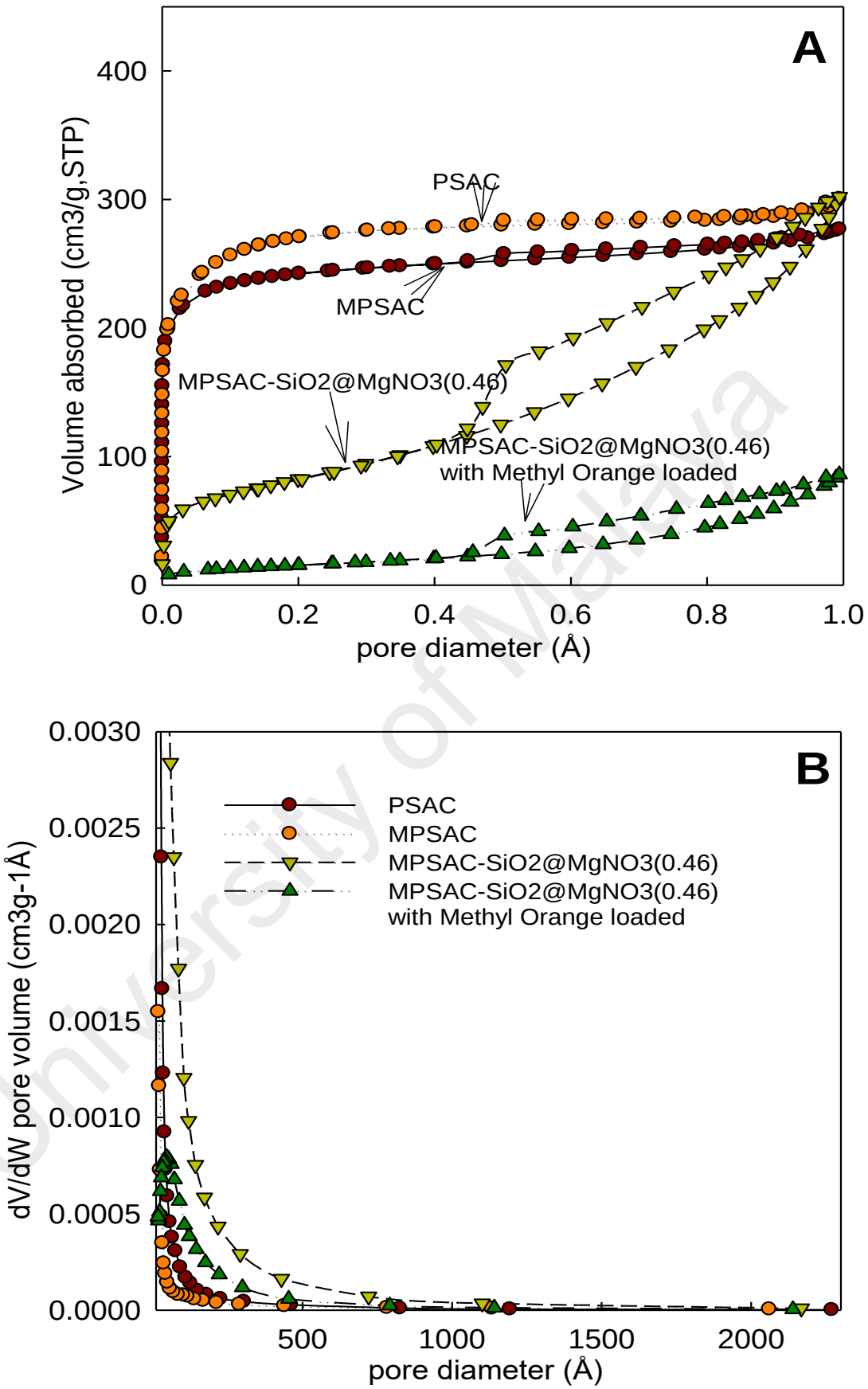

Figure 4.18 (A) N_2 adsorption and desorption isotherms (B) pore size distribution (BJH) curve of PSAC, MPSAC, MPSAC-SiO2@$MgNO_3$(0.46) and MPSAC-SiO_2@$MgNO_3$ (0.46) with Methyl Orange loaded at pH 6, C_i = 1300mg L^{-1}, 1 g L^{-1} of adsorbent.

University of Malaya

Figure 4.18 shows the N_2 gas isotherm and BJH pore size distribution of the PSAC, MPSAC, MPSAC-SiO_2@$MgNO_3$ (0.46) and MPSAC-SiO_2@$MgNO_3$ (0.46) loaded with Methyl Orange. By referring to the IUPAC standard classification (Thommes et al., 2015), PSAC and MPSAC showed type I isotherm curve to represent the long horizontal knee feature of the isotherm. Predominantly, consisting of the micropore structures proved the magnetization of the unmodified PSAC by using the film coating method, which caused a thin nano-magnetite layer on the adsorbent surface that produced MPSAC with a microporous structure. Meanwhile, MPSAC-SiO_2@$MgNO_3$ (0.46) shows the type IV isotherm curve, which indicated the initial curve that is assigned to a monolayer and multilayer adsorption with hysteris loop, H4 that were attributed to MPSAC-SiO_2@$MgNO_3$ (0.46), consisting of a narrow slit-like pore (Harris, Kowalewski, & de Menezes, 1998). This is to show when SiO_2 and $MgNO_3$ were incorporated on the surface of MPSAC-SiO_2@$MgNO_3$ (0.46), it caused a significant reduction to the microporous structure that was carried by the adsorbent. Instead. a mesoporous structure was developed. The 3D crystal structure of $MgNO_3$ built on the nano-magnetite layer at a different angle completely covered the porous structure. After methyl orange was loaded on the MPSAC-SiO_2@$MgNO_3$ (0.46), the isotherm curve showed type V, which indicated a weak adsorbent-adsorbate interaction and was believed to be the cause of the ion-dipole forces, dipole-dipole forces, van der Waals forces, and the dispersion forces arising from the delocalized π electrons.

University of Malaya

Table 4.13 Porosity characterization of PSAC, MPSAC, MPSAC-SiO_2@$MgNO_3$(0.46) and MPSAC-SiO_2@$MgNO_3$(0.46) with Methyl Orange

Samples	BET surface area (m^2g^{-1})	total pore volume (cm^3g^{-1})	Micropore Area (m^2g^{-1})	Volume (cm^3g^{-1})	primary mesopore		
					Area (m^2g^{-1})	Volume (cm^3g^{-1})	Size (W_{KJ}s,Å)
PSAC	1558.2	1.762	984.851	0.4953	296.8	1.357	7.75
MPSAC	1,022.5	0.465	775.012	0.3087	247.5	0.046	18.18
MPSAC-SiO_2@$MgNO_3$ (0.46)	296.1	0.459	26.464	0.0098	269.6	0.398	61.94
MPSAC-SiO_2@$MgNO_3$ (0.46) with Methyl Orange	53.9	0.133	0.619	-0.0004	55.9	0.128	94.25

Based on Table 4.13, PSAC has the highest BET surface area (1558.2 m^2g^{-1}) and micropore area (984.85 m^2g^{-1}), followed by MPSAC with BET surface area (1022.5m^2g^{-1}) and micropore area (775.01m^2g^{-1}) showing both adsorbent carried a dominant micropore structure. Meanwhile, the incorporation of SiO_2 and $MgNO_3$ caused the BET surface area to experience a large reduction of 80% (296.1 m^2g^{-1}) followed by 97% reduction of the micropore area (26.464 m^2g^{-1}). After Methyl Orange was loaded, the BET surface area is further reduced to 97% reduction (53.9 m^2g^{-1}) and micropore area was reduced to 99% (0.619 m^2g^{-1}). However, the mesopore size was observed to increase from 7.75 Å to 94.25 Å with 91.7% increment, proving the adsorbent surface was covered with $MgNO_3$ crystal structure and Methyl Orange accumulation.

University of Malaya

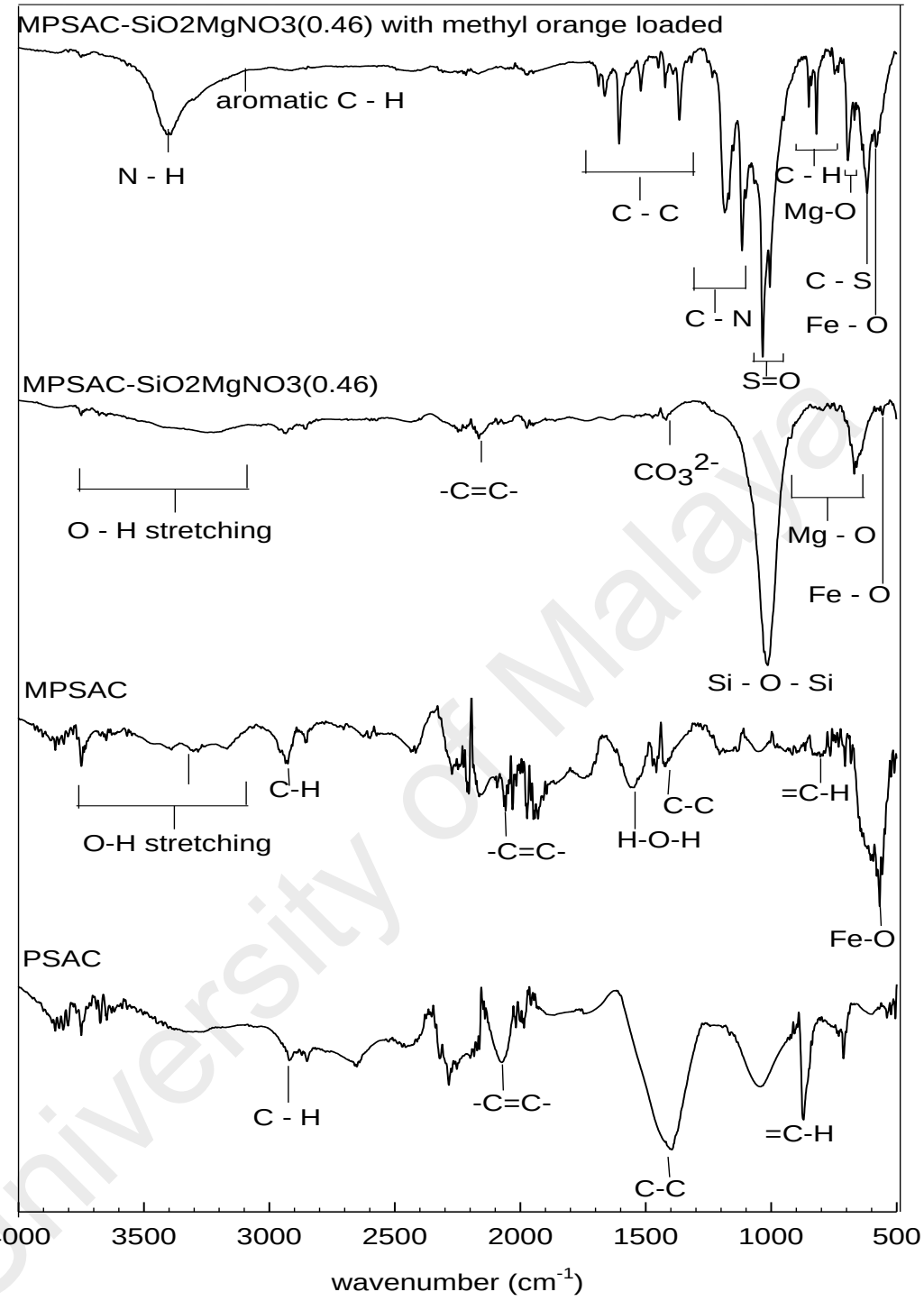

Figure 4.19 FT-IR spectra of PSAC, MPSAC, MPSAC-SiO_2@$MgNO_3$ (0.46) and MPSAC-SiO_2@$MgNO_3$ (0.46) with Methyl Orange loaded at pH 6, C_i = 1300mg L^{-1}, 1 g L^{-1} of adsorbent.

University of Malaya

The FT-IR spectra of PSAC, MPSAC, MPSAC-SiO_2@$MgNO_3$ (0.46) and MPSAC-SiO_2@$MgNO_3$ (0.46) with Methyl Orange loaded were described in Figure 4.19. Based on the illustrated figure, both PSAC and MPSAC have the same IR peaks at 900, 1409, 2100, and 2900 cm^{-1} in the IR spectra and were examined to be =C-H, C-C (aromatic stretching), -C=C- (carbonyl) and C-H, respectively. However, MPSAC has different peaks emerged at 612 cm^{-1} and 3150-3850 cm^{-1} which were assigned to Fe-O stretching and O-H stretching. These were to show that MPSAC was coated with magnetite.

When SiO_2 and $MgNO_3$ were incorporated, the IR peaks of C-C, =C-H and C-H disappeared and only –C=C- remained. The new IR peak at 1040cm-1 were indicated to be SiO2 layer. Meanwhile, the Fe-O stretching and O-H stretching were observed to experience slight reduction, which may be due to the incorporation of SiO_2 and $MgNO_3$ on the surface of magnetite layer (Quy et al., 2013). The characteristic of Mg-O stretching vibration was noticed at 570-860 cm-1 and the CO_3^{2-} ions were indicated at 1440 cm-1 IR spectra. The CO_3^{2-} ions might be entrapped into the porous oxide and were chemisorbed as monodentate onto the MgO when it is exposed to the atmosphere and formed $MgCO_3$ (I. H. Chowdhury et al., 2016).

University of Malaya

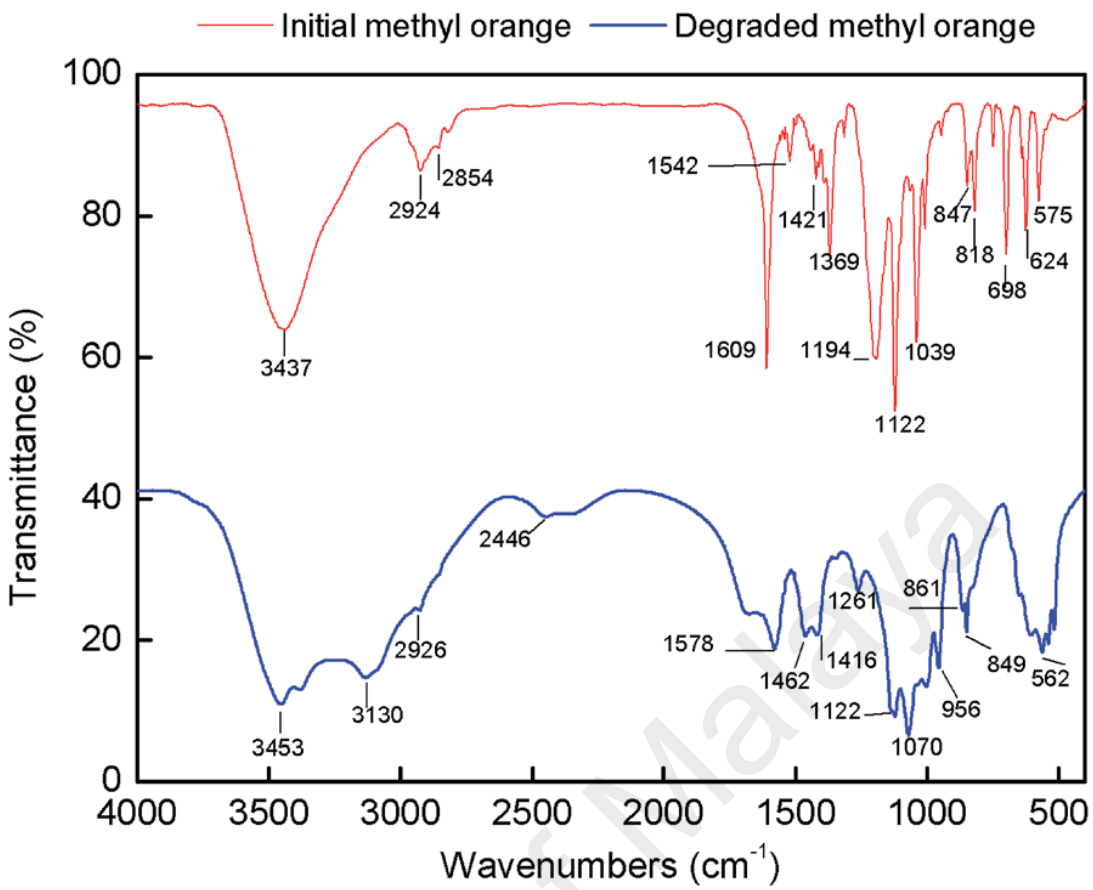

Figure 4.20 FT-IR spectra of initial Methyl Orange dye and degraded Methyl Orange dye
(Shen, Jiang, et al., 2015)

Figure 4.20 shows IR spectra of initial Methyl Orange and degraded Methyl Orange dye reported by Shen et al. (2015). By referring to the degraded Methyl Orange IR spectra data, we managed to analyze the MPSAC-SiO_2@$MgNO_3$ (0.46) with Methyl Orange loaded IR spectra.

Back to Figure 4.19, MPSAC-SiO_2@$MgNO_3$ (0.46) with Methyl Orange loaded, Mg-O and Fe-O stretching vibration were reduced. However, a broad peak of N-H and aromatic C-H was seen at 3450cm-1 and 3100cm-1 IR spectra, which was similar to the degraded Methyl Orange IR spectra. This could happened when the conjugated double bond of N=N (azo bond) is broken down causing the conjugated π-π interaction (Baiocchi et al., 2002). On the other hand, peaks at 1450cm^{-1} – 1650cm^{-1} were noticed to be the C-C benzene skeleton vibration, 1350 cm^{-1} -1450 cm^{-1} for C-N aromatic stretching

University of Malaya

vibrations, 1060 cm^{-1} -980 cm^{-1} for S=O stretching vibrations. 850 cm^{-1} -870 cm^{-1} for the aromatic C-H vibration and 640 cm^{-1} for the C-S bond formation of the new products with a benzene ring or sulfonated aromatic ring (Shen, Jiang, et al., 2015). On the other hand, Shen et al. (2015) also discussed the destruction of azo bond and formation of other degradation intermediates containing benzene ring, which were proven to show the easy decolorization of Methyl Orange dye. However, the destruction of the benzene ring was shown to be difficult.

University of Malaya

CHAPTER 5: CONCLUSION & RECOMMENDATIONS

6.1 Arsenic Removal Study

In this study, highly-effective sorption materials for the removal of arsenate were prepared through the magnetization of PSAC followed by Lanthanum incorporation using a wetness impregnation and calcination. The isotherm study showed that the arsenate adsorption capacity and K_L value were significantly increased with the increment of Lanthanum impregnated to MPSAC. MPSAC–La (0.36) had about 16.5 or 1.6 times higher q_{max} (227.6 mg g^{-1}) for arsenate removal than the PSAC or MPSAC. Specifically, it had 230 times higher K_L than MPSAC, showing that Lanthanum impregnation had a much stronger sorption affinity for arsenate. The experimental results of pH effect on arsenate removal and speciation modeling revealed that arsenate is dominantly removed by precipitation at pH < 8 while it complexes on the surface of $La(OH)_3$ was at pH > 8. In addition, the nano-magnetite might have a strong binding strength to stabilize Lanthanum, providing a lesser dissolution. XRD, FTIR, SEM–EDS and N_2 gas isotherms disclosed that the nano-magnetite coating gave a considerable micropore clogging of PSAC, but increased the meso and macropores due to the space created between the nano-magnetite particles. Nevertheless, LO/LH cemented the spaces of nano-magnetite to eliminate most of the pore structures and had an effective removal function of arsenate as $LaAsO_4$ at pH 6. Established on the results of batch tests, the granular-sized MPSAC–La (0.36) has a potential to be a competitive and economic media because of the extremely high sorption capabilities, easy magnetic separation and high regeneration rates.

University of Malaya

6.2 Dye Removal Study

Both Methylene Blue dye (cationic) and Methyl Orange dye (anionic) carried different ionic properties that were used to represent the common textile dye used in the textile manufacturing industry. Highly effective $MgNO_3$ with silica coated magnetically palm shell waste-based activated carbon with a different $MgNO_3$: urea molar ratio adsorbent was prepared through the triple modification method. The isotherm study showed the modified adsorbent with the highest $MgNO_3$: urea ratio where the MPSAC-SiO_2@$MgNO_3$ (0.46) gives the highest q_{max} value of 1019.61 mg g^{-1}, which is 2.7 times higher than the unmodified PSAC in Methyl Orange dye removal study and 1.15 times higher than the unmodified PSAC in Methylene Blue dye removal study. Based on the kinetic data, the pseudo first order, pseudo second order, and the intra particle diffusion kinetic model was plotted and used to analyze the Methyl Orange and Methylene Blue dyes removal mechanism by MPSAC-SiO_2@$MgNO_3$ (0.46), which revealed that the chemisorption may influence the removal mechanism. The experimental results for MPSAC-SiO_2@$MgNO_3$ (0.46) effects on pH showed that the Methyl Orange dye adsorption capacity pattern were influenced by pH but not for Methylene Blue dye. Based on the XRD, FESEM+EDX, FT-IR and BET+N2 gas analyses, the incorporation of $MgNO_3$: urea into the MPSAC-SiO_2 resulted to the formation of $MgCO_3$ instead of $MgO/Mg(OH)_2$ and caused the development of the 3D-rhombohedral structure with plate-like nanostructure consisting of the hydromagnesite. The morphological structure was changed after the Methyl Orange dye uptake resulted to the formation of 3D cuboidal block structure with a smooth and shiny surfaces, which indicated the accumulation of Methyl Orange dye. As a result, the micropore structure had totally disappeared and the mesopore was significantly developed. It was believed that other than the electrostatic attraction force between MPSAC-SiO_2@$MgNO_3$ (0.46) and the anionic Methyl Orange dye, the ion-dipole, dipole-dipole, van der Waals, and π-π electron donor acceptor and

University of Malaya

pore filling might have happened during the adsorption process. Established on the results of batch tests, the granular-sized MPSAC-SiO_2@$MgNO_3$ (0.46) developed has a potential to be a competitive and economic media for Methyl Orange dye removal because of the extremely high sorption capabilities, easy magnetic separation and high regeneration rates.

6.3 Major Contribution

Through time, a new material with a better removal efficiency than the current material will always tried to be developed. The major contribution of both developed material is to provide an alternative for water and wastewater treatment. Recently, researchers have put more interest in using recycled material as their basic raw material. In this study, both of the developed material used palm shell waste-based activated was used as a basic adsorbent. Palm shell waste is available in abundance in Malaysia.

a) Arsenic Removal study

The major contribution of arsenic removal study towards the world are:

- **A new highly efficient adsorbent**

As reported in section 4.1, the developed material, MPSAC-La (0.36) was reported to have the capability to remove Arsenic (V) at high performance. This material can be used in real groundwater treatment for drinking water usage as the capability of developed material to remove Arsenic (V) is very high. Even though, the current highest concentration of arsenic in groundwater did not achieve more than 1 mg L^{-1}, meanwhile, the MPSAC-La (0.36) is capable to remove 227.6 mg L^{-1}.

University of Malaya

- **A fast sorption rate adsorbent**

As in the laboratory, shaker was used to mix the adsorbent, while in a real treatment process, agitator will be used to agitate the adsorbent. Thus, the adsorbent will continuously move in a uniform movement for a better adsorption performance. The agitation process consumed high electricity rate and eventually will incurred a high treatment cost. As reported in section 4.2, MPSAC-La (0.36) has a very fast sorption rate in Arsenic (V) removal at initial concentration=350mg L^{-1}. It is believed that the agitation time taken to remove the arsenic from water to be treated will be reduced significantly as the common arsenic concentration in real groundwater is <1 mg L^{-1}.

- **Simple, easy to implement and cost-effective**

Until now, developing countries such as Bangladesh and India still reported to contain high arsenic contamination in groundwater. Most of the region in India still uses tube wells at shallow aquifer for groundwater uptake because of the low installation and operation cost. Thus, it is believed that the newly developed material, MPSAC-La (0.36) is applicable to be used for arsenic (V) groundwater treatment as the adsorption process is simple and no high installation cost will be incurred. The magnetic characteristic carried by MPSAC-La (0.36) will make the separation method of adsorbent from treated water much easier by using the external magnetic field. On the other hand, MPSAC-La (0.36) also can be regenerated and reused again up to three times and this will contribute to low operation cost.

University of Malaya

b) Dye removal study

The major contribution of dye removal study towards the textile manufacturing industry and environment are:

- **A new highly efficient adsorbent**

As reported in section 4.7, MPSAC-SiO_2@$MgNO_3$ (0.46) was reported to show a high performance in Methyl Orange dye and Methylene Blue dye uptake. It shows that the developed material is capable to adsorb both dyes, which carry different ionic properties. Meanwhile, Methyl Orange and Methylene Blue dyes are commonly used in textile manufacturing industry. Thus, it is believed that the newly develop material is capable to be applied in real dye wastewater. In addition, MPSAC-SiO_2@$MgNO_3$ (0.46) showed a high adsorption capacity of about 1091 mg g^{-1} and 471 mg g^{-1} for Methyl Orange and Methylene Blue dye uptake, respectively. Hence, it showed that the developed material is capable to remove both dyes at a high concentration level.

- **Simple, easy to implement and cost-effective**

In real textile manufacturing industry, a simple and easy to implement textile wastewater treatment will be aimed. But, most of the simple textile wastewater treatment is not very efficient in the dye removal uptake. Thus, it is believed by developing a new adsorbent material with a magnetic characteristic, it will make the developed material to be a good adsorbent alternative, as the used-adsorbent can be separated by external magnetic field from the treated wastewater at the end of the treatment process. On the other hand, the developed material has the ability to be regenerated and re-used for another several adsorption treatment cycle, which will eventually reduce the treatment cost.

University of Malaya

6.5 Recommendation of future works

The method used in both studies has driven very promising results for arsenic in groundwater contamination problem and dye wastewater treatment for the textile manufacturing industry. However, there are several extents that need further analysis. In both studies, simulated arsenic solution and dye solution were prepared in the laboratory. In order to simulate real groundwater or dye wastewater, the co-existing anion and competing anion studies were carried out to analyze its adsorption performance. However, because of the time limitation, the developed material was unable to be tested using the real groundwater and dye wastewater. Thus, for future work, it is recommended to use the real groundwater and dye wastewater to support these findings.

In previous section, the synthesized materials were proven to have a high efficient removal capacity for Arsenic (V) and in dye removal. Thus, to commercialize the synthesized material, some convincing additional data needs to be included. Both of the experimental studies were carried out using laboratory scale study, small scale and batch tests. Meanwhile, in real water and wastewater treatment system, the treatment for pollutants are in a large scale and in continuous system. It is believed that the application of the pilot scale study can be used in a full scale study using the synthesized material and column test study data, which will improve the justification of the study and showed the effectiveness of the developed material. On the other hand, a detailed cost including the material preparation cost, operation cost, and disposal cost are recommended to be carried out so that a real sustainable (economic, environmental, social and engineering) approach can be selected.

University of Malaya

The development of both MPSAC-La (0.36) and MPSAC-SiO_2@$MgNO_3$ (0.46) were developed by several modification techniques. The modification techniques applied had helped to improve the efficiency of Arsenic (V) and dye adsorption. However, the procedure of the modification is still quite complicated. To encounter this problem, simpler modification needs to be investigated in the future. Furthermore, the possibility of incorporating a larger amount of Lanthanum and $MgNO_3$ into the synthesized material during the modification needs to be investigated.

In the dye removal study, $MgNO_3$ salt was used as the modification material. It is recommended to investigate the adsorption performance, pore size, volume and structure, and the morphological structure of the synthesized material by using other types of Magnesium salt, such as $MgSO_4$ and $MgCl_2$.

University of Malaya

REFERENCES

Aghazadeh, M., Golikand, A. N., Ghaemi, M., & Yousefi, T. (2011). A novel lanthanum hydroxide nanostructure prepared by cathodic electrodeposition. *Materials Letters, 65*(10), 1466-1468.

Ahmaruzzaman, M. (2008). Adsorption of phenolic compounds on low-cost adsorbents: a review. *Advances in Colloid and Interface Science, 143*(1), 48-67.

Ahmaruzzaman, M. (2011). Industrial wastes as low-cost potential adsorbents for the treatment of wastewater laden with heavy metals. *Advances in Colloid and Interface Science, 166*(1–2), 36-59. doi: http://dx.doi.org/10.1016/j.cis.2011.04.005

Ahmed, M. F. (2001). *An overview of arsenic removal technologies in Bangladesh and India.* Paper presented at the Proceedings of BUET-UNU International Workshop on Technologies for Arsenic Removal from Drinking Water, Dhaka.

Ai, L., Zhang, C., & Meng, L. (2011). Adsorption of methyl orange from aqueous solution on hydrothermal synthesized Mg–Al layered double hydroxide. *Journal of Chemical & Engineering Data, 56*(11), 4217-4225.

Al-Degs, Y. S., El-Barghouthi, M. I., El-Sheikh, A. H., & Walker, G. M. (2008). Effect of solution pH, ionic strength, and temperature on adsorption behavior of reactive dyes on activated carbon. *Dyes and Pigments, 77*(1), 16-23.

Alberghina, G., Bianchini, R., Fichera, M., & Fisichella, S. (2000). Dimerization of Cibacron Blue F3GA and other dyes: influence of salts and temperature. *Dyes and Pigments, 46*(3), 129-137.

Ali, I., Asim, M., & Khan, T. A. (2012). Low cost adsorbents for the removal of organic pollutants from wastewater. *Journal of Environmental Management, 113*, 170-183. doi: http://dx.doi.org/10.1016/j.jenvman.2012.08.028

Amin, N. K. (2008). European Desalination Society and Center for Research and Technology Hellas (CERTH), Sani Resort 22–25 April 2007, Halkidiki, GreeceRemoval of reactive dye from aqueous solutions by adsorption onto activated carbons prepared from sugarcane bagasse pith. *Desalination, 223*(1), 152-161. doi: http://dx.doi.org/10.1016/j.desal.2007.01.203

Anjaneyulu, Y., Chary, N. S., & Raj, D. S. S. (2005). Decolourization of industrial effluents–available methods and emerging technologies–a review. *Reviews in Environmental Science and Bio/Technology, 4*(4), 245-273.

Apostol, I., Mamasakhlisi, J., & Subotta, D. (2015). *Engaging the Public to Fight the Consequences of Terrorism and Disasters*: IOS Press.

Asadullah, M., Jahan, I., Ahmed, M. B., Adawiyah, P., Malek, N. H., & Rahman, M. S. (2014). Preparation of microporous activated carbon and its modification for arsenic removal from water. *Journal of Industrial and Engineering Chemistry, 20*(3), 887-896. doi: http://dx.doi.org/10.1016/j.jiec.2013.06.019

University of Malaya

Azami, M., Bahram, M., Nouri, S., & Naseri, A. (2012). A central composite design for the optimization of the removal of the azo dye, methyl orange, from waste water using the Fenton reaction. *J Serb Chem Soc, 77*, 235-246.

Babu, B. R., Parande, A., Raghu, S., & Kumar, T. P. (2007). Cotton textile processing: waste generation and effluent treatment. *Journal of cotton science*.

Baiocchi, C., Brussino, M. C., Pramauro, E., Prevot, A. B., Palmisano, L., & Marcì, G. (2002). Characterization of methyl orange and its photocatalytic degradation products by HPLC/UV–VIS diode array and atmospheric pressure ionization quadrupole ion trap mass spectrometry. *International Journal of Mass Spectrometry, 214*(2), 247-256.

Blaas, H., & Kroeze, C. (2016). Excessive nitrogen and phosphorus in European rivers: 2000–2050. *Ecological Indicators, 67*, 328-337. doi: http://dx.doi.org/10.1016/j.ecolind.2016.03.004

Blomqvist, A. (1996). Food and fashion: Water management and collective action among irrigation farmers and textile industrialists in South India.

Cavaco, S. A., Fernandes, S., Quina, M. M., & Ferreira, L. M. (2007). Removal of chromium from electroplating industry effluents by ion exchange resins. *Journal of Hazardous Materials, 144*(3), 634-638.

Chakraborti, D., Das, B., Rahman, M. M., Kumar, U., Chowdhury, B. B., Goswami, A., . . . Sengupta, S. A. (2009). Research Article Status of groundwater arsenic contamination in the state of West Bengal, India: A 20-year study report. *Mol. Nutr. Food Res, 53*, 542-551.

Chakraborti, D., Rahman, M. M., Das, B., Nayak, B., Pal, A., Sengupta, M. K., . . . Saha, K. C. (2013). Groundwater arsenic contamination in Ganga–Meghna–Brahmaputra plain, its health effects and an approach for mitigation. *Environmental earth sciences, 70*(5), 1993-2008.

Chakraborti, D., & Roy, S. (1997). Groundwater arsenic calamity in Bangladesh. *Current Science, 73*(1), 4859.

Chakraborty, S., De, S., Basu, J., & DasGupta, S. (2005). Treatment of a textile effluent: application of a combination method involving adsorption and nanofiltration. *Desalination, 174*(1), 73-85.

Chen, B., Liu, Y., Chen, S., Zhao, X., Meng, X., & Pan, X. Magnetically recoverable cross-linked polyethylenimine as a novel adsorbent for removal of anionic dyes with different structures from aqueous solution. *Journal of the Taiwan Institute of Chemical Engineers*. doi: http://dx.doi.org/10.1016/j.jtice.2016.07.014

Chen, X., Chen, G., & Yue, P. L. (2000). Separation of pollutants from restaurant wastewater by electrocoagulation. *Separation and purification technology, 19*(1), 65-76.

Chowdhury, I. H., Chowdhury, A. H., Bose, P., Mandal, S., & Naskar, M. K. (2016). Effect of anion type on the synthesis of mesoporous nanostructured MgO, and its

University of Malaya

excellent adsorption capacity for the removal of toxic heavy metal ions from water. *Rsc Advances, 6*(8), 6038-6047.

Chowdhury, S. R., Yanful, E. K., & Pratt, A. R. (2011). Arsenic removal from aqueous solutions by mixed magnetite–maghemite nanoparticles. *Environmental earth sciences, 64*(2), 411-423.

Christie, R. M. (2007). *Environmental Aspects of Textile Dyeing*: Elsevier Science.

Compounds, W. A. (2001). Environmental Health Criteria 224. *World Health Organisation, Geneva*.

contributors, N. W. E. Methylene blue (pp. 984958): New World Encyclopedia,. Retrieved from http://www.newworldencyclopedia.org/p/index.php?title=Methylene_blue&oldid=984958.

contributors, W. ion exchange: Wikipedia, The Free Encyclopedia.

contributors, W. Methyl orange: Wikipedia, The Free Encyclopedia.

contributors, W. Methylene blue: Wikipedia, The Free Encyclopedia.

Cornell, R. M., & Schwertmann, U. (2003). *The Iron Oxides*. Weinheim: Wiley-VCH.

Crittenden, J. C., Howe, K. J., Hand, D. W., Tchobanoglous, G., & Trussell, R. R. (2012). *Principles of Water Treatment*: John Wiley & Sons, Incorporated.

Das, D. P., Das, J., & Parida, K. (2003). Physicochemical characterization and adsorption behavior of calcined Zn/Al hydrotalcite-like compound (HTlc) towards removal of fluoride from aqueous solution. *Journal of colloid and interface science, 261*(2), 213-220.

Daud, W. M. A. W., & Ali, W. S. W. (2004). Comparison on pore development of activated carbon produced from palm shell and coconut shell. *Bioresource Technology, 93*(1), 63-69.

Dávila-Jiménez, M., Elizalde-Gonzalez, M., & Peláez-Cid, A. (2005). Adsorption interaction between natural adsorbents and textile dyes in aqueous solution. *Colloids and Surfaces A: Physicochemical and Engineering Aspects, 254*(1), 107-114.

Demirbas, E., Kobya, M., & Konukman, A. (2008). Error analysis of equilibrium studies for the almond shell activated carbon adsorption of Cr (VI) from aqueous solutions. *Journal of Hazardous Materials, 154*(1), 787-794.

Demirbas, E., & Nas, M. (2009). Batch kinetic and equilibrium studies of adsorption of Reactive Blue 21 by fly ash and sepiolite. *Desalination, 243*(1), 8-21.

Donnan, F. G. (1995). Theory of membrane equilibria and membrane potentials in the presence of non-dialysing electrolytes. A contribution to physical-chemical physiology. *Journal of Membrane Science, 100*(1), 45-55.

University of Malaya

Dutta, K., Mukhopadhyay, S., Bhattacharjee, S., & Chaudhuri, B. (2001). Chemical oxidation of methylene blue using a Fenton-like reaction. *Journal of Hazardous Materials, 84*(1), 57-71. doi: http://dx.doi.org/10.1016/S0304-3894(01)00202-3

Emamjomeh, M. M., & Sivakumar, M. (2009). Review of pollutants removed by electrocoagulation and electrocoagulation/flotation processes. *Journal of Environmental Management, 90*(5), 1663-1679.

Envirowise. (1997). 'Water and Chemical Use in the Textile Dyeing and Finishing Industry *GG62* (pp. 37): Environmental Technology Best Practice Program.

Fakhri, A., & Adami, S. (2014). Adsorption and thermodynamic study of Cephalosporins antibiotics from aqueous solution onto MgO nanoparticles. *Journal of the Taiwan Institute of Chemical Engineers, 45*(3), 1001-1006. doi: http://dx.doi.org/10.1016/j.jtice.2013.09.028

Faust, S. D., & Aly, O. M. (2013). *Adsorption processes for water treatment*: Elsevier.

Feng, G., Hu, D., Yang, L., Cui, Y., Cui, X.-a., & Li, H. (2010). Immobilized-metal affinity chromatography adsorbent with paramagnetism and its application in purification of histidine-tagged proteins. *Separation and purification technology, 74*(2), 253-260. doi: http://dx.doi.org/10.1016/j.seppur.2010.06.013

Figueiredo, J., Pereira, M., Freitas, M., & Orfao, J. (1999). Modification of the surface chemistry of activated carbons. *Carbon, 37*(9), 1379-1389.

Fisli, A., Yusuf, S., Krisnandi, Y. K., & Gunlazuardi, J. (2014). *Preparation and Characterization of Magnetite-Silica Nano-Composite as Adsorbents for Removal of Methylene Blue Dyes from Environmental Water Samples.* Paper presented at the Advanced Materials Research.

Forgacs, E., Cserháti, T., & Oros, G. (2004). Removal of synthetic dyes from wastewaters: a review. *Environment international, 30*(7), 953-971. doi: http://dx.doi.org/10.1016/j.envint.2004.02.001

Gao, C., Zhang, W., Li, H., Lang, L., & Xu, Z. (2008). Controllable fabrication of mesoporous MgO with various morphologies and their absorption performance for toxic pollutants in water. *Crystal Growth and Design, 8*(10), 3785-3790.

Gaur, V. (2012). SURFACE MODIFICATION OF ACTIVATED CARBON FOR THE REMOVAL OF WATER IMPURITIES. *DISINFECTION.* Retrieved 30 August 2016, from http://www.watertechonline.com/surface-modification-of-activated-carbon-for-the-removal-of-water-impurities/

Gebbie, P. (2006). *An operator's guide to water treatement coagulants.* Paper presented at the 31st Annual QLD Water Industry Workshop—Operations Skills.

Ghasemian, E., & Palizban, Z. (2016). Comparisons of azo dye adsorptions onto activated carbon and silicon carbide nanoparticles loaded on activated carbon. *International Journal of Environmental Science and Technology, 13*(2), 501-512.

University of Malaya

Ghorai, S., & Pant, K. (2005). Equilibrium, kinetics and breakthrough studies for adsorption of fluoride on activated alumina. *Separation and purification technology, 42*(3), 265-271.

Golob, V., Vinder, A., & Simonič, M. (2005). Efficiency of the coagulation/flocculation method for the treatment of dyebath effluents. *Dyes and Pigments, 67*(2), 93-97.

Gong, R., Ye, J., Dai, W., Yan, X., Hu, J., Hu, X., . . . Huang, H. (2013). Adsorptive removal of methyl orange and methylene blue from aqueous solution with finger-citron-residue-based activated carbon. *Industrial & Engineering Chemistry Research, 52*(39), 14297-14303.

Griffin, R., & Jurinak, J. (1974). Kinetics of the phosphate interaction with calcite. *Soil Science Society of America Journal, 38*(1), 75-79.

Guivarch, E. (2004). Organic Pollutant Treatment in Aqueous Medium by Electrochemical Advanced Oxidation Process Electro-Fenton: Application to the Mineralization of Synthetic Dyes. *University of l\/larne-La-Vallee, France, Pages, 232*.

Guo, C., Xu, J., He, Y., Zhang, Y., & Wang, Y. (2011). Photodegradation of rhodamine B and methyl orange over one-dimensional TiO 2 catalysts under simulated solar irradiation. *Applied Surface Science, 257*(8), 3798-3803.

Guo, Y., Zhu, Z., Qiu, Y., & Zhao, J. (2012). Adsorption of arsenate on Cu/Mg/Fe/La layered double hydroxide from aqueous solutions. *Journal of Hazardous Materials, 239–240*, 279-288. doi: http://dx.doi.org/10.1016/j.jhazmat.2012.08.075

Gupta, A. D. (2008). Implication of environmental flows in river basin management. *Physics and Chemistry of the Earth, Parts A/B/C, 33*(5), 298-303.

Gupta, G., Prasad, G., Panday, K., & Singh, V. (1988). Removal of chrome dye from aqueous solutions by fly ash. *Water, Air, and Soil Pollution, 37*(1-2), 13-24.

Gupta, V. K., Ali, I., Saleh, T. A., Nayak, A., & Agarwal, S. (2012). Chemical treatment technologies for waste-water recycling—an overview. *Rsc Advances, 2*(16), 6380-6388.

Gupta, V. K., Pathania, D., Sharma, S., Agarwal, S., & Singh, P. (2013). Remediation and recovery of methyl orange from aqueous solution onto acrylic acid grafted Ficus carica fiber: isotherms, kinetics and thermodynamics. *Journal of Molecular Liquids, 177*, 325-334.

Gupta, V. K., Rastogi, A., & Nayak, A. (2010). Biosorption of nickel onto treated alga (Oedogonium hatei): application of isotherm and kinetic models. *Journal of colloid and interface science, 342*(2), 533-539.

Hafeznezami, S., Lam, J. R., Xiang, Y., Reynolds, M. D., Davis, J. A., Lin, T., & Jay, J. A. (2016). Arsenic mobilization in an oxidizing alkaline groundwater: Experimental studies, comparison and optimization of geochemical modeling

University of Malaya

parameters. *Applied Geochemistry, 72*, 97-112. doi: http://dx.doi.org/10.1016/j.apgeochem.2016.07.011

Hai, F. I., Yamamoto, K., & Fukushi, K. (2007). Hybrid treatment systems for dye wastewater. *Critical Reviews in Environmental Science and Technology, 37*(4), 315-377.

Hamdaoui, O., & Naffrechoux, E. (2007). Modeling of adsorption isotherms of phenol and chlorophenols onto granular activated carbon: Part II. Models with more than two parameters. *Journal of Hazardous Materials, 147*(1), 401-411.

Hao, L., Liu, Q., Li, X., Du, Z., & Wang, P. (2014). A potentially low-cost modified sawdust (MSD) effective for rapid Cr (VI) and As (V) removal from water. *RSC Advances, 4*(91), 49569-49576.

Haque, E., Jun, J. W., & Jhung, S. H. (2011). Adsorptive removal of methyl orange and methylene blue from aqueous solution with a metal-organic framework material, iron terephthalate (MOF-235). *Journal of Hazardous Materials, 185*(1), 507-511. doi: http://dx.doi.org/10.1016/j.jhazmat.2010.09.035

Haque, N., Morrison, G., Cano-Aguilera, I., & Gardea-Torresdey, J. L. (2008). Iron-modified light expanded clay aggregates for the removal of arsenic(V) from groundwater. *Microchemical Journal, 88*(1), 7-13. doi: http://dx.doi.org/10.1016/j.microc.2007.08.004

Harris, R. K., Kowalewski, J., & de Menezes, S. C. (1998). International Union of Pure and Applied Chemistry Physical Chemistry Division Commission on Molecular Structure and Spectroscopy. Parameters and symbols for use in nuclear magnetic resonance (IUPAC recommendations 1997). *Magnetic Resonance in Chemistry, 36*(2), 145-149.

He, T., Feng, X., Guo, Y., Qiu, G., Li, Z., Liang, L., & Lu, J. (2008). The impact of eutrophication on the biogeochemical cycling of mercury species in a reservoir: a case study from Hongfeng Reservoir, Guizhou, China. *Environmental Pollution, 154*(1), 56-67.

Heath, A. G. (1995). *Water Pollution and Fish Physiology*: Taylor & Francis.

Heishman, J. O., Olson, N. O., & Shelton, D. C. (1960). Control of Chronic Respiratory Disease. II. The Effect of Low Calcium Diet, Terephthalic acid and Chlortetracycline. *Avian Diseases, 4*(4), 413-418. doi: 10.2307/1587691

Hendricks, D. W. (2006). *Water treatment unit processes: physical and chemical*: CRC press.

Ho, Y., & McKay, G. (1998). A comparison of chemisorption kinetic models applied to pollutant removal on various sorbents. *Process Safety and Environmental Protection, 76*(4), 332-340.

Ho, Y., Porter, J., & McKay, G. (2002). Equilibrium isotherm studies for the sorption of divalent metal ions onto peat: copper, nickel and lead single component systems. *Water, Air, and Soil Pollution, 141*(1-4), 1-33.

University of Malaya

Ho, Y. S., & McKay, G. (1998). Sorption of dye from aqueous solution by peat. *Chem. Eng. J., 70*(2), 115-124.

Holt, P. K., Barton, G. W., & Mitchell, C. A. (2005). The future for electrocoagulation as a localised water treatment technology. *Chemosphere, 59*(3), 355-367.

Hong, J., Zhu, Z., Lu, H., & Qiu, Y. (2014). Synthesis and arsenic adsorption performances of ferric-based layered double hydroxide with α-alanine intercalation. *Chemical Engineering Journal, 252*, 267-274. doi: 10.1016/j.cej.2014.05.019

Hong, S., Wen, C., He, J., Gan, F., & Ho, Y.-S. (2009). Adsorption thermodynamics of Methylene Blue onto bentonite. *Journal of Hazardous Materials, 167*(1), 630-633.

Hopenhayn-Rich, C., Biggs, M. L., Fuchs, A., Bergoglio, R., Tello, E. E., Nicolli, H., & Smith, A. H. (1996). Bladder cancer mortality associated with arsenic in drinking water in Argentina. *Epidemiology, 7*(2), 117-124.

Hughes, M. F., Beck, B. D., Chen, Y., Lewis, A. S., & Thomas, D. J. (2011). Arsenic Exposure and Toxicology: A Historical Perspective. *Toxicological Sciences, 123*(2), 305-332. doi: 10.1093/toxsci/kfr184

Humans, I. W. G. o. t. E. o. C. R. t., Organization, W. H., & Cancer, I. A. f. R. o. (2004). *Some Drinking-water Disinfectants and Contaminants, Including Arsenic: IARC Monographs on the Evaluation of Carcinogenic Risks to Human*: World Health Organization.

Jain, R., Bhargava, M., & Sharma, N. (2003). Electrochemical studies on a pharmaceutical azo dye: Tartrazine. *Industrial & Engineering Chemistry Research, 42*(2), 243-247.

Jain, R., & Sikarwar, S. (2008). Removal of hazardous dye congored from waste material. *Journal of Hazardous Materials, 152*(3), 942-948.

Jang, M., Park, J. K., & Shin, E. W. (2004). Lanthanum functionalized highly ordered mesoporous media: implications of arsenate removal. *Microporous and mesoporous materials, 75*(1), 159-168.

Jedryczko, D., Pohl, P., & Welna, M. (2016). Inorganic arsenic speciation in natural mineral drinking waters by flow-through anodic stripping chronopotentiometry. *Talanta, 150*, 265-271. doi: http://dx.doi.org/10.1016/j.talanta.2015.12.032

Kabata-Pendias, A., & Pendias, H. (1992). *Trace elements in soils and plants*: CRC Press.

Kabra, K., Chaudhary, R., & Sawhney, R. L. (2004). Treatment of Hazardous Organic and Inorganic Compounds through Aqueous-Phase Photocatalysis: A Review. *Industrial & Engineering Chemistry Research, 43*(24), 7683-7696. doi: 10.1021/ie0498551

Kaiya, Y., Itoh, Y., Fujita, K., & Takizawa, S. (1996). Study on fouling materials in the membrane treatment process for potable water. *Desalination, 106*(1), 71-77.

University of Malaya

Karim, M. M., Das, A. K., & Lee, S. H. (2006). Treatment of colored effluent of the textile industry in Bangladesh using zinc chloride treated indigenous activated carbons. *Analytica chimica acta, 576*(1), 37-42.

Kasaoka, S., Sakata, Y., Tanaka, E., & Naitoh, R. (1987). PREPARATION OF ACTIVATED FIBROUS CARBON FROM PHENOLIC FABRIC AND ITS MOLECULAR-SIEVING PROPERTIES. *Nippon Kagaku Kaishi*(6), 990-1000.

Katsoyiannis, I. A., Hug, S. J., Ammann, A., Zikoudi, A., & Hatziliontos, C. (2007). Arsenic speciation and uranium concentrations in drinking water supply wells in Northern Greece: correlations with redox indicative parameters and implications for groundwater treatment. *Science of The Total Environment, 383*(1), 128-140.

Kavitha, D., & Namasivayam, C. (2007). Experimental and kinetic studies on methylene blue adsorption by coir pith carbon. *Bioresource Technology, 98*(1), 14-21.

Kim, W., Suh, C.-Y., Cho, S.-W., Roh, K.-M., Kwon, H., Song, K., & Shon, I.-J. (2012). A new method for the identification and quantification of magnetite–maghemite mixture using conventional X-ray diffraction technique. *Talanta, 94*(0), 348-352. doi: http://dx.doi.org/10.1016/j.talanta.2012.03.001

Knaebel, K. S. (2008). Adsorbent selection. *Adsorption Research, Inc*.

Kong, S., Wang, Y., Hu, Q., & Olusegun, A. K. (2014). Magnetic nanoscale Fe–Mn binary oxides loaded zeolite for arsenic removal from synthetic groundwater. *Colloids and Surfaces A: Physicochemical and Engineering Aspects, 457*, 220-227.

Kumar, P. R., Chaudhari, S., Khilar, K. C., & Mahajan, S. (2004). Removal of arsenic from water by electrocoagulation. *Chemosphere, 55*(9), 1245-1252.

Kundu, S., & Gupta, A. (2006). Arsenic adsorption onto iron oxide-coated cement (IOCC): regression analysis of equilibrium data with several isotherm models and their optimization. *Chemical Engineering Journal, 122*(1), 93-106.

Kuo, S., & Lotse, E. (1972). Kinetics of phosphate adsorption by calcium carbonate and Ca-kaolinite. *Soil Science Society of America Journal, 36*(5), 725-729.

Kuokkanen, V., & Kuokkanen, T. (2013). Recent applications of electrocoagulation in treatment of water and wastewater—a review.

Lagergren, S. (1898). About the theory of so-called adsorption of soluble substances.

Lakshmi, U. R., Srivastava, V. C., Mall, I. D., & Lataye, D. H. (2009). Rice husk ash as an effective adsorbent: Evaluation of adsorptive characteristics for Indigo Carmine dye. *Journal of Environmental Management, 90*(2), 710-720. doi: http://dx.doi.org/10.1016/j.jenvman.2008.01.002

Langmuir, I. (1916). THE CONSTITUTION AND FUNDAMENTAL PROPERTIES OF SOLIDS AND LIQUIDS. PART I. SOLIDS. *Journal of the American Chemical Society, 38*(11), 2221-2295.

University of Malaya

Laszlo, K., & Szűcs, A. (2001). Surface characterization of polyethyleneterephthalate (PET) based activated carbon and the effect of pH on its adsorption capacity from aqueous phenol and 2, 3, 4-trichlorophenol solutions. *Carbon, 39*(13), 1945-1953.

Laxman, M. (2009). Pollution and its control in textile industry. *Dyes and Chemicals*.

Ledakowicz, S., Solecka, M., & Zylla, R. (2001). Biodegradation, decolourisation and detoxification of textile wastewater enhanced by advanced oxidation processes. *Journal of biotechnology, 89*(2), 175-184.

Libera, J., Elam, J., & Pellin, M. (2008). Conformal ZnO coatings on high surface area silica gel using atomic layer deposition. *Thin Solid Films, 516*(18), 6158-6166.

Limousin, G., Gaudet, J.-P., Charlet, C., Szenknect, S., Barthès, V., & Krimissa, M. (2007). Sorption isotherms: A review on physical bases, modeling and measurement. *Applied Geochemistry, 22*(2), 249-275.

Lin, B., & Moubarak, M. (2013). Decomposition analysis: change of carbon dioxide emissions in the Chinese textile industry. *Renewable and Sustainable Energy Reviews, 26*, 389-396.

Liu, C.-H., Chuang, Y. H., Chen, T.-Y., Tian, Y., Li, H., Wang, M.-K., & Zhang, W. (2015). Mechanism of arsenic adsorption on magnetite nanoparticles from water: thermodynamic and spectroscopic studies. *Environmental Science and Technology, 49*, 7726-7734.

Liu, J., Zhou, Q., Chen, J., Zhang, L., & Chang, N. (2013). Phosphate adsorption on hydroxyl–iron–lanthanum doped activated carbon fiber. *Chemical Engineering Journal, 215*, 859-867.

Liu, Y., Zeng, G., Tang, L., Cai, Y., Pang, Y., Zhang, Y., . . . He, Y. (2015). Highly effective adsorption of cationic and anionic dyes on magnetic Fe/Ni nanoparticles doped bimodal mesoporous carbon. *Journal of Colloid and Interface Science, 448*, 451-459. doi: http://dx.doi.org/10.1016/j.jcis.2015.02.037

Lloyd, D. S., Koenings, J. P., & Laperriere, J. D. (1987). Effects of turbidity in fresh waters of Alaska. *North American Journal of Fisheries Management, 7*(1), 18-33.

Lloyd, R. (1992). *Pollution and freshwater fish*: Fishing News Books Ltd.

Lopez-Ramon, M. V., Stoeckli, F., Moreno-Castilla, C., & Carrasco-Marin, F. (1999). On the characterization of acidic and basic surface sites on carbons by various techniques. *Carbon, 37*(8), 1215-1221. doi: http://dx.doi.org/10.1016/S0008-6223(98)00317-0

Lu, Y., Jiang, B., Fang, L., Ling, F., Gao, J., Wu, F., & Zhang, X. (2016). High performance NiFe layered double hydroxide for methyl orange dye and Cr (VI) adsorption. *Chemosphere, 152*, 415-422.

Lua, A. C., & Guo, J. (2001). Microporous oil-palm-shell activated carbon prepared by physical activation for gas-phase adsorption. *Langmuir, 17*(22), 7112-7117.

University of Malaya

Ma, J., Yu, F., Zhou, L., Jin, L., Yang, M., Luan, J., . . . Chen, J. (2012). Enhanced adsorptive removal of methyl orange and methylene blue from aqueous solution by alkali-activated multiwalled carbon nanotubes. *ACS applied materials & interfaces, 4*(11), 5749-5760.

Maity, D., Kale, S., Kaul-Ghanekar, R., Xue, J.-M., & Ding, J. (2009). Studies of magnetite nanoparticles synthesized by thermal decomposition of iron (III) acetylacetonate in tri (ethylene glycol). *Journal of magnetism and magnetic materials, 321*(19), 3093-3098.

Mandal, B. K., & Suzuki, K. T. (2002). Arsenic round the world: a review. *Talanta, 58*(1), 201-235.

Méndez, M., Carvajal, J. J., Cesteros, Y., Aguiló, M., Díaz, F., Giguère, A., . . . Marsal, L. F. (2010). Sol–gel Pechini synthesis and optical spectroscopy of nanocrystalline La2O3 doped with Eu3+. *Optical Materials, 32*(12), 1686-1692. doi: http://dx.doi.org/10.1016/j.optmat.2010.02.018

Mezohegyi, G., van der Zee, F. P., Font, J., Fortuny, A., & Fabregat, A. (2012). Towards advanced aqueous dye removal processes: a short review on the versatile role of activated carbon. *Journal of Environmental Management, 102*, 148-164.

Mondal, P., Bhowmick, S., Chatterjee, D., Figoli, A., & Van der Bruggen, B. (2013). Remediation of inorganic arsenic in groundwater for safe water supply: a critical assessment of technological solutions. *Chemosphere, 92*(2), 157-170.

Mousavi, H., Hosseynifar, A., Jahed, V., & Dehghani, S. (2010). Removal of lead from aqueous solution using waste tire rubber ash as an adsorbent. *Brazilian Journal of Chemical Engineering, 27*(1), 79-87.

Murcott, S. (2012). *Arsenic contamination in the World: an international sourcebook 2012*: IWA Publishing.

Naden, D. (1984). Ion exchange technology.

Nam, W., Kim, J., & Han, G. (2002). Photocatalytic oxidation of methyl orange in a three-phase fluidized bed reactor. *Chemosphere, 47*(9), 1019-1024.

Naqvi, S. M., Vaishnavi, C., & Singh, H. (1994). Toxicity and metabolism of arsenic in vertebrates. *ADVANCES IN ENVIRONMENTAL SCIENCE AND TECHNOLOGY-NEW YORK-, 27*, 55-55.

Naujokas, M. F., Anderson, B., Ahsan, H., Aposhian, H. V., Graziano, J. H., Thompson, C., & Suk, W. A. (2013). The broad scope of health effects from chronic arsenic exposure: update on a worldwide public health problem. *Environmental Health Perspectives (Online), 121*(3), 295.

Nga, N. K., Hong, P. T. T., Dai Lam, T., & Huy, T. Q. (2013). A facile synthesis of nanostructured magnesium oxide particles for enhanced adsorption performance in reactive blue 19 removal. *Journal of colloid and interface science, 398*, 210-216.

University of Malaya

Nilforoushan, M. R., & Otroj, S. (2008). Absorption of lead ions by various types of steel slag. *Iranian Journal of Chemistry and Chemical Engineering (IJCCE), 27*(3), 69-75.

Parida, S. K., Dash, S., Patel, S., & Mishra, B. K. (2006). Adsorption of organic molecules on silica surface. *Advances in Colloid and Interface Science, 121*(1–3), 77-110. doi: http://dx.doi.org/10.1016/j.cis.2006.05.028

Parsons, S. (2004). *Advanced Oxidation Processes for Water and Wastewater Treatment*: IWA Publishing.

Patnaik, P. (2017). *Handbook of Environmental Analysis: Chemical Pollutants in Air, Water, Soil, and Solid Wastes, Third Edition*: CRC Press.

Pattanayak, J., Mondal, K., Mathew, S., & Lalvani, S. (2000). A parametric evaluation of the removal of As (V) and As (III) by carbon-based adsorbents. *Carbon, 38*(4), 589-596.

Pehlivan, E., Tran, H., Ouédraogo, W., Schmidt, C., Zachmann, D., & Bahadir, M. (2013). Sugarcane bagasse treated with hydrous ferric oxide as a potential adsorbent for the removal of As (V) from aqueous solutions. *Food chemistry, 138*(1), 133-138.

Peterson, P. J., Benson, L. M., & Zieve, R. (1981). Metalloids. In N. W. Lepp (Ed.), *Effect of Heavy Metal Pollution on Plants: Effects of Trace Metals on Plant Function* (pp. 279-342). Dordrecht: Springer Netherlands.

Pierce, M. L., & Moore, C. B. (1982). Adsorption of arsenite and arsenate on amorphous iron hydroxide. *Water Research, 16*(7), 1247-1253. doi: http://dx.doi.org/10.1016/0043-1354(82)90143-9

Prasertsan, S., & Prasertsan, P. (1996). Biomass residues from palm oil mills in Thailand: an overview on quantity and potential usage. *Biomass and Bioenergy, 11*(5), 387-395.

Quy, D. V., Hieu, N. M., Tra, P. T., Nam, N. H., Hai, N. H., Thai Son, N., . . . Luong, N. H. (2013). Synthesis of silica-coated magnetic nanoparticles and application in the detection of pathogenic viruses. *Journal of Nanomaterials, 2013*.

Rahman, M. A., Amin, S. R., & Alam, A. S. (2012). Removal of methylene blue from waste water using activated carbon prepared from rice husk. *Dhaka University Journal of Science, 60*(2), 185-189.

Ravenscroft, P., Brammer, H., & Richards, K. (2009). *Arsenic pollution: a global synthesis* (Vol. 28): John Wiley & Sons.

Reddy, P. M. K., Krushnamurty, K., Mahammadunnisa, S., Dayamani, A., & Subrahmanyam, C. (2015). Preparation of activated carbons from bio-waste: effect of surface functional groups on methylene blue adsorption. *International Journal of Environmental Science and Technology, 12*(4), 1363-1372.

University of Malaya

Rehman, S. u., Siddiq, M., Al-Lohedan, H., Aktas, N., Sahiner, M., Demirci, S., & Sahiner, N. (2016). Fast removal of high quantities of toxic arsenate via cationic p(APTMACl) microgels. *Journal of Environmental Management, 166*, 217-226. doi: http://dx.doi.org/10.1016/j.jenvman.2015.10.026

Report, S. U. A. D. W., Toxicology, C., Toxicology, B. E. S., Studies, D. E. L., & Council, N. R. (2001). *Arsenic in Drinking Water: 2001 Update*: National Academies Press.

Reports of Societies. (1887). *British Medical Journal, 2*(1406), 1280-1283.

Reza, R. A., & Ahmaruzzaman, M. (2015). A novel synthesis of Fe 2 O 3@ activated carbon composite and its exploitation for the elimination of carcinogenic textile dye from an aqueous phase. *Rsc Advances, 5*(14), 10575-10586.

Rios, R. R. A., Alves, D. E., Dalmázio, I., Bento, S. F. V., Donnici, C. L., & Lago, R. M. (2003). Tailoring activated carbon by surface chemical modification with O, S, and N containing molecules. *Materials Research, 6*(2), 129-135.

Robati, D. (2013). Pseudo-second-order kinetic equations for modeling adsorption systems for removal of lead ions using multi-walled carbon nanotube. *Journal of nanostructure in Chemistry, 3*(1), 1-6.

Robinson, T., McMullan, G., Marchant, R., & Nigam, P. (2001). Remediation of dyes in textile effluent: a critical review on current treatment technologies with a proposed alternative. *Bioresource Technology, 77*(3), 247-255.

Rott, U., & Minke, R. (1999). Overview of wastewater treatment and recycling in the textile processing industry. *Water Science and Technology, 40*(1), 137-144.

Ryan, P. A. (1991). Environmental effects of sediment on New Zealand streams: a review. *New Zealand journal of marine and freshwater research, 25*(2), 207-221.

Sahu, O., Mazumdar, B., & Chaudhari, P. (2014). Treatment of wastewater by electrocoagulation: a review. *Environmental science and pollution research, 21*(4), 2397-2413.

Sánchez-Rodas, D., Luis Gómez-Ariza, J., Giráldez, I., Velasco, A., & Morales, E. (2005). Arsenic speciation in river and estuarine waters from southwest Spain. *Science of The Total Environment, 345*(1–3), 207-217. doi: http://dx.doi.org/10.1016/j.scitotenv.2004.10.029

Sarkar, A. K., Saha, A., Panda, A. B., & Pal, S. (2015). pH Triggered superior selective adsorption and separation of both cationic and anionic dyes and photocatalytic activity on a fully exfoliated titanate layer–natural polymer based nanocomposite. *Chemical Communications, 51*(89), 16057-16060.

Sarkar, S., Greenleaf, J. E., Gupta, A., Ghosh, D., Blaney, L. M., Bandyopadhyay, P., . . . SenGupta, A. K. (2010). Evolution of community-based arsenic removal systems in remote villages in West Bengal, India: assessment of decade-long operation. *Water Research, 44*(19), 5813-5822.

University of Malaya

Serizawa, T., Kamimura, S., & Akashi, M. (2000). Electrostatic adsorption of polystyrene particles with different surface charges onto the surface of an ultrathin polymer film. *Colloids and Surfaces A: Physicochemical and Engineering Aspects, 164*(2–3), 237-245. doi: http://dx.doi.org/10.1016/S0927-7757(99)00399-4

Shannon, R., & Strayer, D. (1989). Arsenic-induced skin toxicity. *Human & Experimental Toxicology, 8*(2), 99-104.

Shen, T., Jiang, C., Wang, C., Sun, J., Wang, X., & Li, X. (2015). A TiO2 modified abiotic-biotic process for the degradation of the azo dye methyl orange. *Rsc Advances, 5*(72), 58704-58712. doi: 10.1039/C5RA06686G

Shen, T., Luo, J., Zhang, S., & Luo, X. (2015). Hierarchically mesostructured MIL-101 metal–organic frameworks with different mineralizing agents for adsorptive removal of methyl orange and methylene blue from aqueous solution. *Journal of Environmental Chemical Engineering, 3*(2), 1372-1383.

SHUKLA, S. K., KUMAR, V., & BANSAL, M. (2008). Application of Membrane Filtration for Reuse of Bleaching Plant Effluent in the Process. *ENVIRONMENT and GEOSCIENCE*.

Singh, R., Singh, S., Parihar, P., Singh, V. P., & Prasad, S. M. (2015). Arsenic contamination, consequences and remediation techniques: a review. *Ecotoxicology and environmental safety, 112*, 247-270.

Singh, T. S., & Pant, K. K. (2004). Equilibrium, kinetics and thermodynamic studies for adsorption of As(III) on activated alumina. *Separation and purification technology, 36*(2), 139-147. doi: http://dx.doi.org/10.1016/S1383-5866(03)00209-0

Smedley, P., & Kinniburgh, D. (2002). A review of the source, behaviour and distribution of arsenic in natural waters. *Applied Geochemistry, 17*(5), 517-568.

Smith, E., MacCarthy, P., Yu, T., & Mark Jr, H. (1977). Sulfuric acid treatment of peat for cation exchange. *Journal (Water Pollution Control Federation)*, 633-638.

Soni, M., Sharma, A. K., Srivastava, J. K., & Yadav, J. (2012). Adsorptive removal of methylene blue dye from an aqueous solution using water hyacinth root powder as a low cost adsorbent. *International Journal of Chemical Sciences and Applications, 3*(3), 338-345.

Suffet, I. H., Maccarthy, P., MacCarthy, P., & Suffet, I. H. (1988). PREFACE, Introduction *Aquatic Humic Substances* (Vol. 219, pp. xiii-xxx): American Chemical Society.

Sun, Q., & Yang, L. (2003). The adsorption of basic dyes from aqueous solution on modified peat–resin particle. *Water research, 37*(7), 1535-1544.

Szymczyk, M., El-Shafei, A., & Freeman, H. S. (2007). Design, synthesis, and characterization of new iron-complexed azo dyes. *Dyes and Pigments, 72*(1), 8-15.

University of Malaya

Tabbara, M., & El Jamal, M. (2012). A kinetic study of the discoloration of methylene blue by Na2SO3, comparison with NaOH. *Journal of the University of Chemical Technology and Metallurgy, 47*(3), 275-282.

Tchobanoglous, G., & Burton, F. L. (1991). Wastewater engineering. *Management, 7*, 1-4.

Tholoana, M. (2007). Water Management at a Textile Industry: A Case Study in Lesotho. *University of Pretoria*.

Thommes, M., Kaneko, K., Neimark, A. V., Olivier, J. P., Rodriguez-Reinoso, F., Rouquerol, J., & Sing, K. S. (2015). Physisorption of gases, with special reference to the evaluation of surface area and pore size distribution (IUPAC Technical Report). *Pure and Applied Chemistry, 87*(9-10), 1051-1069.

Trivedi, H., Patel, V., & Patel, R. (1973). Adsorption of cellulose triacetate on calcium silicate. *European Polymer Journal, 9*(6), 525-531.

Tüfekci, N., Sivri, N., & Toroz, İ. (2007). Pollutants of textile industry wastewater and assessment of its discharge limits by water quality standards. *Turkish journal of fisheries and aquatic sciences, 7*(2).

Umoren, S., Etim, U., & Israel, A. (2013). Adsorption of methylene blue from industrial effluent using poly (vinyl alcohol). *J Mater Environ Sci, 4*, 75-86.

USEPA. (2016). Table of Regulated Drinking Water Contaminants. Retrieved 9 August 2016 https://www.epa.gov/ground-water-and-drinking-water/table-regulated-drinking-water-contaminants

Vijayaraghavan, K., Padmesh, T., Palanivelu, K., & Velan, M. (2006). Biosorption of nickel (II) ions onto Sargassum wightii: application of two-parameter and three-parameter isotherm models. *Journal of Hazardous Materials, 133*(1), 304-308.

VITO. (2010, February 2010). Water Treatment Selection System. *Ion Exchange.* Retrieved 22 August 2016, from https://emis.vito.be/en/techniekfiche/ion-exchange

Wang, C., Luo, H., Zhang, Z., Wu, Y., Zhang, J., & Chen, S. (2014). Removal of As (III) and As (V) from aqueous solutions using nanoscale zero valent iron-reduced graphite oxide modified composites. *Journal of Hazardous Materials, 268*, 124-131.

Wang, H., Yuan, X., Zeng, G., Leng, L., Peng, X., Liao, K., . . . Xiao, Z. (2014). Removal of malachite green dye from wastewater by different organic acid-modified natural adsorbent: kinetics, equilibriums, mechanisms, practical application, and disposal of dye-loaded adsorbent. *Environmental science and pollution research, 21*(19), 11552-11564.

Waters, T. F. (1995). *Sediment in streams: sources, biological effects, and control*: American Fisheries Society.

University of Malaya

Weber, W., & Morris, J. *Advances in water pollution research: removal of biologically resistant pollutants fromwastewaters by adsorption.* Paper presented at the International Conference onWater Pollution Symposium.

Weber, W. J., & Morris, J. C. (1963). Kinetics of adsorption on carbon from solution. *Journal of the Sanitary Engineering Division, 89*(2), 31-60.

Wedepohl, K. H. (1969). *Handbook of geochemistry*.

Wikipedia. (2016, 20 July 2016). Water pollution. Retrieved 8 August 2016, from https://en.wikipedia.org/w/index.php?title=Water_pollution&oldid=730736569

Worch, E. (2012). *Adsorption technology in water treatment: fundamentals, processes, and modeling*: Walter de Gruyter.

Wu, F.-C., Tseng, R.-L., & Juang, R.-S. (2009). Initial behavior of intraparticle diffusion model used in the description of adsorption kinetics. *Chemical Engineering Journal, 153*(1–3), 1-8. doi: http://dx.doi.org/10.1016/j.cej.2009.04.042

Wu, K., Liu, R., Li, T., Liu, H., Peng, J., & Qu, J. (2013). Removal of arsenic(III) from aqueous solution using a low-cost by-product in Fe-removal plants—Fe-based backwashing sludge. *Chemical Engineering Journal, 226*(0), 393-401. doi: http://dx.doi.org/10.1016/j.cej.2013.04.076

Xie, J., Wang, Z., Lu, S., Wu, D., Zhang, Z., & Kong, H. (2014). Removal and recovery of phosphate from water by lanthanum hydroxide materials. *Chemical Engineering Journal, 254*, 163-170.

Xu, J., Chu, W., & Luo, S. (2006). Synthesis and characterization of mesoporous V-MCM-41 molecular sieves with good hydrothermal and thermal stability. *Journal of Molecular Catalysis A: Chemical, 256*(1–2), 48-56. doi: http://dx.doi.org/10.1016/j.molcata.2006.03.078

Yan, J., Moreno, L., & Neretnieks, I. (2000). The long-term acid neutralizing capacity of steel slag. *Waste Management, 20*(2), 217-223.

Yang, L., Shahrivari, Z., Liu, P. K., Sahimi, M., & Tsotsis, T. T. (2005). Removal of trace levels of arsenic and selenium from aqueous solutions by calcined and uncalcined layered double hydroxides (LDH). *Industrial & Engineering Chemistry Research, 44*(17), 6804-6815.

Yin, C. Y., Aroua, M. K., & Daud, W. M. A. W. (2007). Review of modifications of activated carbon for enhancing contaminant uptakes from aqueous solutions. *Separation and purification technology, 52*(3), 403-415.

Yoon, J., Lee, Y., & Kim, S. (2000). Investigation of the reaction pathway of OH radicals produced by Fenton oxidation in the conditions of wastewater treatment. *Water science and technology: a journal of the International Association on Water Pollution Research, 44*(5), 15-21.

University of Malaya

Yu, B. Y., & Kwak, S.-Y. (2010). Assembly of magnetite nanocrystals into spherical mesoporous aggregates with a 3-D wormhole-like pore structure. *Journal of Materials Chemistry, 20*(38), 8320-8328.

Yu, J., Jiang, D., Hao, Q., & Liu, J. (2015). Silica-coated Magnetic Nanocomposites as an Adsorbent for the Removal of Methylene Blue Dyes from Water: Preparation and Characterization.

Yu, Y., Zhuang, Y.-Y., Li, Y., & Qiu, M.-Q. (2002). Effect of dye structure on the interaction between organic flocculant PAN-DCD and dye. *Industrial & Engineering Chemistry Research, 41*(6), 1589-1596.

Yuan, Y.-l., Wen, Y.-z., Li, X.-y., & Luo, S.-z. (2006). Treatment of wastewater from dye manufacturing industry by coagulation. *Journal of Zhejiang University Science A, 7*(2), 340-344.

Yürüm, A., Kocabaş-Ataklı, Z. Ö., Sezen, M., Semiat, R., & Yürüm, Y. (2014). Fast deposition of porous iron oxide on activated carbon by microwave heating and arsenic (V) removal from water. *Chemical Engineering Journal, 242*, 321-332. doi: http://dx.doi.org/10.1016/j.cej.2014.01.005

Zeldowitsch, J. (1934). Adsorption site energy distribution. *Acta phys. chim. URSS, 1*, 961-973.

Zeng, L., Xie, M., Zhang, Q., Kang, Y., Guo, X., Xiao, H., . . . Luo, J. (2015). Chitosan/organic rectorite composite for the magnetic uptake of methylene blue and methyl orange. *Carbohydrate Polymers, 123*, 89-98. doi: http://dx.doi.org/10.1016/j.carbpol.2015.01.021

Zhang, S., Li, X.-Y., & Chen, J. P. (2009). An XPS study for mechanisms of arsenate adsorption onto a magnetite-doped activated carbon fiber. *Journal of Colloid and Interface Science, 343*, 232-238.

Zhang, S., Li, X.-y., & Chen, J. P. (2010). Preparation and evaluation of a magnetite-doped activated carbon fiber for enhanced arsenic removal. *Carbon, 48*(1), 60-67.

Zhang, W., Fu, J., Zhang, G., & Zhang, X. (2014). Enhanced arsenate removal by novel Fe–La composite (hydr) oxides synthesized via coprecipitation. *Chemical Engineering Journal, 251*, 69-79.

Zhang, Y., Yang, M., Dou, X.-M., He, H., & Wang, D.-S. (2005). Arsenate adsorption on an Fe-Ce bimetal oxide adsorbent: role of surface properties. *Environmental science & technology, 39*(18), 7246-7253.

Zhu, M.-X., Li, Y.-P., Xie, M., & Xin, H.-Z. (2005). Sorption of an anionic dye by uncalcined and calcined layered double hydroxides: a case study. *Journal of Hazardous Materials, 120*(1–3), 163-171. doi: http://dx.doi.org/10.1016/j.jhazmat.2004.12.029

Zongliang, H., Senlin, T., & Ping, N. (2012). Adsorption of arsenate and arsenite from aqueous solutions by cerium-loaded cation exchange resin. *Journal of Rare Earths, 30*(6), 563-572.

University of Malaya

Zouboulis, A. I., & Katsoyiannis, I. A. (2005). Recent advances in the bioremediation of arsenic-contaminated groundwaters. *Environment international*, *31*(2), 213-219. doi: http://dx.doi.org/10.1016/j.envint.2004.09.018

University of Malaya

LIST OF PUBLICATION

a) Symposium

Farahin mohd jais, shaliza ibrahim, yeomin yoo, min jang. Enhanced arsenate removal by lanthanum and nano–magnetite composite incorporated palm shell waste–based activated carbon. Sustainable symposium. 2016. University of malaya.

a) Journal

Jais, F.M., Ibrahim, S.,Yoon, Y., & Jang, M. (2016). Enhanced arsenate removal by Lathanum and nano-magnetite composite incorporated palm shell waste-based activated carbon. Separation and purification technology, 169, 93-102. Doi:http://dx.doi.org/10.1016/j.seppur.2016.05.034

University of Malaya